

Shape optimisation of a second skin



A.O. van Tilburg
MSc Thesis, May 2019

Shape optimisation of a second skin

What can be achieved - in terms of structural and building physics performance - when an existing skin of a building is removed and replaced by a new facade.

by

A.O. van Tilburg

Master Thesis Building Engineering

Faculty of Civil Engineering and Geosciences · Delft University of Technology

| | | |
|-------------------|----------------------------|--------------------|
| Student number: | 4303695 | |
| Public defence | May 7, 2019 at 15:00 | |
| Thesis committee: | Prof. Ir. R. Nijse, | TU Delft, chairman |
| | Ir. T. Bristogianni | TU Delft |
| | Ir. L.P.L. van der Linden | TU Delft |
| | Dr. Ir. W.H. van der Spoel | TU Delft |

Preface

I would like to express my gratitude to everyone who helped me with the thesis, starting with the thesis committee. The guidance and feedback of each committee member helped me set out the course for the whole project, especially at the beginning of the project.

I would like to thank Professor Nijse for guiding the overall process as chair of the committee and his spot-on remarks during the meetings.

Also, I want to thank Telesilla Bristogianni for her contribution, in particular at the beginning of the project.

Moreover, I want to thank Lennert van der Linden, every meeting the project as a whole got a bit better and grow to the product it is now. The meetings contained both in dept advise and general guidance, which was both very welcome.

The last commission member I want to thank is Willem van der Spoel for his contribution, helping with the building physics. I liked that the meetings were not a one-way stream; you were interested in all the aspects of the thesis also the structural part. The advice about the ventilation partly given by Peter van den Engel, I want to thank him as well. The meetings with Peter van den Engel were often an eye-opener.

Finally, I want to thank my family for their patience and understanding during these busy months. My parents always supported my study and helped me to get the most out of it. I am very grateful for that. Also, I want to thank my oldest sister for improving the language and the structure of the report.

*A.O. van Tilburg
Dinteloord, April 2019*

Contents

| | | |
|----------|---|-----------|
| 1 | Introduction | 3 |
| 1.1 | The Background | 3 |
| 1.2 | Problem description: | 3 |
| 1.3 | Objective | 4 |
| 1.3.1 | Structural Improvement | 4 |
| 1.3.2 | Improvement of building physics | 5 |
| 1.4 | Research question | 5 |
| 1.5 | Delimitations | 5 |
| 1.6 | Research methodology | 6 |
| I | Literature study | 7 |
| 2 | Parametric design and optimisation | 9 |
| 2.1 | Parametric design. | 10 |
| 2.2 | Parametric tools. | 10 |
| 2.3 | Optimisation in general. | 12 |
| 2.4 | Structural optimisation | 13 |
| 2.5 | Genetic algorithms | 14 |
| 3 | Wind engineering | 17 |
| 3.1 | Atmospheric boundary layer | 18 |
| 3.1.1 | Source of the wind | 18 |
| 3.1.2 | Velocity profile. | 18 |
| 3.2 | CFD basics | 19 |
| 3.2.1 | Discretisation | 19 |
| 3.2.2 | Defining domain. | 19 |
| 3.2.3 | Building mesh | 20 |
| 3.2.4 | Mesh Structures | 20 |
| 3.2.5 | Stability and convergence | 20 |
| 3.3 | Wind tunnel configuration | 20 |
| 3.3.1 | Computational domain | 20 |
| 3.3.2 | Boundary conditions. | 21 |
| 3.3.3 | Inlet and outlet. | 21 |
| 3.3.4 | Cp-values | 22 |
| 3.4 | Retrospect of existing research | 23 |
| 3.4.1 | Experimental research | 23 |
| 3.4.2 | Theoretical research | 24 |
| 3.5 | Wind availability | 25 |
| 4 | Structure | 29 |
| 4.1 | Survey of freeform gridshells | 30 |
| 4.2 | Nodes. | 32 |
| 4.2.1 | Welded node | 32 |
| 4.2.2 | 3D printed nodes | 32 |
| 4.2.3 | Bolted connection | 33 |
| 4.3 | Maintenance | 33 |
| 4.3.1 | Internal | 33 |
| 4.3.2 | External | 33 |

| | | |
|-----------|---|-----------|
| 5 | Ventilation | 35 |
| 5.1 | Physical Fundamentals | 36 |
| 5.1.1 | Stack effect | 36 |
| 5.1.2 | Wind driven | 38 |
| 5.1.3 | Combined | 38 |
| 5.2 | Ventilation principles | 38 |
| 5.2.1 | Natural. | 39 |
| 5.2.2 | Mechanical ventilation. | 39 |
| 5.2.3 | Hybrid ventilation | 39 |
| 5.3 | Survey of naturally ventilated buildings. | 40 |
| 5.3.1 | Single sided ventilation | 41 |
| 5.3.2 | Cross ventilation. | 41 |
| 5.3.3 | Stack ventilation | 42 |
| 5.3.4 | Double skin | 42 |
| 5.4 | Critical barriers | 44 |
| 5.4.1 | Safety | 44 |
| 5.4.2 | Noise. | 45 |
| 5.4.3 | Air pollution | 45 |
| 5.4.4 | Draughts & condensation | 45 |
| 5.4.5 | User ignorance Patterns of use | 45 |
| II | The Design | 47 |
| 6 | CFD analysis set-up and shape optimisation | 49 |
| 6.1 | Case study: Mijnbouwstraat 106-112 Delft | 50 |
| 6.2 | Comparing Butterfly with existing research | 51 |
| 6.2.1 | Eurocode | 51 |
| 6.3 | Mesh set-up. | 52 |
| 6.3.1 | Mesh generation | 53 |
| 6.4 | Grid sensitivity | 54 |
| 6.4.1 | Rectangular buildings | 54 |
| 6.4.2 | Freeform buildings. | 54 |
| 6.5 | Residuals | 55 |
| 6.6 | Genetic algorithm. | 56 |
| 6.6.1 | Galapagos | 56 |
| 6.6.2 | Genetic algorithm in Python. | 57 |
| 6.7 | Shape optimisation | 57 |
| 6.7.1 | Design variable: Floor offset | 57 |
| 6.7.2 | Performance indicator: Resultant wind force | 58 |
| 6.7.3 | Process. | 61 |
| 6.7.4 | Results | 63 |
| 7 | Structural model set-up and optimisations | 67 |
| 7.1 | Freeform gridshell | 68 |
| 7.1.1 | Optimal grid | 68 |
| 7.1.2 | Translation of a freeform facade to a gridshell | 68 |
| 7.1.3 | Translation of a freeform roof to a gridshell | 69 |
| 7.2 | Supports and connections | 71 |
| 7.2.1 | Supports types | 71 |
| 7.2.2 | Supports | 72 |
| 7.2.3 | Mechanic scheme | 72 |
| 7.2.4 | Stiffness supports | 73 |
| 7.2.5 | Connections | 74 |
| 7.3 | Materials and elements | 74 |
| 7.3.1 | Materials. | 74 |
| 7.3.2 | Cross section. | 75 |

| | | |
|------------|--|------------|
| 7.4 | Loads | 75 |
| 7.4.1 | Load cases | 75 |
| 7.4.2 | Load combinations | 77 |
| 7.5 | Structural requirements | 77 |
| 7.5.1 | Displacement | 78 |
| 7.5.2 | Strength | 78 |
| 7.5.3 | Buckling | 78 |
| 7.6 | Structural optimisation | 78 |
| 7.6.1 | Design variables | 78 |
| 7.6.2 | Performance indicator: Material usage. | 79 |
| 7.6.3 | Process. | 79 |
| 7.6.4 | Results | 81 |
| 7.7 | Structural and shape optimisation | 83 |
| 7.8 | Benchmark: Karamba and GSA | 84 |
| 7.8.1 | Displacement | 84 |
| 7.8.2 | Forces and Moments. | 85 |
| 7.9 | Global buckling | 87 |
| 7.10 | Testing spring supports | 88 |
| 7.10.1 | Negative support reactions. | 89 |
| 7.10.2 | Relation between support stiffness and support reactions | 90 |
| 8 | Ventilation concept | 93 |
| 8.1 | Ventilation concept: mean idea | 94 |
| 8.2 | Ventilation demand | 94 |
| 8.3 | Behaviour of the openings | 94 |
| 8.4 | Position openings. | 95 |
| 8.4.1 | Stack-effect | 95 |
| 8.4.2 | Wind. | 95 |
| 8.5 | Design ventilation openings | 97 |
| 8.5.1 | Type of opening | 97 |
| 8.6 | Calculation procedure | 97 |
| 8.6.1 | Equations | 97 |
| 8.6.2 | CIBSE spreadsheet. | 98 |
| 8.6.3 | Contam | 99 |
| 8.6.4 | Contam result | 100 |
| 8.7 | The uptime of the ventilation system | 100 |
| III | Conclusion & Reflection | 103 |
| 9 | Conclusion & Reflection | 105 |
| 9.1 | Conclusion | 105 |
| 9.1.1 | Shape optimisation | 105 |
| 9.1.2 | Structural optimisation | 106 |
| 9.1.3 | Ventilation | 107 |
| 9.2 | Further research | 108 |
| IV | Appendix | 109 |
| A | Python code highlights | 111 |
| A.1 | Python code to adjust panels | 111 |
| A.2 | Genetic algorithm in Python | 111 |
| B | Ventilation excel tool | 115 |
| B.1 | Basis formulas | 115 |
| C | Contam verification | 119 |
| C.1 | Example Wind | 119 |
| C.2 | Example Buoyancy | 121 |

| | |
|--|------------|
| D Glass calculation | 125 |
| E Estimation stiffness supports | 127 |
| E.1 Supports at ground level | 127 |
| E.2 Supports attached to the Building. | 130 |
| E.2.1 Wind load | 130 |
| E.2.2 Results | 132 |
| E.3 Support reactions | 132 |
| E.3.1 Ground supports. | 132 |
| E.3.2 Supports attached to building | 132 |
| F Resultant wind force | 135 |
| G Galapagos-Colibri setup | 137 |
| Bibliography | 141 |

Summary

Chapter one introduces the main incentive of the thesis which is the low rate of refurbishment. To reach the European Union climate targets of 2020 the rate of refurbishment must increase [1]. This thesis looks at the improvement, that can be made when replacing an existing skin by a new facade.

The second chapter introduces one of the main driving forces of this thesis, parametric design and optimisation. A parametric design is crucial for this thesis to perform a variation study. By combining the variation study with an optimisation algorithm, the performance of the variation study is supervised.

Chapter three gives the background information for the CFD simulations. The chapter starts with the theoretical background about the source of the wind and the behaviour of it in the atmosphere. It is crucial to understand the input and processes of the simulation, to avoid a black box problem. Therefore, the sections contain information about the set-up and the simulation process itself. Lastly, existing research provides background information for proper verification of the CFD simulation.

The next chapter provides background information but about the structural model. The design of the grid-shell is supported by the survey of existing gridshells like the Yas Island Marina. Besides that, the chapter provides information to choose the type of node and type of supports.

In Chapter five ventilation is discussed. Natural ventilation is driven by buoyancy, wind or a combination of the two. Those natural forces are not available throughout the year. Therefore, relying on natural ventilation alone is not possible. An option is to use hybrid ventilation which is a combination of mechanical and natural ventilation, when using mechanical ventilation the indoor climate changes and the energy usage increases.

The structural and building physics performance of the Mijnbouwstraat 106-112 is increased to illustrate the improvements that can be made. In chapter 6 the knowledge gained in the previous chapters is put to practice. The CFD simulation is set-up, verified and adjusted for the variation study. The main difference with the common practice is that not just one design is tested, but a couple of hundred designs. Doing this by hand is not an option; an optimisation program can control the simulation. Standard optimisation programs do not work because the CFD simulation is a complex calculation. Therefore a custom made Python script controls the CFD simulations. The Python script demonstrates its added value by reducing the wind load on the facade.

The structural optimisation extends the shape optimisation in chapter seven. By using a structural model, to calculate the required amount of material, the material savings are quantified. This model substantiates that the reduction of the wind load translates to material savings. The second step is another optimisation strategy; here the shape and structural optimisation are executed simultaneously. The different strategy quantifies the importance of the simultaneous execution of the optimisation.

Chapter eight explains what can be achieved regarding the ventilation system and emphasizes the importance of integrating the ventilation system with the second skin. First, the integration is explained by means of a design. The design builds upon the results of the CFD simulation and the structural model. The ventilation system itself is unique and requires more attention (in the design and construction stage) than a conventional ventilation system. Secondly, the performance of the system is quantified by determining the usage of natural resources.

The last chapter discusses the conclusion and reflection. One of the conclusions is that shape can reduce the wind load. The reduction of the wind load results in a reduction of the material usage. Combining the structural and shape optimisation is recommended. In the case study, the shape optimisation minimizes the height of the structure because a lower structure has less wind resistance. On the contrary, a small increase in height reduces the amount of steel which is needed to construct the facade, it appears that increasing the height is more advantageous. The best solution is founded when the shape optimisation and structural optimisation are executed simultaneously.



Introduction

1.1. The Background

The human population is increasing at a high rate, which causes serious problems and pressure on primary resources and the environment. According to UN reports [1] the global human population will grow from 7.2 billion in 2013 to 9.6 billion people in 2050. The European Union climate target states that in 2020 the GHG emission must reduce with 20%, renewable energy must increase by 20%, and the energy efficiency must improve by 20%. To achieve these targets the building sector could contribute significantly because they account for 40% of the total energy consumption in the European Union. The Energy Performance of Buildings Directive [1], published the nearly zero energy concept which will be mandatory in 2021.

A Zero Energy Building (ZEB) is a sustainable building which uses renewable energy sources to fulfil the required energy consumption. Besides the use of non-polluting energy sources, the ZEB's reduce the energy demand by using methods of energy efficiency. The remaining energy needs are fulfilled by renewable energy generation. Because most ZEB's are connected to the grid, the excess or lack of generated energy can be sent to or taken from the grid. This method ensures that the buildings energy balance on an annual basis is zero. When there are better storage technologies, a 'Net-Zero-Energy Building' can be reached with different methods [2].

These nearly zero energy buildings are part of the solution, but when the majority of the existing buildings is unsatisfactory, renovation is more important [3]. The current rate of refurbishment might be too low to meet the challenging climate targets. Only 1.2% of the existing building stock is renovated, and 0.1% is demolished. Even if the renovations utilise the full energy-saving potential the rate is too low to reach the energy targets [1]. To improve the building stock, the speed and quality of the refurbishment must increase.

1.2. Problem description:

In order to meet the European Union Climate targets, the current number of renovations should increase. Since the current rate of renovations, assuming they reach full energy saving potential, is too low to reach the targets. This low rate of renovations is caused by many known and unknown barriers which can obstruct a successful renovation. In order to give an overview of the possible barriers and possible solutions, the most important economic and technological barriers will be discussed.

Economic

Hviid and Svendsen [4] describes barriers like high capital costs, imperfect information, confidence in the investment and various forms of uncertainty (technical, political, etc.). According to Greco et al. [5] the main barriers are financially related.

Economic barriers are challenging to overcome entirely because, as with many projects, there are different stakeholders with different cost-effectiveness perspectives. For example, investors are interested in an af-

fordable investment, and an expensive zero energy refurbishment is more advantageous from an ecological perspective. A zero energy refurbishment is a less competing investment option because the benefit of energy improvement is not visible enough. On top of that, energy efficiency alone is not an attractive purchase because of the long payback period [1]. To make a renovation feasible, the benefits of renovation must extend beyond energy savings. These extra benefits can increase the value of the building, which can help investors to gain confidence in the investment. An example of a renovation which is feasible is the VROM building in the Hague, where the indoor climate is improved, and extra floor space is created due to the atria, see Figure 1.1. Also, the energy savings are high because the facade area is minimised due to the atrium. Initially, the building was H-shaped, but the gaps were closed off with multiple atria.



Figure 1.1: Ministry Vrom The Hague [6]

Technologic

Innovative and practical solutions to renew office facades could support the refurbishment of office buildings [7]. However, according to Antinucci et al. [1] technical barriers like unfamiliarity with innovative solutions, technical risks (related to ventilation, moisture etc.) and technical constraints in the building envelope must be solved. Refurbishment can be difficult because many buildings are unique and need individual solutions. Facade refurbishment is limited due to technical constraints in the building envelope, and technical details about the building get lost over time. Therefore it is tempting to demolish a building and create a completely new building. Even buildings with high refurbishment potential are kept in poor condition or get demolished, which is a waste of money and embodied energy.

Concluding, a solution must overcome most technical and economic barriers to be successful. Moreover, the main barriers are financially related; thus a suitable solution must be more competitive in terms of price.

1.3. Objective

The problem is that there are many barriers to refurbishment, which causes a low rate and low quality. The objective is to overcome these barriers and stimulate facade refurbishment. This thesis will focus on improving the structural efficiency and touch upon building physics. For a feasible project, the structure and building physics must be well integrated. The disciplines can even go a step further and profit from each other. By showing that the structure is not a solution on its own, some building physics aspects (ventilation) will be integrated into the design.

1.3.1. Structural Improvement

First of all, the cost can be influenced by minimising the amount of material by altering: the shape of the beam, cross-sections, beam distances, etc. More important than minimising material usage is minimising

the embodied energy. By minimising the embodied energy, the environmental impact can be lowered. Environmental impact has got more attention over the years, and environmental considerations have to be integrated into different decision makers by business, individuals and policymakers [8]. These environmental considerations can be quantified by, for example, shadow costs where each material has a certain price per kg equivalent [9].

Secondly, by altering the shape of the facade a more aerodynamic building can be created. When the curvature increases, the wind load can be reduced which can make the structure more efficient. The reduction factors for cylindrical buildings and dome structures can be found in the Eurocode [10]. If the shape of the building diverges from those shapes, the reduction factors can be estimated with the computational fluid dynamics (CFD).

1.3.2. Improvement of building physics

A level A quality refurbishment is needed to reach European targets. However, a zero energy refurbishment is very rare [5]. To design such a building, structural and building physics engineers must create an integrated design. The synergy between the two disciplines can improve the design, for example, the pressure coefficients calculated by the structural engineer can be used to design a better ventilation system. Also, renewing the technical installations and facade construction is not misaligned because the technical lifespan of building services and the facade construction are both 30 years [11].

On the contrary, modern architecture tends to build more and more transparent buildings. Architects like the daylight, view and aesthetics that come with it [12]. However, to reach the targets set by the European Union, the operational energy must be minimised to create energy-efficient buildings. Large glass areas consume a lot of energy to preserve a comfortable temperature. By making use of ventilation, the cooling energy can be reduced.

1.4. Research question

Main question:

What can be achieved - in terms of structural and building physics performance - when an existing skin of a building is removed and replaced by a new facade?

Subquestions:

1. How to perform a shape optimisation of a facade to reduce the wind load by making the building more aerodynamic?
2. What is the effect of integrating a structural optimisation with a shape optimisation?
3. How to integrate a low energy ventilation system in the design and what can be achieved?

1.5. Delimitations

The parametric design can be used to model a preliminary structure. Creating a detailed design with a parametric model is overambitious and is out of the scope of this thesis. The focus of the thesis is to show what can be achieved with shape optimisation of the facade, instead of a detailed design.

The improvement of the buildings has been restricted to office buildings only. In the Netherlands still, 15.9% of the office buildings are vacant [13], and despite a large number of rentable buildings, new office buildings are built because of the lack of quality. It is better to stimulate renovation and avoid loss of embodied energy by minimising demolition. Also, office buildings are the most energy intensive typologies and use over 50% of the total energy consumption of non-domestic buildings [14].

1.6. Research methodology

The thesis consists of nine chapters subdivided into three parts. First the literature study, which provides background information. Part 2, The Design, consists out of three chapters and each chapter answers one (sub) research question. The last part answers the main research question and presents the conclusion.

Part I: Literature study

Firstly, parametric design and optimisation, in general, will be addressed. The software which is used will be addressed followed by different optimisation processes. Structural optimisation can be categorised into three classes namely topology, shape and size optimisation [15]. Secondly, gridshells buildability and maintenance will be reviewed. Thirdly, wind in general but also wind engineering concerning computational fluid dynamics will be explained. Lastly, ventilation and the problems and opportunities of hybrid ventilation will be discussed.

Part II: The Design

The findings in the literature study will be put to practice by implementing the findings in a design. As a basis, the setup of computational fluid analysis will be discussed. This analysis will be used for the ventilation system and the structural optimisation. The ventilation concept, which elaborates on the outcome of the computational fluid design, will be explained together with the availability of the ventilation system. After that two optimisations will be applied on a case: Mijnbouwstraat 106-112. Namely, a shape optimisation followed by a structural optimisation. Each optimisation starts with the explanation of the input parameters and the performance indicators, which are necessary for the optimisation. The optimisations will explore the design space with a parametric design including the creation of the grid and structural calculations.

Part III: Conclusion & Reflection

A comparison will be made between the original building and the building after renovation by means of a case study to substantiate the improvement of the facade. This comparison can be used to substantiate and answer the research question. The thesis will conclude with a conclusion and proposal for further research.

I

Literature study

2

Parametric design and optimisation

This chapter introduces two important aspects of this thesis, namely parametric design and optimisation. The first two sections discuss parametric design and parametric tools. After those sections, structural optimisation is introduced and followed by genetic algorithms.

2.1. Parametric design

With conventional design tools, it is relatively easy to create an initial model. However, it is more complex to change things in these models. When changing a dimension, it can require that a lot of other parts must be adjusted as well. Since this rework is manual, there can be much work entailed (especially when the model is more developed). In a design, decisions that should be changed can take up too much time which limits the exploration and effectively restricts the design [16].

However, an advantage of conventional design tools is the ease of erasing parts. Since the parts are independent, they can be selected and deleted. The representation does not have to be fixed, because the parts do not have a lasting relationship with other parts, but it can be fixed by adding something which replaces the removed parts [16].

Design variations are effortless when designing in an environment of parametric design [17]. As a parametric designer, one does not create the design by direct manipulation, but first, the relationships which connect the parts is established [16]. A design is build using these relationships and can be modified by changing the relations by observation and selection from the results produced. The designer no longer has to keep the design consistent with relationships (since the system takes care of that), which enables the designer to explore ideas without loads of rework.

With parametric design, the relationship definition phase should be considered as an integral part of the design process [16]. The quality of a parametric design thus depends on the willingness and ability of the designer to implement this the relationship definition. The designer should focus on the logic behind the design instead of beginning with the direct activity of design. This different approach requires formal notation and additional (new) concepts which were not a part of the design thinking before.

2.2. Parametric tools

There are many tools available to support a parametric design. Initially, the tool-set existed out of physical models alone, but over time different programs have been created and replaced the need for physical models. This thesis relies on parametric software, with Grasshopper ¹ is used which is an extension of Rhinoceros ² as the main contributor. The benefit of Grasshopper is that it is quite popular, has good support and many plugins are available.

Many Grasshopper plugins are used for this thesis but the most important ones are (see Figure 2.1):

- Karamba (version 1.2.2)
- Butterfly (version 0.0.04)
- Python

¹Grasshopper version 0.9.0076 is used

²Rhinoceros version 5.13 is used

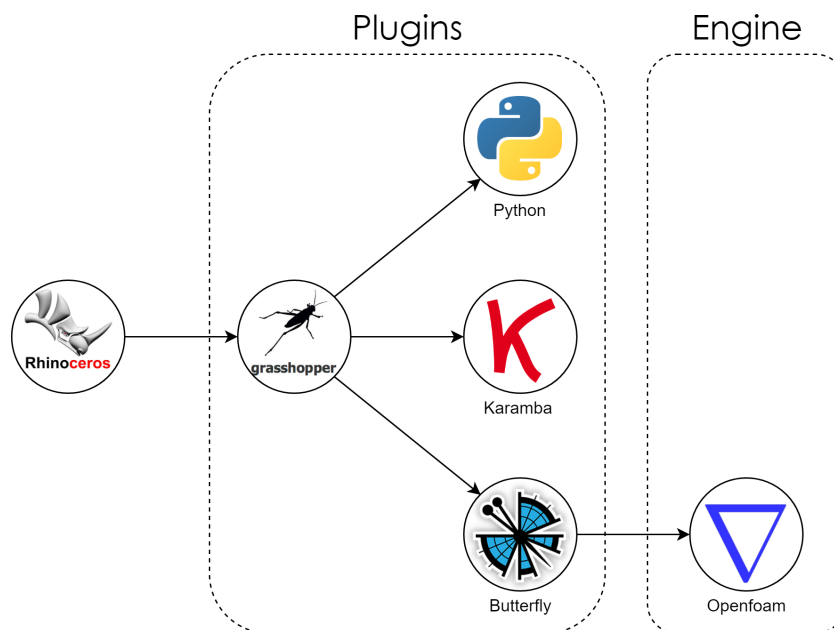


Figure 2.1: Overview the most important tools which are used in this thesis

Karamba and GSA

For the structural calculations, two programs are used. Firstly, Karamba is used for the iterative calculations and exploration of the design space. The results of Karamba are less reliable than a software package like GSA³. Therefore only the iterative calculations are done in Karamba and later on verified with GSA. Not all solutions are verified; only the best performing designs are checked with GSA.

Python

Python needs some further explanation because it is different from the other plugins. Python, C# and Visual Basic .NET are all programming languages which can be executed within Grasshopper. Most Grasshopper users never use it because the diversity of Grasshopper makes these plugins more or less obsolete, but some things can only be done with these scripting components.

For this thesis >500 CFD analyses have been done to optimise the shape of a building. Normally, to do a CFD analysis, several actions must be performed to do an analysis. In Butterfly many of these processes are automated but still only one building can be analysed at a time. To start a new analysis human interaction is needed. It took much effort to automate these clicks to let Butterfly run continuously. This was not possible without a scripting component like Python. Appendix A discusses the solution for this problem more thoroughly.

Butterfly: notes for future research

In this section, some guidelines will be given for future research. In this thesis, low-rise buildings are analysed with a height of around 15 m. The CFD computations are heavy and time-consuming even for a low-rise building. Ideally, the residual values are 1.0×10^{-5} or lower, but to speed up the process 1.0×10^{-4} is accepted. These "draft" calculation are used to do a variation study, and a calculation takes roughly 3-5 hours. For the structural analysis, the limit is set to 1.0×10^{-5} , and such a calculation takes 10-24 hours.

Butterfly recomputes the canvas at certain intervals, which influences everything inside the canvas. Ideally, Butterfly works in its own grasshopper environment, so the generation of the geometry and structural calculations run in a different grasshopper environment. This can be accomplished by running grasshopper on two different PCs and let them communicate over the network by JSON-files or Excel-files. An example of an

³GSA version 8.7 is used

Excel-file to communicate is given in Table 2.1. Each row is one simulation where the last column refers to a Rhino file containing the geometry of the facade. The other columns describe the settings which will be loaded to the panels in Butterfly, see Figure 2.2. The settings will be loaded to a panel with a Python script which can be found in Appendix A Section A.1. When all the settings are loaded, the Butterfly simulation will run. After the run, the following model will be simulated by reading the next row and loaded the information to Butterfly. The simulations will stop when all the rows are read.

| refineLevels_ | Windspeed | _landscape_ | _Rotation | _Building |
|----------------------|------------------|--------------------|------------------|---|
| (7,10) | 15 | 1 | 65 | ff4563cce5cec3470d011ab865a4e607_mijn.3dm |
| (7,10) | 15 | 1 | 65 | a36532cbd85dea58da5ec9170da153da_mijn.3dm |
| (7,10) | 15 | 1 | 65 | 324c00d093b0379c542b6059dda3cc6c_mijn.3dm |
| (7,10) | 15 | 1 | 65 | 4c62433ce922a41f87f0a1dab6c7514f_mijn.3dm |
| (7,10) | 15 | 1 | 65 | 0e2f5aeb11bdf058ce5b02621b730b1d_mijn.3dm |
| (8,10) | 15 | 1 | 65 | 41be4a198c368c00d35c4a13db9d59be_mijn.3dm |
| (8,10) | 15 | 1 | 65 | c19a042d45793afb0457ee1a09f9ed42_mijn.3dm |
| (8,10) | 15 | 1 | 65 | 41ab4d3dbac459cc031fe2d3a3eeaa2d_mijn.3dm |
| (8,10) | 15 | 1 | 65 | 541ff706f84e27f3877a2fbd3d0af736_mijn.3dm |

Table 2.1: Example of an excel file to communicate between two grasshopper files.

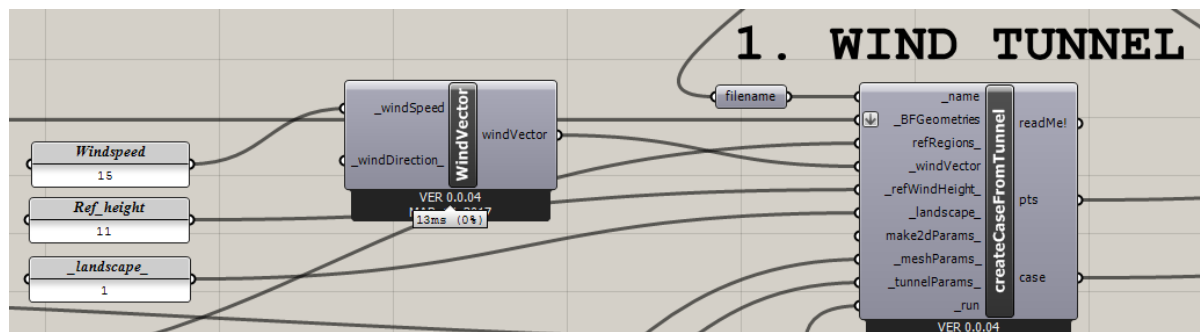


Figure 2.2: These three panels adjust the properties of the wind they are altered before running the simulation

Lastly, CFD models require a lot of memory. For this thesis, a computer with 32GB of ram is used, which was not superfluous. It is important to note that the required amount of memory is linked to the number of cells, as a rule of thumb 1×10^6 cells require 1GB of ram. Besides that, the computational domain is linked to the height. If the height doubles the computational domain will almost double as well, see Section 3.3.1 for more details. Besides that, also storage-space is required; in the end, 1.6 TB is required to store roughly 500 simulations.

Other tools

The tools mentioned above are not the only tools which are used. Many grasshopper plugins are used, but their contribution is smaller, examples of them are Colibri, Galapagos and Kangaroo. Those plugins will be mentioned in the text and get a brief introduction together with an example. Also, Paraview is used to post process and visualise the results from Butterfly and DesignExplorer is also for visualisation.

2.3. Optimisation in general

Optimization is the process or procedure in which an object is made as perfect, functional or effective as possible. This object can be a design, a system or a decision. In the context of science (mathematics, statistics and other sciences), optimization means finding the best solution for a problem from a given set of alternatives. In the context of building performance simulation (BPS), optimization does not always mean finding the most optimal solution for a given problem [18]. The optimal solution might be impossible as a consequence of the

nature of the problem [19] or the simulation program itself [19]. Therefore the simulation-based optimization community uses the term optimization for an automated process which is completely based on numerical simulation and mathematical optimization [18]. This process is automated in a conventional building optimization study by the coupling between a building simulation program and one or several algorithms or strategies which form the 'optimization engine' [18]. In Figure 2.3 a summary is given of the most representative strategy of simulation-based optimization.

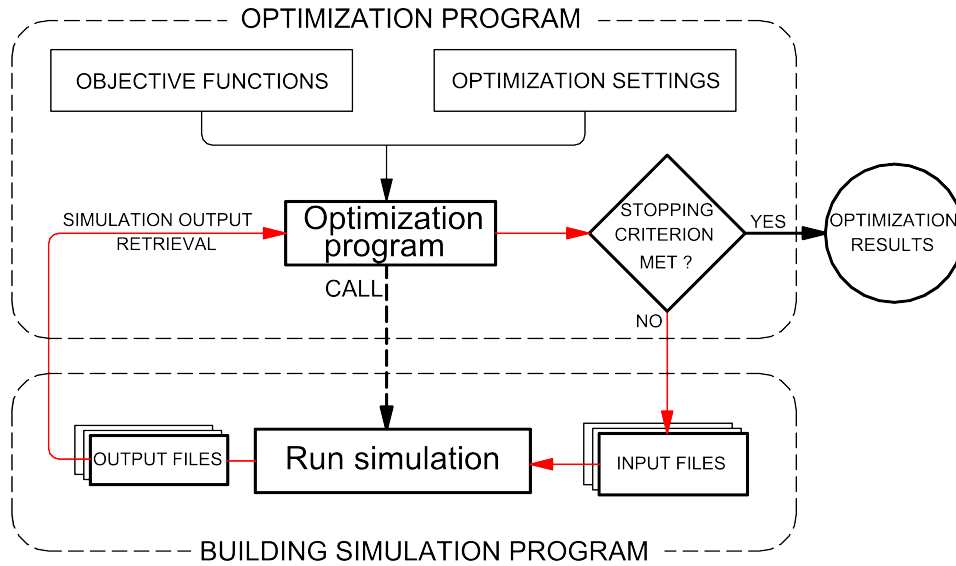


Figure 2.3: The most general strategy of simulation-based optimisation in building engineering studies [18]

2.4. Structural optimisation

In this paragraph, x will represent a geometric feature of a structure, like thickness or the position of a beam. Depending on the geometric feature, there are three types of structural optimisation problems, see Figure 2.4.

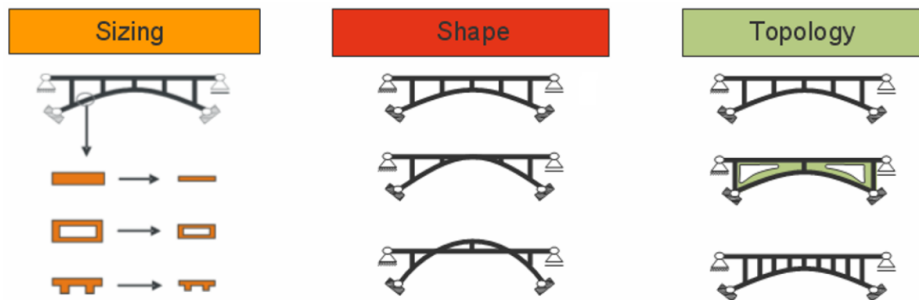


Figure 2.4: The three structural optimisation types [20]

Sizing optimisation

When x represents a kind of structural thickness, a sizing optimisation problem is formulated. The cross-sectional areas of truss members can be optimised, or the thickness distribution of a sheet. [15]

Shape optimisation

With a shape optimisation problem, x represents the form or contour of some part of the boundary of the structural domain. For example a solid body, which state is described by a set of partial differential equations. The optimisation process chooses the integration domain for the differential equations in an optimal way. It should be noted that the shape optimisation does not change the connectivity of the structure: there are no new boundaries formed. [15]

Topology optimisation

The last form of structural optimisation is topology optimisation, which is the most general form of structural optimisation. This form of optimisation will be clarified by a discrete case, by a two-dimensional continuum-type structure and a three-dimensional case. When performing a discrete case optimisation, like a truss, it is achieved by taking cross-sectional areas as design variables. These variables are allowed to take the value zero, thus removing the bars from the truss. This means that the topology of the truss changes, since the connectivity of the nodes is variable. [15]

An example of a continuum type structure is a two-dimensional sheet. When the thickness of the sheet takes the value zero, topology changes can be achieved. When other features are disregarding, the optimal thickness takes the value zero or a maximum sheet thickness. When using the topology optimisation for a three-dimensional case, the optimal thickness can be achieved by letting x be a density-like variable that can only take the values 0 and 1. [15]

The different forms of optimisation have similarities in practical or theoretical respects. Shape optimisation is, in ideal form, a subclass of topology optimisation, but they are based on very different techniques. Therefore they are treated separately. On the other hand sizing and topology optimisation are, from a fundamental point of view very different, but are practically close related. [15]

2.5. Genetic algorithms

A search technique based on the principles of natural evolution is the Genetic Algorithm (GA). It is based on operators which are analogues of the evolutionary processes of mating, mutation and natural selection to explore multi-dimensional parameter spaces.

The Genetic Algorithm can be used for each problem where the variables ('genes') which need to be optimised and can be coded to form a string ('chromosome'). Each string formed represents a possible solution to the problem. The values of the individual variables can be called 'alleles', just like in biology. A string of variables forms the chromosome, or individual, see Figure 2.5. In GA a group or population of individuals evolves for a certain amount of generations. This can be fixed in advance or can depend on a convergence criterion. [21]

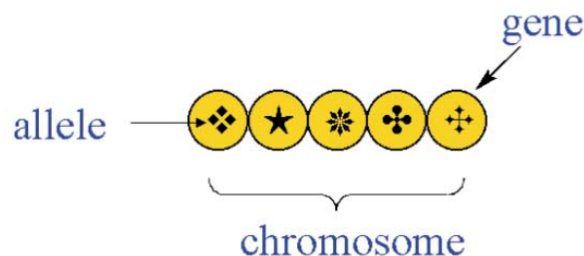


Figure 2.5: Schematisation of an individual or chromosome in a genetic optimisation. The individual represents a chromosome of string of variables [21]

The starting set of individuals which will be evolved by the GA is called the initial population. This population can be created random, but it can be wise to use any available prior knowledge although it should be prevented to bias the research too much [21].

When optimising a function the quality of the trial solution can be expressed as 'fitness'. This is the quality of the string which represents the trial solution. A high fitness thus means a high value (maximising problem) or a low value (minimising problem). When the upper or lower limit of the function to be optimised is known, absolute fitness can be used. If the upper or lower limit is unknown, dynamic fitness scaling can be used. For each generation, the highest or lowest values of individuals are scaled relative to the highest or lowest values of the current population. Fitness is an important measure when determining the probability of an individual taking part in a crossover and in determining which individuals will survive in the next generation. [21]

Choosing individual members of the population for the subsequent crossover is called selection. There are different selection methods, of which roulette wheel and tournament selection are most popular. The roulette

wheel chooses individuals randomly and selects them for crossover if the fitness value is greater than a randomly generated number between 0 and 1. If the fitness value is lower than the generated number, the selection starts again, and a new individual is chosen. [21]

The tournament selection method chooses a couple of random strings from the population to form a tournament pool. The two strings with the highest fitness values are designated as the parents of this pool. [21]

How the 'genetic information' of two or more parents is combined and generates offspring, is called crossover. There are two commonly used forms of crossover: one-point and two-point. With the first form, the parents are cut at the same point, and the offspring are formed by combining the complementary parts (genes) of both parents. With the second form (two-point crossover), the parents are cut at two points. The offspring is formed by combining the centre genes of the first parent into the second parent and vice versa. Another example of crossover is uniform offspring. With this form of crossover, the offspring is formed by combining a number of genes from each parent, regardless of where these genes originally occurred in the string. [21]

Since crossover is formed by mixing the genetic material and not by adding new material, it can lead to a lack of population diversity or end in stagnation. This means that the population can converge to a non-optimal solution. Therefore the GA mutation operator introduces new genetic material and helps to increase the diversity. The mutation can be accomplished by making a random change in one or more random genes of an individual. If a completely random value causes the change of the mutated gene, it is called static mutation. On the other hand, if the value of the mutated gene is changed by a small random amount of the original value it is called dynamic mutation. [21]

Survival of the fittest is with the concept of natural selection an important evolutionary driving force. Although the selection in a GA is not natural, the individuals who will survive to the next generation are selected on the bases of their fitness value. In this selection procedure, there are different variations on the selection step. For example, all mutants can be accepted, none of the parents or only the best parents. The last variation is also called the 'elitist' strategy and prevents that the best of each population gets worse over the next generations. [21]

The GA approach can operate effectively in a parallel manner. This means that many different regions of the design space are investigated simultaneously. On top of that, the crossover procedure actively passes information of different regions of parameter space between individual strings. This takes care of the information distribution across the entire population. The GA is an intelligent search mechanism and can learn which regions of the search space represent good solutions, though the recognition of schemata. A schema is a common building block between different strings. For example when there are three strings of 7 variables with a common variable on position 2 and 4. The schema exists of the variables on position 2 and 4, see Figure 2.6.

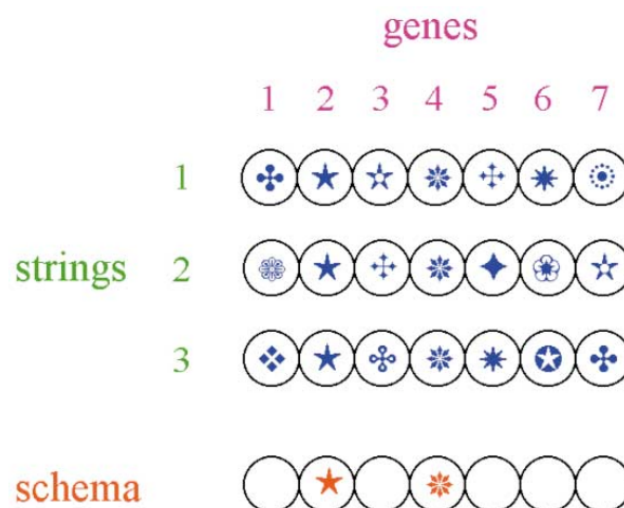


Figure 2.6: Visualisation of schemata or building blocks in GA [21]

3

Wind engineering

Before answering the research question, some background information is needed to perform a CFD analysis. The required background information is given in this chapter. The first section is about wind in the atmospheric boundary layer. The wind velocity profile is an essential input for the CFD analysis. The second section addresses the CFD basics like defining the domain and building a mesh to perform a CFD analysis. The following step is to define the wind tunnel configuration which has agreements with an actual wind tunnel. Lastly, an overview of existing research is given. The existing research will be used to validate the CFD set-up.

3.1. Atmospheric boundary layer

3.1.1. Source of the wind

The source of energy in the atmosphere is solar radiation. This solar energy heats the Earth's surface more at the equator than at the poles. These different air temperatures cause rising and descending air particles, eventually leading to high and low-pressure zones. Since gaseous substances flow from high to low-pressure zones, the air moves from the high-pressure zones to the low-pressure zones. This generates several global flows, resulting in a global circulation of the air. Besides this, instabilities in the global circulation, assisted by local temperature differences and the earth rotations, transfer energy into the weather systems. [22]

3.1.2. Velocity profile

The wind speed is not only influenced by the solar energy and high/low-pressure fields, but also by the surface and obstacles near the surface. This causes the wind speed to decrease from gradient velocity at gradient height to zero at the Earth's surface, and this is shown in Figure 3.1. This phenomenon occurs in the atmospheric layer called 'Atmospheric Boundary Layer'. [22]

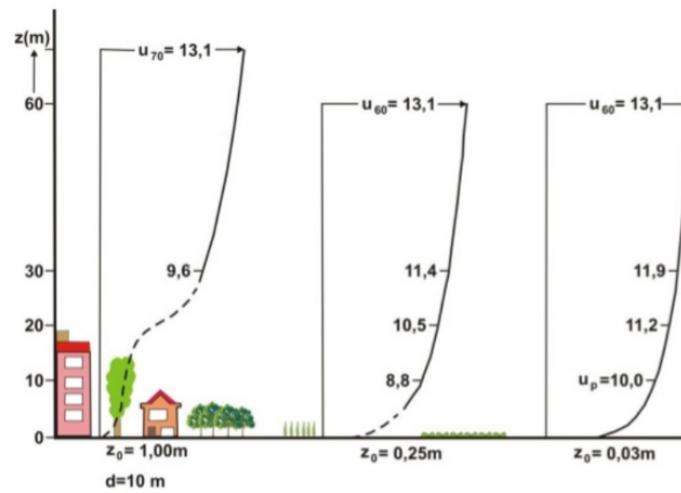


Figure 3.1: Different characteristic wind profiles varying by surface roughness [23]

When the surface has a certain roughness the flow of the wind is brought to rest at the surface due to friction, while the flow at higher levels is hardly affected. A higher roughness results in a larger boundary level, more turbulence, more mixing of layers, a lower velocity near the surface and a slower approach to the constant velocity in the atmospheric boundary layer.

To describe the profile of the wind, the log law (equation 3.1 [24]) and the power law (equation 3.2 [25]) can be used. In the Netherlands, the log is used which is more accurate. The log law uses the surface roughness (z_0), friction velocity (U^*), the height (h), the zero-plane displacement (z_g) and the Von Karman constant ($\kappa = 0.41$). The zero plane displacement corresponds to the average height of buildings.

$$U(z) = \frac{U^*}{\kappa} \cdot \ln\left(\frac{z - z_g + z_0}{z_0}\right) \quad \text{with} \quad U^* = \kappa \frac{U_{ref}}{\ln\left(\frac{z_{ref} + z_0}{z_0}\right)} \quad (3.1)$$

$$U(z) = U(z_{ref}) \cdot \left(\frac{z - d_0}{z_{ref} - d_0}\right)^\alpha \quad (3.2)$$

It is assumed that the velocity profile starts from the average height of the buildings and shifts up. This does not mean that there is no flow of wind between the ground and the average roof height. However, since this flow is in arbitrary directions, canalized by the buildings, the net flow is assumed to be zero. Depending

on the surface, it can be classified as aerodynamically smooth or rough. The Earth is always classified as aerodynamically rough instead of aerodynamically smooth, because of the large sizes of rough elements, for example, fences, hedges, trees and buildings. The surface roughness according to Butterfly is shown in table 3.1.

| Case | Surface roughness [m] | Description |
|------|-----------------------|---|
| 0 | 0.0002 | Open sea |
| 1 | 0.005 | Smooth: featureless land surface |
| 2 | 0.03 | Open: country with low vegetation |
| 3 | 0.1 | Roughly: open or moderately open country |
| 4 | 0.25 | Rough: cultivated or natural area with high crops or crops of varying height |
| 5 | 0.5 | Very rough: intensively cultivated landscape with many rather large obstacles |
| 6 | 1.0 | Skimming: Landscape regularly covered with similar-size large obstacles. |
| 7 | 2.0 | Chaotic: City centres with mixture of low-rise and high-rise buildings |

Table 3.1: Surface roughness according to Butterfly

3.2. CFD basics

OpenFOAM does all the processes like discretisation and building a mesh. These processes will be discussed briefly.

3.2.1. Discretisation

A representative wind velocity is translated into a representative pressure on (a part of) a structure, similar as with the wind tunnel. These pressures induce a mechanical response of the structure, which is checked based on different criteria. When these criteria are met, the structure meets the requirements regarding wind load. To determine this wind load on structures, Computational Fluid Dynamics can be used. This method uses numerics to determine the flow of a fluid in a set domain, where the Navier-Stokes equations define the behaviour of the fluid. These equations are derived from the findings of Newton and Euler concerning three conservation rules: conservation of mass, energy and momentum. [22]

The Navier-Stokes equations can be used to calculate values like wind speed and pressure for an infinite amount of entries. In other words, these equations are continuous. To use a computer for these calculations, they need to be described as discrete equations. A discrete equation is an equation which provides values for a finite amount of positions in space. The process of transforming a continuous equation to a discrete equation is called discretisation.[22]

When using the Navier-Stokes equations for the building in this thesis, it is necessary to discretise a part of the continuous space around the building, namely the computational domain. The computational domain is spatially discretised, and the Navier-Stokes equations are numerically discretised. In other words, the computational domain is divided into a finite amount of points, elements or volumes. Each of those points, elements or volumes are solved with a known set of initial equations and boundary conditions. [22]

3.2.2. Defining domain

The airflow near a structure interacts with the structure. To determine the flows and the wind loading, the area should be determined in which the flow is affected by the presence of the structure. This area around the structure is often used as a computational domain. On the edge of the affected area, the boundary conditions are set.

3.2.3. Building mesh

Regardless of the method, the computational domain is subdivided into a finite amount of elements, points or volumes. These points are used to build a mesh or grid, dependent on the discretisation method. Besides the discretisation method, other elements influence the building mesh. For example, the computational costs of the mesh, the features of the modelled flow and the topology of the mesh can influence the building mesh.[22]

All numerical methods assume that the flow variables change between the points or within an element or volume. This variation is often assumed to be linear, but non-linear variations are also possible. When designing a mesh, the simulation must be able to take flow features into account. For example, when the gradients of the variables are high, the mesh has to fulfil different requirements than at places where no gradients occur. Therefore a large number of grid points is necessary at critical regions to describe the process accurately. This leads to a fine grid in critical regions.[22]

3.2.4. Mesh Structures

There are different discretising methods, which all use different types of meshes. These different types of meshes can be constructed out of points or nodes, volumes or cells and elements, depending on the method used. The most widely used discretising method in CFD is the Finite Volume Method (FVM). With this method, the spatial domain is discretised into small cells which form a grid or mesh. Then the equations for all cells are solved using a suitable algorithm.

During the process of mesh creation, the used elements are structured in a specific way. This is known as the structure or topology of the mesh. There are three different structures or topologies. The first structure is the regular one, which can be used to be manipulated into several other geometries. These other geometries are called structured meshes. The second possibility is irregular structures, which are qualified as unstructured meshes. The points of these meshes are not structured in a specific way. Lastly, a mesh can be formed out of structured and unstructured parts. This form of meshes is called a hybrid grid or multi-block mesh. [22]

3.2.5. Stability and convergence

When solving a numerical problem with an approximation, it is important to determine when the solution is adequate. To increase accuracy, the solution might require a large number of repetitions. Therefore convergence and stability are two important concepts regarding the number of iterations. Convergence is the ability of a set of numerical equations to represent the numerical solution if this solution exists. When the iterations tend to infinity, the solution is said to converge. When that happens, the numerical solution tends to the analytical solution. Stability means that the equations move towards a converged solution while proceeding the numerical process will not swamp the results by errors in the discrete solution.

When there is no analytical solution to compare the numerical solution with, as with most physical CFD problems, convergence is defined as the process when the values of the variables at each point in the domain tend to move towards fixed values as the solution progresses [22].

3.3. Wind tunnel configuration

3.3.1. Computational domain

For the overall dimensions of the computational domain, the guideline of Franke [26] has been used. The guideline defines the computational domain based on the height of the building, see Figure 3.2. Different structures are tested, and the height of the building varies per design, therefore the computational domain changes as well. In one of the designs, the building has a height of 15 m. In this case, the computational domain is around $330 \times 195 \times 105 \text{ m}^3 = L \cdot B \cdot H$. The height the domain is chosen so that the influence of the building above the domain is negligible.

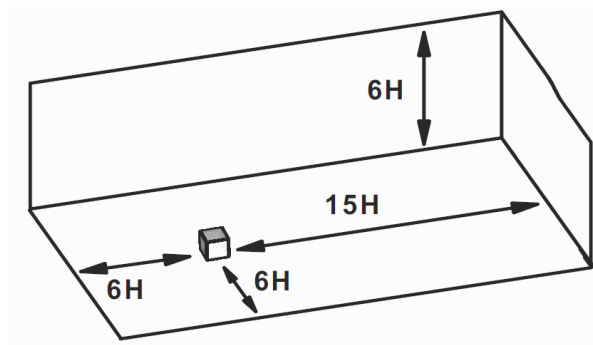


Figure 3.2: Computational domains for the flow simulation [26]

3.3.2. Boundary conditions

Similar to a physical wind tunnel, the boundary conditions determine the behaviour of the wind, the boundary conditions are shown in Figure 3.3. OpenFOAM is free and opensource which gives the user many possibilities to customize the settings. In this thesis, the default values for an outdoor wind simulation will be used. The behaviour of the wind speed concerning the boundary conditions will be discussed to illustrate the importance of proper boundary conditions. The sidewalls of a physical wind tunnel must have a small resistance in OpenFOAM; this is defined as slip. To the contrary, at the ground and the facade, the wind speed is defined with a fixed value of 0 m/s. In reality, the wind speed at the facade is also approximately zero but only very close to the facade.

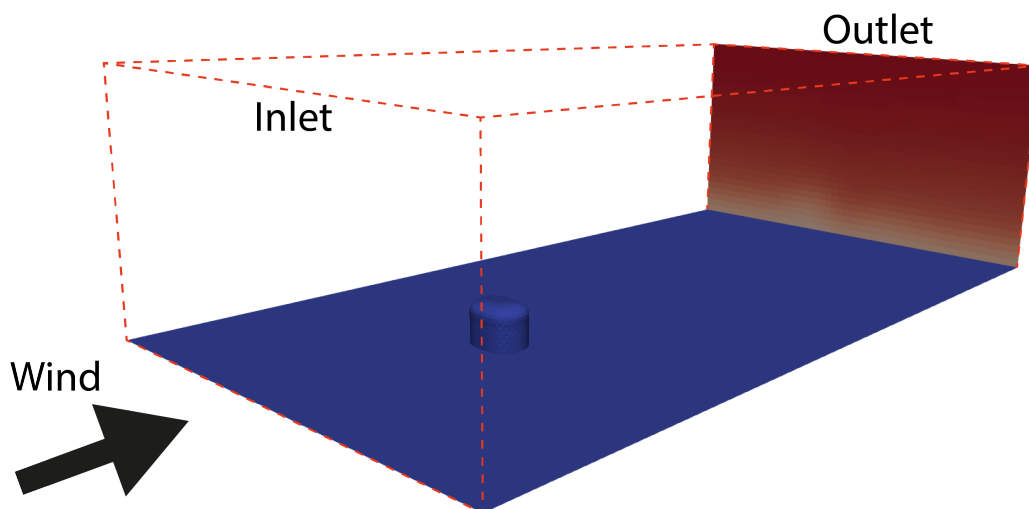


Figure 3.3: Visualization of the digital wind tunnel, the blue areas indicate the positions where the windspeed is zero.

3.3.3. Inlet and outlet

The inlet and outlet are indicated in Figure 3.3. The inlet must match the outdoor environment as good as possible including the wind profile over height. The velocity profile is already discussed in paragraph 3.1.2 and can be described with the Expression 3.1. To avoid mistakes, it is good to test if the given velocity profile matches the output. In Figure 3.4a the velocity profile is defined with Expression 3.1 where $z_0 = 0.01$ m and $U_{ref} = 15$ m/s and $Z_{ref} = 10$ m. The log law matches the data in the cells at the inlet, but at the outlet the velocity profile is different. The building in the wind tunnel influences the velocity profile in such a way that at the outlet the wind speed below 30 m has decreased and the wind speed above 30 m has increased. At the top of the wind tunnel, at 105 m, the wind speed is not influenced, after all the variance in wind speed above

the domain must be neglectable. This behaviour is identical to the behaviour seen in the paper of Hunte [22], see Figure 3.4b.

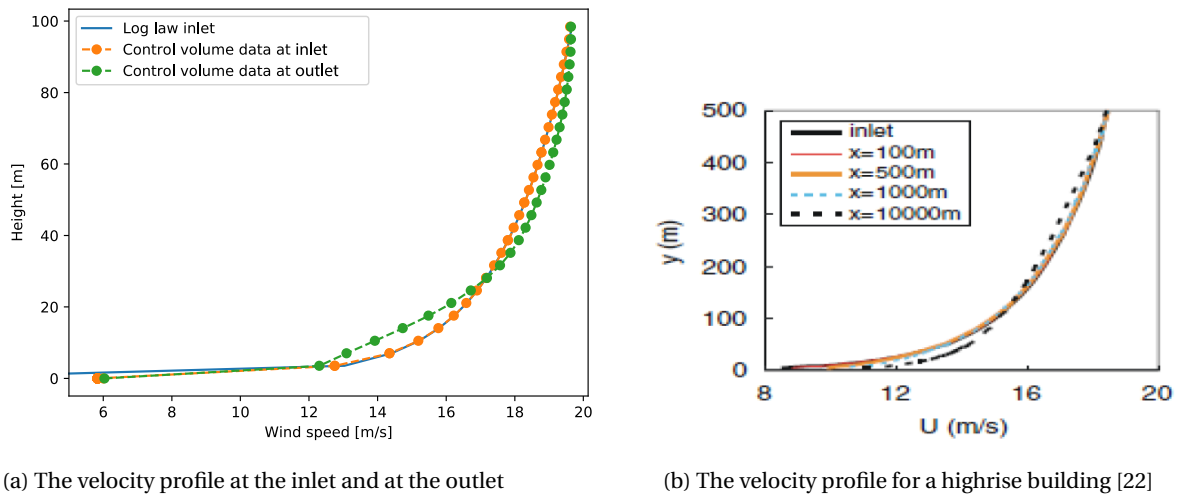


Figure 3.4: Velocity profiles for two different test [27]

3.3.4. Cp-values

The formula for Cp-value is Equation 3.3 [28], where p is the pressure at the facade, p_0 is the static pressure and U_h is the wind speed at the building height. The cp-values are important to calculate the forces on the structure but also to compare different CFD analyses. Cp-values are independent of the wind speed which makes it possible to compare wind analyses with different wind speeds. The reason for this is that p increases quadratically when the wind speed increases, by dividing by U_h^2 a dimensionless factor is calculated. This is tested by comparing two CFD analyses, see Figure 3.5. The surface roughness used in the analyses is 0.01 m when the surface roughness is higher; the results can differ.

$$C_p = \frac{p_{wi} - p_0}{0.5 \cdot \rho \cdot U_h^2} \quad (3.3)$$

- p_{wi} is the pressure at the facade, calculated with the CFD analysis in Butterfly.
- p_0 is the static pressure, close to 0 pa in most analyses
- $\rho = 1.225 \text{ kg/m}^3$, the density air
- U_h is the windspeed at the building height, can be determined by reading the windspeed at the inlet (Section 3.3.3) or calculate the windspeed with the log law (Equation 3.1)

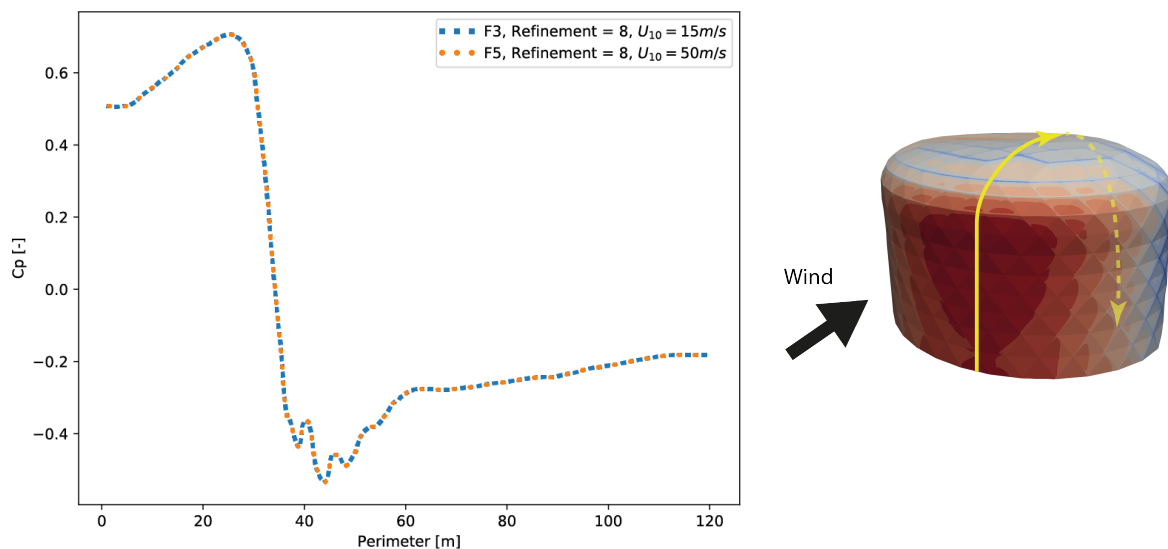


Figure 3.5: The cp-values around the facade following the yellow line starting from the base of the structure

3.4. Retrospect of existing research

3.4.1. Experimental research

Doing a wind-tunnel test is expensive and out of the scope of this thesis. A good alternative is to compare the CFD models with current research. Many researchers have validated their CFD models with experiments, mostly standard buildings. An example of such a standard (tall) building is the CAARC building (Commonwealth Advisory Aeronautical Research Council). This is a well-acknowledged model to validate and calibrate CFD models [29]. Because this thesis focuses on low-rise buildings, a standard cube of 6m (Silsoe cube) will be used to validate the CFD model. Multiple researchers tested a scale model of the 6m cube like Lim et al. [28] and Wright and Easom [30] but also a full-scale model of the 6m cube is tested by Richards et al. [31]. It is important to note that full-scale models often are considered as true results. A full-scale model is not vulnerable to scaling errors, but it is still difficult to control the flow conditions like the reference pressure and thermal stratification which will obscure the data. The error of the measurements of a well-conditioned wind-tunnel test will probably be smaller than for a full-scale model [25].

The mean pressure coefficients are determined at the facade at different locations, and these locations follow the line from A to D, see Figure 3.6. The values are correlated especially at the windward and leeward side when the roof shows more variance. Only experiments with the same boundary conditions are compared. A few characteristics of the different cases are shown in 3.2. Because of the scaling differences, a comparison of the surface roughness is not correct. Indirectly the surface roughness can be compared with the Jensen number, $Je = h/z_0$ [28]. If the Jensen number is 600 and the cube is 6 m then the surface roughness (z_0) is 0.01 m.

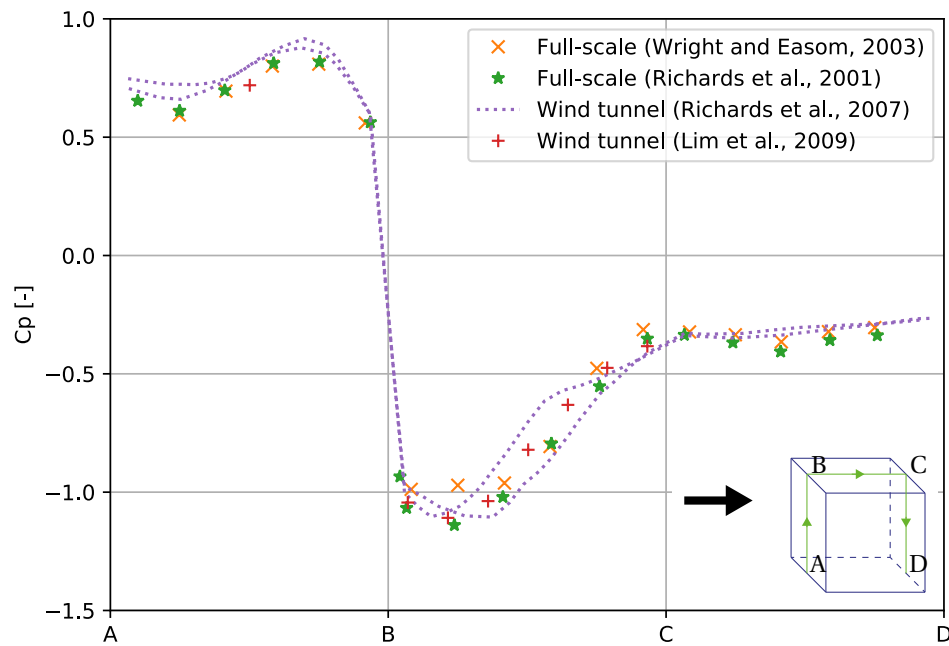


Figure 3.6: Comparison of mean pressure coefficients of several experimental results

| Test | Cube dimensions [m] | Jenson number | Windspeed [m/s] |
|----------------------------------|---------------------|---------------|-----------------|
| Full-scale Wright and Easom [30] | 6 x 6 x 6 | 600 | 10 |
| Full-scale Richards et al. [31] | 6 x 6 x 6 | 600–1000 | 9.52 |
| Wind tunnel Richards et al. [32] | 0.15 x 0.15 x 0.15 | 600–1000 | 6.4 |
| Wind tunnel Lim et al. [28] | 0.08 x 0.08 x 0.08 | 600 | - |

Table 3.2: Characteristics existing research

3.4.2. Theoretical research

All the researchers mentioned in Table 3.2 have presented the results of their CFD model besides the experimental results. The input parameters of the CFD models are identical to the experimental research (Table 3.2). In Figure 3.7 the CFD models and experimental results can be compared. The grey area contains the experimental results which are shown previously (Figure 3.6). The CFD models are not in full compliance with the experimental results. Especially at the roof, the results deviate, and at most other locations the CFD models underestimate the situation. At location B, both on the windward side and the roof, the CFD models show higher values than the experimental results. The most accurate CFD model is the LES model, but more computer power is needed for such an analysis [28]. Therefore the LES-model will not be used in this thesis.

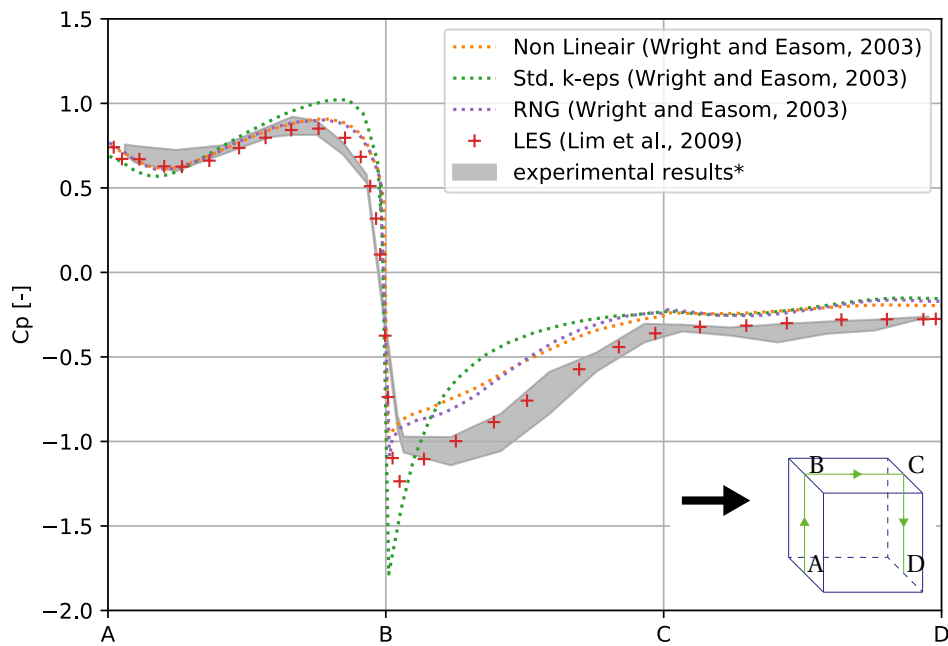


Figure 3.7: Comparison of mean pressure coefficients of several CFD model
 * Wright and Easom [30], Richards et al. [31], Lim et al. [28]

In Section 6.2 the literature will be compared with the CFD models made by Butterfly. The results from Butterfly are used for the structural optimisation and the ventilation concept.

3.5. Wind availability

When designing a ventilation system, it is important to know how much wind there is available. The KNMI has several weather stations in the Netherlands and measures weather data like wind speed (at 10m height), wind direction and temperature. The weather station closest to Delft is station 344 Rotterdam (51.962N, 4.447E). The station is positioned in an open area near an airfield. To use the data the wind speeds in the open country must be converted to the wind speeds in the city. This can be accomplished with equation 3.4, where U_{met} is the measured wind speed at 10m height in open country, k and a are defined in table 3.3 and z is the height above ground [33].

$$U = U_{met} \cdot k \cdot z^a \tag{3.4}$$

| Terrain | k | a |
|------------------------------------|------|------|
| Open flat country | 0.68 | 0.17 |
| Country with scattered wind breaks | 0.52 | 0.2 |
| Urban | 0.35 | 0.25 |
| City | 0.21 | 0.33 |

Table 3.3: Terrain coefficients [33]

The function of the building determines which time window is most interesting. For an office building, the most important time is during working hours when the building is occupied. Because the case considered in part II Design is an office building, a time window between 7:00 and 19:00 will be checked. A histogram

of the wind speed U_{met} from 2000 until 2017 is displayed in Figure 3.8. It is harder to do calculations with the histogram directly, and therefore the Weibull function is used to fit the data. Expression 3.5 is used with a shape parameter k and scale parameter λ [34], the results are shown in Figure 3.8.

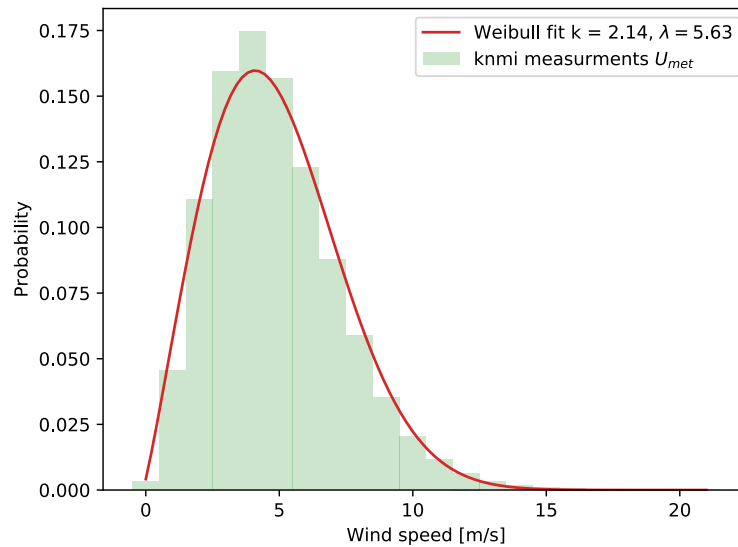


Figure 3.8: The probability density function and histogram of the meteorological wind speed (station 344 Rotterdam) from 01-01-2000 until 31-12-2017, only measurements between 7:00 and 19:00 are included

$$f(x, \lambda, k) = \begin{cases} \frac{k}{\lambda} \cdot \left(\frac{x}{\lambda}\right)^{k-1} \cdot e^{-(x/\lambda)^k} & x \geq 0 \\ 0 & x < 0 \end{cases} \quad (3.5)$$

When the probability density function (PDF) is known the cumulative density function (CDF) can be calculated. With the PDF one can determine the chance that a specific wind speed occurs when a CDF accumulates all of the probability less than or equal to a specific wind speed. The latter is more interesting when designing the ventilation system. In Figure 3.9 the cumulative density function of the meteorological wind speeds is shown. As an example, when a ventilation system must work 80% of the time, the system must perform with wind speeds of 2.77 m/s and higher. To calculate the wind speed required in the city expression 3.4 can be used [33].

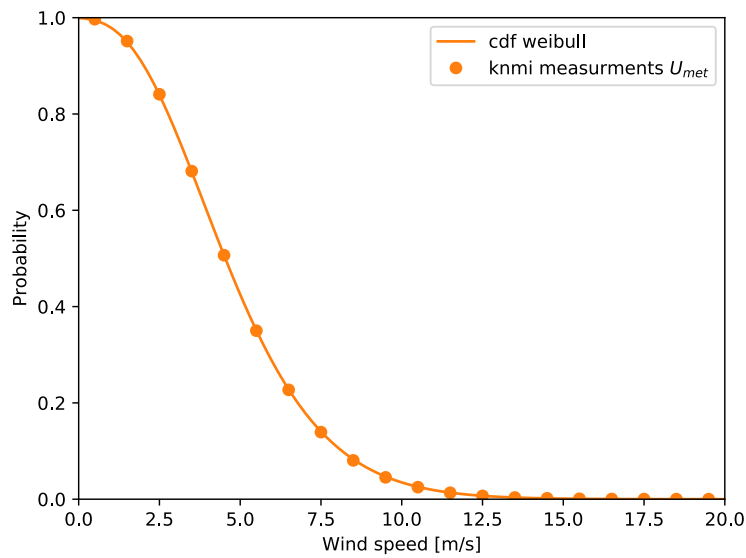


Figure 3.9: The reversed cumulative density function of the meteorological wind speeds (station 344 Rotterdam), only measurements between 7:00 and 19:00 are included

The wind direction is also important. In Rotterdam the dominant wind direction is southwest, see Figure 3.10. The diagram represents 30 years of weather data measured at a weather station in Rotterdam (51.9225N 4.47917E) [35].

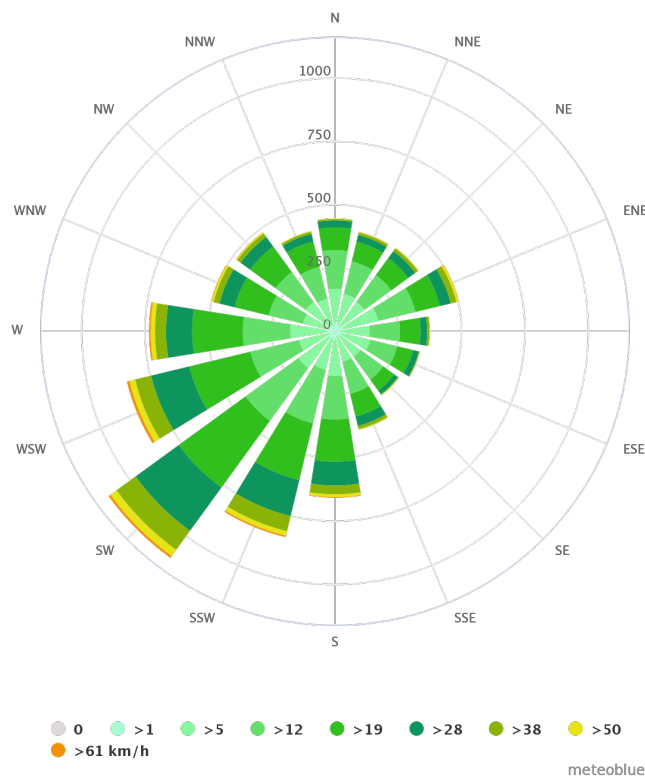


Figure 3.10: Windrose of Rotterdam (51.9225N 4.47917E) based on 30 years of weather data [35]

4

Structure

One aspect of the thesis is to minimise material usage. A structural calculation is needed to determine the material usage, and a structural calculation is bound to many design decisions. This chapter substantiates some of these design decisions needed for the structural calculation. In the first section, existing gridshells will be reviewed. If the elements like supports, nodes and material are applicable they are used in Part II The Design. The second section gives some extra information about the nodes because they have a big influence on structural behaviour. Lastly, maintenance will be discussed.

4.1. Survey of freeform gridshells

Looking at different gridshells over time, different innovative buildings can be distinguished. Four gridshells will be discussed which are performing well in terms of buildability.

Mannheim Multihalle (1975) – Post-formed wooden gridshell

The Mannheim Multihalle is an innovative and very successful building. One of the things that makes this structure interesting is the erection scheme. Steel gridshells with thousands of elements are common where this structure is made out of a wooden lattice mat, see Figure 5a. This mat is constructed at ground level and pushed into the final position. A physical form finding process defines the final shape. When the lattice was in position, the connections were tightened to give the surface its stiffness. The untightened connection had a lot of deformation capacity due to the slotted hole, see Figure 4.1b.

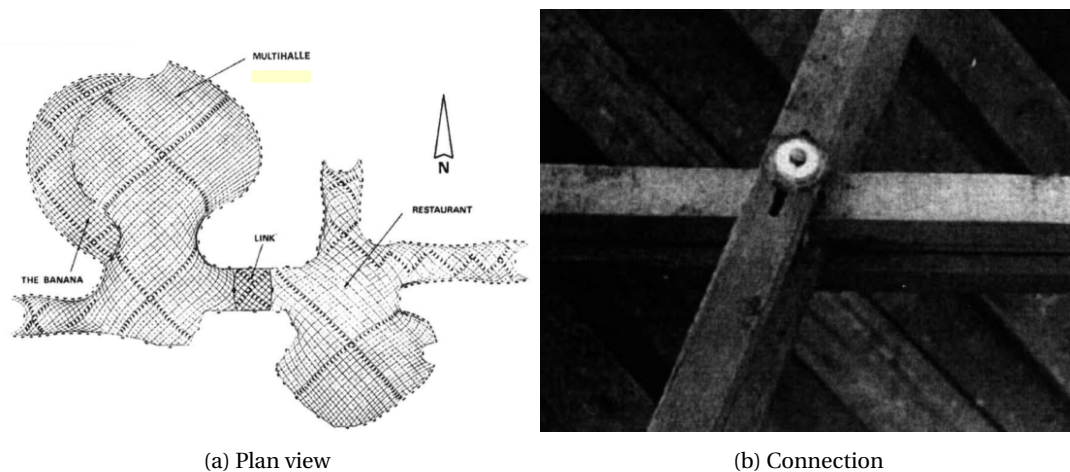


Figure 4.1: Mannheim Multihalle [27]

The drawback of a wooden gridshell is the limited capacity. The Multihalle was covered with a lightweight membrane to reach large spans. To reach the same span with glass panels a stiffer material like steel must be used.

Helsinki zoo observatory – Semi post-formed wooden gridshell

This particular case is added because it is more like a facade than a roof instead of the other way around. Here the wooden pieces were bent in the factory, but to achieve the final shape they had to be bent further. [36]



Figure 4.2: Helsinki zoo observatory [36]

Yas island marina hotel - Steel gridshell

To build a large gridshell with glass panels in an active earthquake area, steel is the only suitable material. Because of the material properties, it is hard to create a post-formed gridshell so everything must be assembled as it is. A drawback of this is the massive amount of parts, especially with a large structure. Not only the amount of parts makes it difficult, but the parts are also unique, this can be seen in Figure 4.3. In the case of the Yas Island Marina hotel, the high amount of components were conveniently maintained using wireframe data. [37]

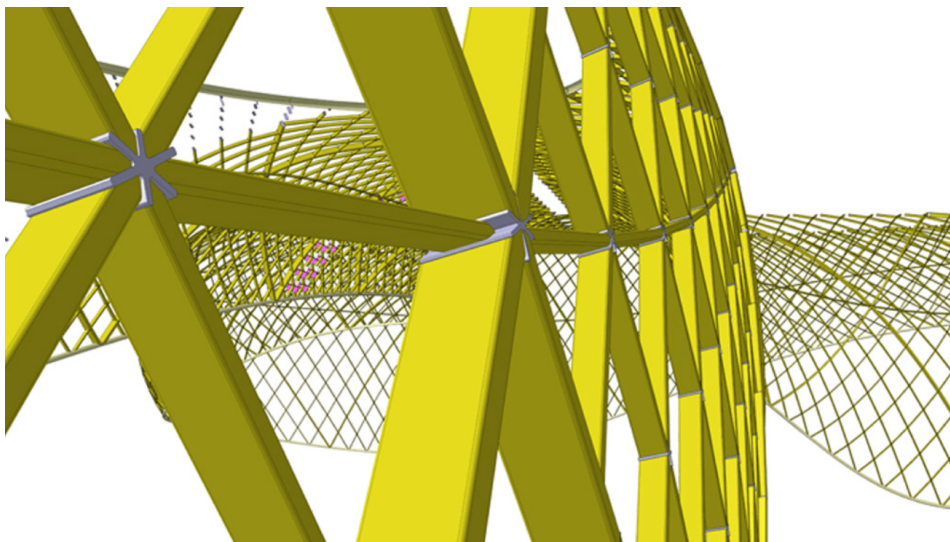


Figure 4.3: Close-up of a connection of the Yas Island Marina hotel where different beam sizes are connected via one node [37]

Museo Soumaya – Rationalisation of panels

The design intent was to create the complete facade out of one single panel. However, due to the high curvature, this was not possible. To make the structure buildable, the panels were grouped into families. Depending on the tolerance of the panels the number of families can be distinguished, see Figure 4.4 [37]



Figure 4.4: Panelisation with seven (left) and 49 families (right) [37]

4.2. Nodes

In this section three types of connections will be elaborated: welded steel nodes, 3D printed nodes and fasteners.

4.2.1. Welded node

A connection type of node in a free form structure is the welded steel node. A couple of advantages of this method are:

- design freedom: there are little limits to the number of bars and the approaching angles since all the nodes are custom made and unique
- Strength and stiffness: the strength and stiffness of the nodes are high.
- aesthetics: the nodes have a clean appearance

Besides that, there is also a disadvantage; the fabrication cost and time are high since the fabrication is labour intensive.

4.2.2. 3D printed nodes

A second connection method is the use of 3D printed nodes. This type of connection is currently in development. The main advantages of the 3D printed nodes are:

- Design Freedom: at a structural level the freedom of design is very high. On detail level, there are some limitations due to the current 3D printing techniques regarding printing angles and minimum material thickness [38].
- Strength and stiffness: the node can be completely optimised for strength and stiffness thanks to the large design freedom
- Weight: if the nodes are designed with topology optimisation, the weight of the node can decrease a lot compared to the welded steel node while retaining a similar strength and stiffness [38].
- Aesthetics: the 3D printed nodes are usually smoothly shaped, which gives these nodes a soft appearance.
- Sustainability: the node can be optimised for minimum material usage, which makes these nodes sustainable.

However, this connection method also has a couple of disadvantages:

- Simplicity: the design process of an optimised 3D printed node is complex
- Ease of fabrication: although the production of a 3D printed node requires less labour, its process is still time-consuming. This disadvantage might disappear in the future when the amount and size of 3D printers increase [38].

- Cost: the production costs are at the moment the largest disadvantage of the 3D printed nodes. This has a negative impact on the development and application of these nodes in construction.

4.2.3. Bolted connection

The third connection method is the connection with bolts. Bolted connections are necessary for post-formed structures like the Mannheim Multihalle, see 4.1a. The advantages of the bolted connection are:

- Low cost: there is almost no extra weight due for the connection
- Simple erection to tighten the bolts less expertise is needed compared to welded connections

impact on the appearance of the tim

- Strength and stiffness: the strength and stiffness of this connection method is limited
- Aesthetics: the bolts are visible, but with some effort, the number of visible bolts can be reduced

Concluding

The welded node is a good solution when high strength and stiffness is required, or a large number of bars meet at one point. However, the 3D printed nodes have, despite the potential of optimising the material usage, high costs. A bolted connection is the best option when a low amount of bars meet at one location, and a limited stiffness and strength is required. Also, this option has low costs.

4.3. Maintenance

4.3.1. Internal

In a double skin facade, the cavity is deep enough to let people enter for cleaning purposes, maintenance for example. At the level of each floor, it is possible to access the cavity via the walkway, see Figure 4.5.

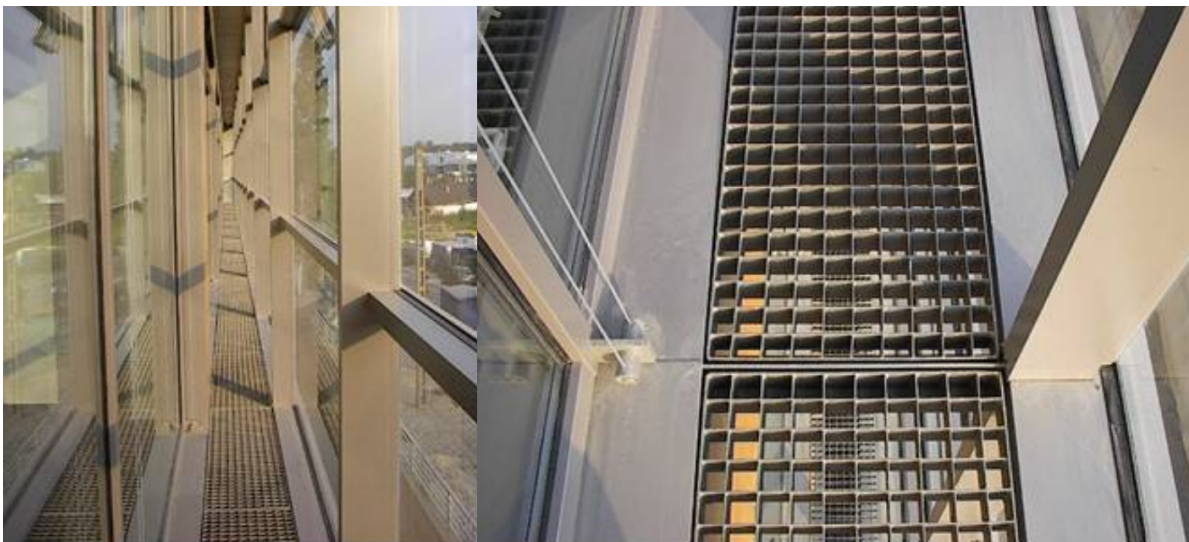


Figure 4.5: Double skin facade with walkway for cleaning purposes and grills to make natural ventilation possible [39]

4.3.2. External

Access for maintenance can be quite challenging when it is not taken into account especially for complex structures. An example where the maintenance and repair were considered at the early stage is the Gardens by the Bay [40]. Movable anchors were positioned to give maintenance workers access to places which were hard

to reach. The anchors were connected to a rail on top of the structure and are called the mobile maintenance units. These maintenance units can also be used to replace glass panels.

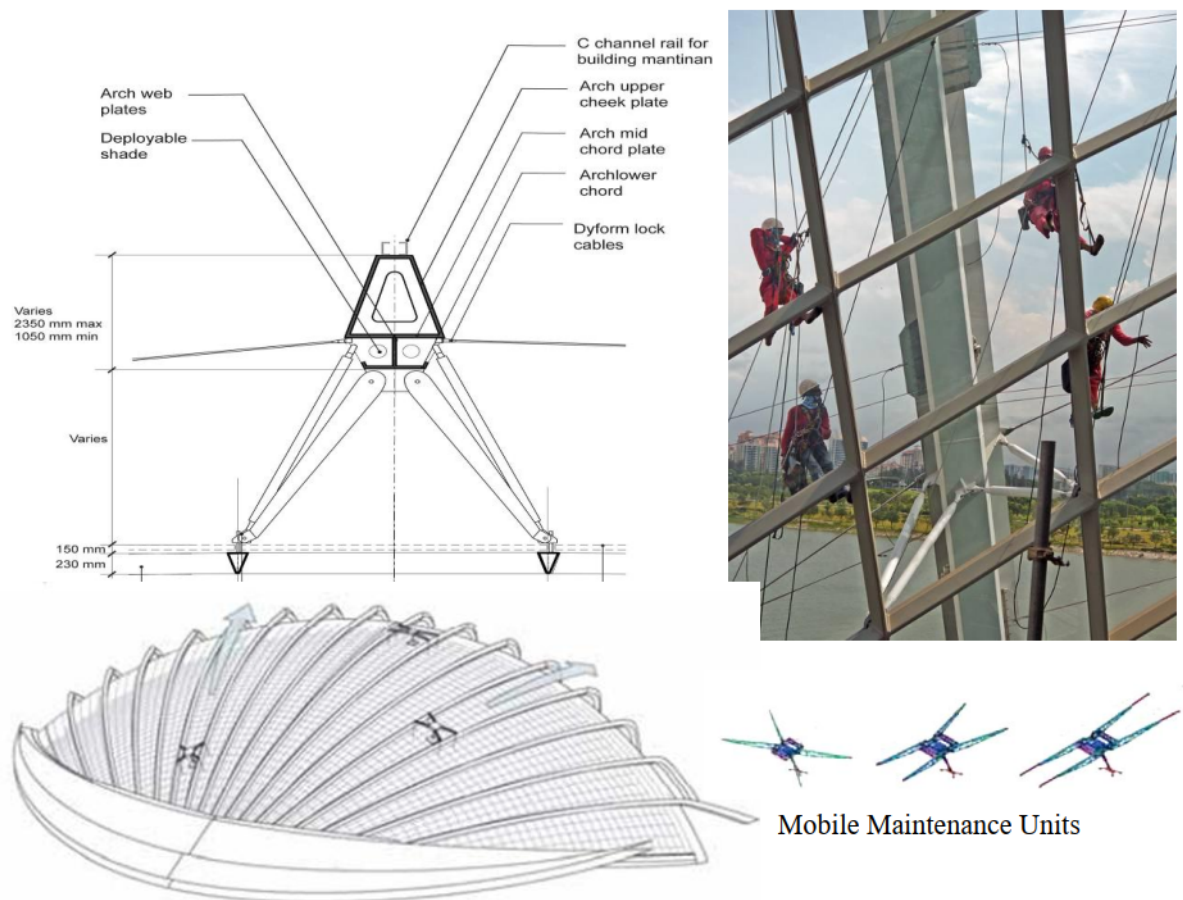


Figure 4.6: The Mobile maintenance unit. Courtesy of Arup Singapore [40]

5

Ventilation

This chapter provides background information for the ventilation concept. The first section explains the physical fundamentals which are needed for natural and hybrid ventilation. The second section explains the ventilation principles. After that different types of ventilation are discussed together with a practical example. In the last section, the critical barriers are addressed, and that information will be used to improve the ventilation concept (Part II The Design).

5.1. Physical Fundamentals

Natural ventilation is influenced by the strength and direction of the natural driving forces like wind and thermal buoyancy. However, also the design of the building influences the flow of the path and thus the magnitude of the natural ventilation. Therefore it is important to design a building according to these two principles.

Before explaining these principles, it is important to notice that most evaluations mentioned are based on a steady-state situation. Since the magnitude of wind and buoyancy vary, wind flows can change or even reverse, which makes designing more difficult. It is also essential to know the ratio between wind and buoyancy forces. Taking an inside-outside temperature difference of 3 K and a wind speed between 1 and 2.2 m/s in a summer design condition, the driving forces of wind and buoyancy are comparable [33]. The inlet and outlet are often static, but since the angle of the wind varies, most designs work only for a specific wind angle. There are examples of multi-directional ventilation systems like the design of Calautit et al. [41] (see Figure 5.1), but they perform not good for multi-story buildings and do not use buoyancy. Because buoyancy is a more stable driving force design practices mainly focus on the size of the openings based on stack effects only. In addition, engineers can design the building so that wind can increase the driving forces.

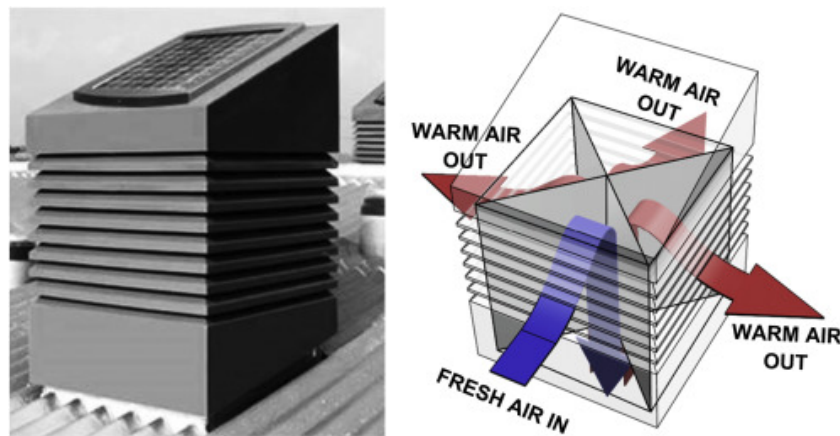


Figure 5.1: A commercial multi-directional wind tower [41]

Thus, there are different physical processes influencing the ventilation rate. Ventilation rate is the number of air changes per hour. A variety of natural ventilation concepts are based on these processes. These processes are described in the next section.

5.1.1. Stack effect

The density of warm air is lower than the density of cold air. Thus, when warm and cold are brought together, the colder denser air will fall, and the warmer lighter air rises. The force that causes this movement is called air buoyancy. The pressure at a point depends on the height, while the rate of decrease/ increase of pressure with height is dependent on the density (thus temperature) of the fluid. When the pressure gradients of cold and warm air are drawn schematically, the pressure gradient of cold air decreases faster with height than the pressure gradient of warm air. This means that there are pressure differences across the walls that divide the inside air from the outside air, see Figure 5.2a.

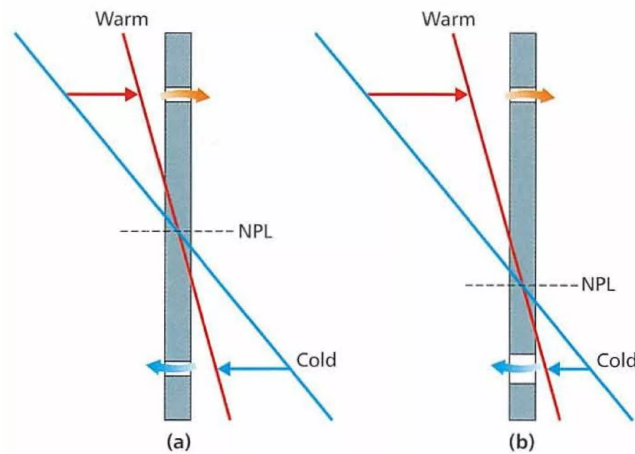


Figure 5.2: The impact of size on an opening [33]

When there are holes positioned in the wall, the outside and inside air will be exchanged according to the relative pressure differences. This means that at lower levels, the cold air has a higher pressure; thus the air will flow from the outside of the building to the inside. At higher levels, the opposite will occur. At a certain height, the outside pressure is similar to the inside pressure. This is called the neutral pressure level (NPL). The air will flow from the higher pressure area to the lower pressure area until the pressure drops across the two openings are the same. [33]

The airflow described is controlled by three physical relationships:

- Conservation of mass: the inflow of the air must be equal to the outflow of the air
- Hydrostatic pressures: The pressure gradient is dependent on the temperature. When the temperature is constant, the pressure gradient is also constant, and the relation between height and pressure is linear. If the temperature varies with height, the pressure gradient is not linear.
- Flow equation: the flow of the air is dependent on the opening, the discharge coefficient and the pressure difference. When the opening is larger, and the pressure difference is higher the airflow rate increases.

Most time of the year, the outside temperature is lower than the inside temperature. This means the warm air will rise up in the building and leave through openings at the roof side, while cooler air enters the building through lower openings. In warm summer days, the temperature of the building might be lower than the outside temperature, causing an airflow in the opposite direction. If this is undesirable, unoccupied parts of the building can be made warmer than the outside temperature to maintain a constant direction of the airflow. This can be accomplished by for example solar chimneys [33].

The size of an opening influences the height of the Neutral pressure line (NPL). When the lower opening is larger, the resistance to airflow is also lower. According to the law of conservation of mass, the pressure drop across the lower opening must decrease while the pressure drop at the higher level must increase until the pressure drop across both openings is the same. This results in a lower NPL, as can be seen in Figure 5.2.

This effect is significant when a building has several levels, and each level should exhaust the air. This means that the NPL should be above the highest floor to prevent warm air from lower levels to enter the higher floor levels. This can be achieved by varying the size of the openings on different levels while keeping the flow rates similar. Since the openings on the lower levels must be smaller, this brings security benefits.

So far the stack effect is discussed in the building as a whole, but the stack effect also occurs more locally. The stack effect can occur between every vertically placed opening which is interconnected. Even in a single window, if it is large enough, the air can flow in at the bottom and flow out at the top. This local stack effect can occur, even if the room is not connected with other rooms or openings. [33]

5.1.2. Wind driven

The physical relationships discussed in the section about stack driven ventilation does also account for wind driven ventilation. The main difference between stack and wind-driven ventilation is that the pressure differences are the result of differences in surface pressures instead of hydrostatic pressures. When wind approaches a building, the air is slowed down, and the pressure increases. Wind moving over the roof accelerates and induces a lower pressure. The distribution of these pressure differences depends on the wind speed and its direction relative to the building. The wind speed is influenced by its surrounding. So when a building is placed in open terrain, the wind speed will be higher compared to a building in a city centre. Also, the wind velocity increases with height as can be seen in Figure 5.3. The pressures on the building increase with the square of wind speed [33]. This means that the pressure on the higher parts of a building can be significant when the wind speed is high.

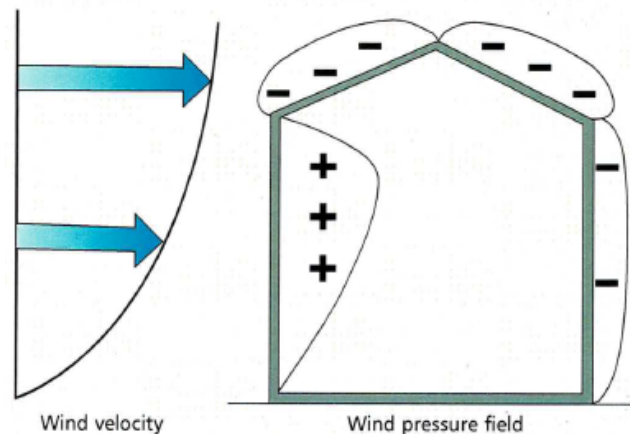


Figure 5.3: The wind pressures acting on a building [33]

Since the pressure differences caused by wind are across the width of the building, the air flow paths of wind-driven ventilation are mainly horizontal. However, it is possible to use the wind forces to increase vertical airflows through the building. Although careful designing of the building and surroundings (trees and other buildings) can maximize the potential of the wind-driven ventilation, the variability of the wind direction must always be considered. [33]

5.1.3. Combined

Although both wind and stack driven ventilation are examples of natural driven ventilation, these effects never act autonomously. The natural ventilation that occurs is the combined effect of wind and stack ventilation. The wind and stack effects can strengthen each other, but they can also counteract. Since the flow through an opening is non-linear, the different pressures must be combined before adding in the flow equations.

5.2. Ventilation principles

The main purpose of ventilation is to provide healthy air inside a building for breathing. Therefore outside air is moved into a building or room and distributed inside a building or room. The ventilation system dilutes the pollutants created in the building and removes the pollutants from it. A building ventilation system has three basic elements: the ventilation rate, the airflow direction and the air distribution of the airflow patterns. These elements are important because they determine the amount of outdoor air, the direction of the air movement and show whether the ventilation system is efficiently moving the air and removing the pollutants. Taking the basic elements into account, there are three types of ventilation: natural, mechanical and hybrid ventilation. [42]

5.2.1. Natural

Natural ventilation is a type of ventilation which depends on the climate, human behaviour and building design. The natural forces of wind and thermal buoyancy drive the outdoor air through openings like windows, doors, solar chimneys and wind towers. To create ventilation with buoyancy and wind, there are several techniques: single sided ventilation, stack ventilation and cross-flow ventilation. [42]

Single-sided ventilation uses wind flow through one side of the building. This is mainly used when cross flow ventilation is not possible or when the room is small. To optimize single sided ventilation the opening for fresh air supply should be low and the opening to drain the air should be high in the facade [42].

Cross flow ventilation uses pressure differences between two facades across the building caused by the wind. This pressure difference leads to an airflow. It is essential to notice that this is only possible when the depth of the building is not too large, and there are not too many obstacles. A rule of thumb for the maximum depth of a building is five times the buildings height [42] [33]. The openings in the opposite facades should be adjustable.

Lastly, stack ventilation is driven by thermal buoyancy forces. Warm air, produced by people and electronics, rises and leaves the air high in the building (often in the roof), while cold fresh air is supplied lower in the building. Adequate routing causes an air flow.

5.2.2. Mechanical ventilation

Mechanical ventilation depends on mechanical fans which drive the air flow. These fans can be installed in windows, walls or in air ducts for supplying or extracting air from a room. There are positive and negative pressure ventilation systems. In a positive pressure ventilation system the room pressure is positive, and the air leaks out of the room through leakages or openings. In a negative ventilation system, the room pressure is negative, and the air is 'sucked' from outside. A balanced mechanical ventilation system is a system where the air supplies and exhausts meet the design specifications. Thus, the room pressure can be slightly positive or negative while being balanced [42].

The climate and the type of room determine which ventilation system is most fitted. For example, in warm climates infiltration may be minimized or prevented, while in cold climates ex-filtration needs to be prevented. Therefore positive pressure ventilation is used in warm climates, and negative pressure ventilation is used in cold climates. Negative pressure is also used in rooms where many pollutants are generated like bathrooms or kitchens [42].

5.2.3. Hybrid ventilation

Hybrid or mixed ventilation uses the natural driving forces to provide the desired air flow rate, but it relies on mechanical ventilation when the air flow rate from natural ventilation is too low. Not only the airflow rate influences the use of mechanical parts with hybrid ventilation, but also the energy use, the thermal comfort and the indoor air quality. Therefore there are various functions in the mechanical parts: filtering, heating, cooling and moisturising [42]. When natural and mechanical ventilation is combined, natural ventilation is used when possible, but mechanical ventilation when necessary [43].

When using mixed-mode ventilation, the fans should be placed and used with care. They should be placed where the air can be exhausted to the outdoor environment directly. The size and the number of fans is dependent on the ventilation rate which should be achieved. This can be tested and measured before installing. Some cons of fans are installation difficulties, noise, influence on the room temperature and the constant need for electrical supply [42].

many factors influence the use of the mechanical parts of the ventilation in different situations, and there are also different forms of hybrid ventilation to distinguish:

- Natural ventilation is leading: the design of the building often uses (automatically) opened windows, air shafts and openings to favour thermal buoyancy forces.
- Passive and free cooling: the design of the building uses night ventilation, sun shading and other forms to limit the internal warming

- Complex control system: different sensors measure the presence of people, CO₂ levels, temperature and humidity and react to it.
- Fluctuating indoor climate conditions: since the airflow rate can vary, the conditions of the indoor climate can be changing.

When designing a hybrid ventilation system, it is important to consider the functions of natural ventilation:

1. Ventilation: The system provides fresh air by extracting the polluted air and supplying fresh air. A suitable ventilation rate in an office building is 6.5 dm³/s per person according to table 3.28 of Bouwbesluit 2012.
2. Free cooling: Free cooling can be used when the outdoor air has enough cooling capacity. When there is no mechanical ventilation necessary, it is called natural free cooling. The maximum ventilation rate is 4.
3. Night cooling: A surplus in heat can be stored at daytime in the building mass. The building mass is cooled at night, if possible by the (natural) airflow, by using night ventilation. Therefore night cooling is mainly used when there are large differences in temperature during the day and night. The ventilation rate necessary is 7 to 10, with a maximum of 15 [42].

There are three main hybrid ventilation principles, which are explained in the next section.

NV and MV two separate systems The first principle is based on two completely separate and autonomous systems. The control system can switch between natural and mechanical ventilation or use one of the systems for individual tasks. Examples of these systems are ventilation systems which rely on natural ventilation in intermediate seasons, but in summer or winter on mechanical ventilation. Also, systems which use mechanical ventilation during daytime and natural ventilation during the nights (for night cooling) are examples of two separate systems. [44]

Fan assisted NV These systems are based on natural ventilation but are supported by an extractor fan. When the natural driving forces are too low or the air flow rate needed is higher, the mechanical fan can increase the pressure difference and increase the airflow.[44]

Stack- and wind-assisted mechanical ventilation The last principle is based on a mechanical ventilation system which uses the natural driving forces as much as possible. Therefore these systems have minimal pressure losses, and natural ventilation is responsible for a large part of the airflow supply.[44]

Better indoor comfort while saving energy

To maximize comfort and indoor air quality, there are several ways to quantify comfort. Firstly, the weighted temperature overrun method which is based on the comfort model of Fanger and can be used at conditioned buildings. A second method is the adaptive temperature limit method (ATG-method) with a variable temperature limit. This method assumes that people habituate to higher outside temperatures (only on the long term), which means that the inside temperatures can be higher as well [43]. The method of adaptive limit values is most relevant when designing hybrid ventilation systems since higher inside temperatures are tolerated under certain circumstances. Therefore this method can be used for buildings with open windows and without (operational) active cooling or dress codes. The adaptive limit value can be increased when there is a higher ventilation rate caused by opened windows or attic fans. With this adaptive thermal comfort, a wider range of temperatures is possible with substantial options to save energy [45].

5.3. Survey of naturally ventilated buildings

Natural ventilation is not a new concept. The first buildings which incorporated air vent systems date back to 3000 BC [46]. Even though these systems are not applicable for modern buildings, the forces driving natural ventilation have not changed over time. More recent buildings which use natural or hybrid ventilation will be discussed.

5.3.1. Single sided ventilation

Single-sided ventilation is the most simple way of ventilating a building, opening a window is sufficient to create this type of ventilation, see Figure 5.4. Many ordinary residential houses use this kind of ventilation.

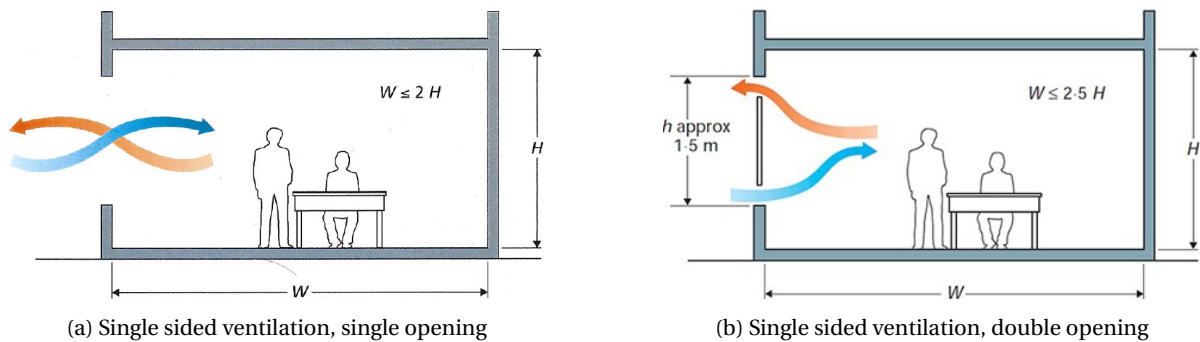


Figure 5.4: Single sided ventilation [33]

5.3.2. Cross ventilation

GSW-headquarters

GSW-headquarters located in Berlin and is a renovated office tower from the 1950s. The refurbished building is designed by architects Sauerbruch Hutton and features cross ventilation from east to west. On top of that energy savings are made by a double skin thermal flue on the west facing facade and automatically and manually operated triple glazed windows with between-pane blinds. [47]



Figure 5.5: GSW Headquarters has a passive ventilation system which reduces the energy demand [47]

5.3.3. Stack ventilation

Solar chimney

The BRE's Environmental Building is designed by the architects Feilden Clegg of Bath and was designed for the use of natural ventilation, maximum use of daylight, maximum use of the mass of the building to moderate the temperature and systems to meet the environmental targets while keeping the occupants satisfied, see Figure 5.6. On top of that, the building made maximum use of recycled and waste materials. [48]

The most striking feature of the building are the five distinctive ventilation shafts. These are a part of the natural ventilation and cooling system. Since the shafts of these solar chimneys are glass fronted, the air inside it will be warmed. This warm air rises and draws the air from the building to replace it. When there is little wind, fans on top of the solar chimneys make sure the airflow is sufficient [48].



Figure 5.6: BRE's Environmental Building [48]

Atrium

Barclaycard headquarters makes use of natural ventilation with an atrium. This permanent natural ventilation is provided by multiple 45 mm diameter plastic tubes, creating a system of 5000 mm²/m. The tubes go through lintels above the fanlight, which are manually operable. The atrium increases the natural stack effect since the roof can reach 40 degrees due to the glass windows. This is a point of attention when mechanical ventilation is combined with vertical zoning. Since a trigger of the top floor can lead to overcooling at the lower floors. [49]

5.3.4. Double skin

ARAG 2000

An example of a double skin facade is the ARAG 2000. The ARAG tower is 125 m high and is situated near Dusseldorf Airport. The tower is completed in 2001 and designed Foster and Partners supported by RKW Architectur +. The double skin facade, with a thermally broken internal skin and a single glazed external skin, combines natural ventilation with electromagnetic vents. Between the two glass skins, an air corridor is situated, see Figure 5.7. The windows in the internal skin can be opened manually, and the motorized sunscreens in the corridor are automated. [50]

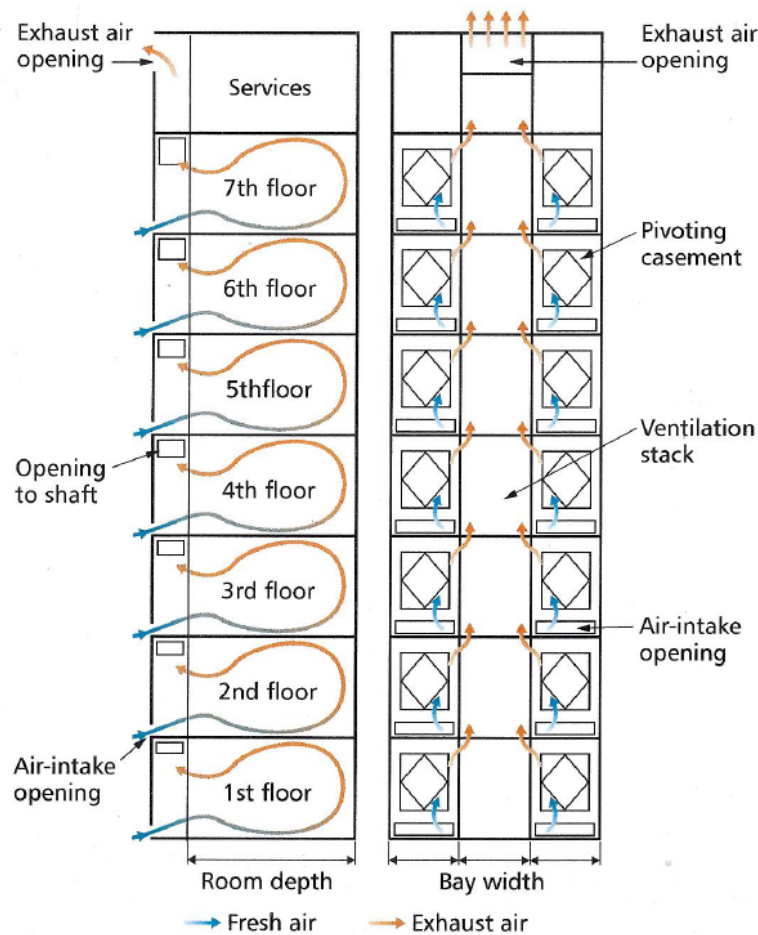


Figure 5.7: Shaft box double skin facade [33]

Stadsdeelcomplex Leidschenveen-Ypenburg

A unique example of a double skin facade is the "Stadsdeelcomplex Leidschenveen-Ypenburg". This building is designed by EGM architects from Dordrecht and built by the construction company Kanters from Barendrecht. This building opened in 2007 and was the first Dutch building which used a wind cowl for the main ventilation. The wind cowl, shaped like a stork, is headed to the wind and ensures under pressure and induces an airflow. Underneath the cowl, a central extraction duct with a diameter of 3 meters is located. The result is that warm, polluted air is withdrawn from the building, while clean air is provided by CO₂ driven grills. The ventilation system is supported by a big fan if there is no wind at all. Besides the use of natural ventilation, the building uses concrete-core activation and a heat pump. [51]

Although the building has won several prizes for the design (Bouwwereld Bouwtechniek Award 2009 and Best Practice Award Gezond Binnen 2008), there are hardly any buildings realized with natural ventilation combined with a cowl. In the Netherlands, there are some buildings with mechanical ventilation in combination with a cowl, but other examples of buildings with (mainly) natural ventilation and a cowl are located abroad. [51]



Figure 5.8: Stadsdeelcomplex Leidschenveen-Ypenburg with a wind cowl improving natural ventilation [51]

5.4. Critical barriers

To let a naturally ventilated building succeed the designer must provide the users with the possibility to implement the system, when desirable, and think of proper solutions for all the problems the users might face. A small unsolved problem might lead to infrequent use of the system. Secondly, it is crucial to let the users know how to use the natural ventilation system and inform them about the advantages and disadvantages of the system. When the users expect a system which maintains an indoor air quality close to the ISO comfort standards, while foolproof and requiring no interaction, the natural ventilation is not the most appropriate solution [24].

5.4.1. Safety

To let natural ventilation succeed, it is essential to find possible solutions for the barriers. One of these barriers is safety. To hinder intrusion of unauthorised people and animals the openings can be limited to max 15 cm with, for example, bars [24]. This is especially important for the openings on the lower floor levels. For bugs or other small intruders, screens or ventilation grills with incorporated screens are suited.

Although these options seem reasonable solutions, there are negative consequences. Smaller openings and screens can cause limitations to the intensity of natural ventilation. Moreover, the bars or screens are not desirable when the windows are intended for daylight or visual contact with the outside. Furthermore, there are additional costs, and bars can eliminate an alternative escape route. Lastly, the rain will enter naturally ventilated buildings if they are not closed manually or automatically before the rain. This is a significant barrier when the building uses night cooling [24].

Therefore it is essential to look at alternative solutions. There are windows with incorporated self-controlled openings for natural ventilation. A second solution is to uncouple the windows from openings for natural ventilation. These openings are well protected against intrusion and can be closed with a remote shutter.

Passive ventilation is often based on large open windows and chimneys. Although this ensures a high free flow of air, it also increases the risks of fire spread. Therefore some general rules must be addressed at the facade level and regarding zoning.

Fire usually spreads through openings, like grilles, louvres and operable windows in the external walls: 'unprotected areas'. When these openings are closable, they increase the fire resistance performance of the wall.

Zoning is another necessary fire restriction. With zoning and subdividing the building into fire resisting compartments, the fire can be isolated for 30 minutes to a few hours [24]. This allows safe evacuation and a minimization of the damage.

5.4.2. Noise

A second barrier is noise. Usually, the sounds from outdoors or from other places in the building are weakened by the boundaries and the reflections of the room. However, with naturally ventilated buildings there are more openings in the envelope leading to less attenuation of the sounds. The use of openings with noise-reducing baffles can overcome this problem. However, it should be noted that the resistance to airflow is high. Therefore a balance should be found between a good airflow and at least the same noise as a mechanical alternative [24].

5.4.3. Air pollution

Air pollution is a common barrier in urban areas, especially during the daytime. The pollution may lead to low air quality, causing problems for occupants, the building materials and furnishings. Thus, in these cases mechanical and chemical filtering may be required and natural ventilation may be a difficult option to implement [24].

To avoid indoor overheating, it is useful to combine natural ventilation with shading. Many forms of shading obstruct the airflow; thus it is important to search for shading devices which take care of shading or privacy protection while allowing enough airflow. Examples of these solutions are outdoor fixed shading devices as vertical fins or horizontal slabs.

5.4.4. Draughts & condensation

The outdoor conditions have a large variety and fluctuate very quickly. In all conditions, the air exchange must be high enough, but not too high. When the air velocity is higher than desirable, it can cause draughts. There must be a balance between enough air exchange, but at the same time avoiding draughts. An often used solution is the use of multiple openings which can be opened partially.

Not only the ventilation speed must be balanced, but also the ventilation temperature. When the ventilation temperature is too low, condensation can occur. This is often a problem with night ventilation [43].

5.4.5. User ignorance Patterns of use

Natural ventilation can take place to control overheating, promote comfort or improve the air quality. Natural ventilation must take place under certain conditions: when the indoor temperature is higher than outside, when the air velocity inside is too low or when the air quality indoor is unacceptable. These different conditions require a controlled start and end of the natural ventilation. If you do not use automatically controlled systems, the building systems must be intuitive and straightforward to operate; otherwise, the solution won't work. Even if the occupants are specialists, the interest gets lost as time goes by [24].

II

The Design

6

CFD analysis set-up and shape optimisation

In this chapter, a shape optimisation is performed on a case study namely the Mijnbouwstraat 106-112 in Delft. After introducing the case study, this chapter will focus on the first sub-question namely: "How to perform a shape optimisation of a facade to reduce the wind load by making the building more aerodynamic?". The answer to this question is given in two parts. First, the set-up of the CFD analysis is discussed to explain how to perform a CFD analysis. The set-up is important to perform an analysis because a small error can cause wrong results. Therefore existing research is reviewed followed by checking the mesh set-up, grid sensitivity and the residual values. Secondly, the optimisation process itself will be explained together with the results in the last section of this chapter.

6.1. Case study: Mijnbouwstraat 106-112 Delft

The validity of the design will be tested with a case study. Mijnbouwstraat 106-112 in Delft is a good subject for a case study because it has an irregular shape and it has an open surrounding, so there is room to extend the building.



Figure 6.1: Mijnbouwstraat 106-112, Delft [52]

The surrounding has a significant influence on the wind load of the structure. The wind will slow down due to the obstacles in the city like buildings and vegetation, but locally the wind pressure can increase. To keep the thesis manageable the surrounding buildings will be neglected. In reality, the building is attached to another building, see Figure 6.2. The drawings of the Mijnbouwstraat are provided by BD Architectuur.



Figure 6.2: Top view of the Mijnbouwstraat 106-112, Delft

6.2. Comparing Butterfly with existing research

To make sure the results are realistic, the CFD model will be compared with existing research. Multiple papers address the 6m cube (the Silsoe cube); these papers cube is already presented in Section 3.4.1. The CFD model in this thesis is made in Butterfly and uses the RNG k-eps turbulence model, see Figure 6.3. The results are in line with the research of Wright and Easom [30]. The results deviate the most at the windward side, and results of Butterfly underestimate the situation. Near the ground at point A the largest difference is present. The experimental results (grey) and Lim et al. [28] also deviate with the Butterfly-model. The difference is most cognizable at the roof, but still, the error is quite consistent so a safety factor could straighten the results.

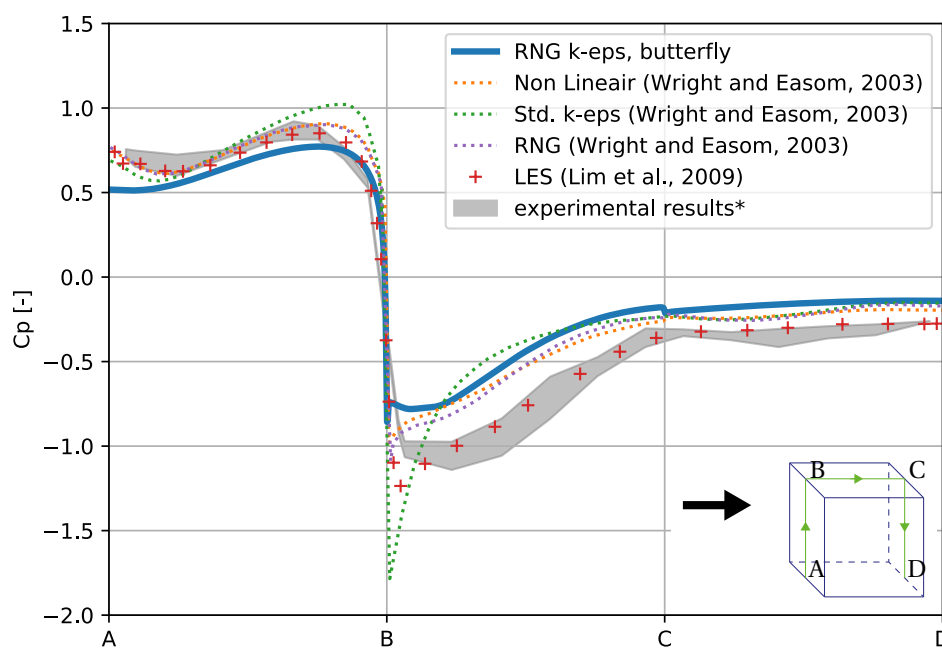


Figure 6.3: Comparing the mean pressure coefficients of this thesis with existing research
*experimental results: Wright and Easom [30], Richards et al. [31], Lim et al. [28]

6.2.1. Eurocode

Lastly, a comparison with the Eurocode NEN-EN 1991-1-4 will be made. The NEN-EN 1991-1-4 defines different pressure coefficients, which depend on h/d . The factors in Figure 6.4 correspond with a cube ($h/d = 1$). There are some similarities between the Eurocode and Butterfly like the constant pressure coefficient on the leeward side. Overall the CFD model underestimates the situation so a safety factor would be appropriate. Each face of a cube can have a separate safety factor, but Butterfly will be used for curved structures in this thesis. The rectangular structures are only used for verification. A less adequate solution is to apply a safety factor on the complete structure. This will be used because it is easy to implement and it is a preliminary calculation. For the final calculation, a different approach is needed, for example, LES-models or wind tunnel tests.

On average the absolute CP-value of Butterfly is 0.42 and the CP-value if the NEN-EN 1991-1-4 is 0.60. When using a safety factor of 1.45, both structures have the same cp-values on average. This factor will be used to avoid an underestimation of the loads.

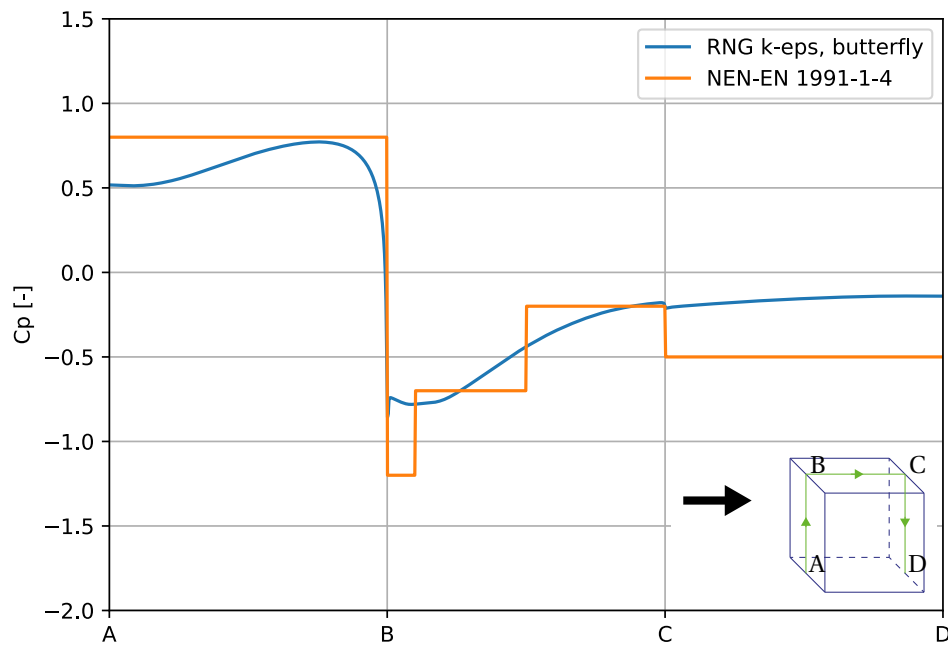


Figure 6.4: Comparison of mean pressure coefficients of several experimental results

6.3. Mesh set-up

Ideally, a mesh has a denser grid in the regions where the velocity or pressure gradients will be high. This is a bit cumbersome because to define the regions with a high gradient a calculation must be done. A workaround is to construct the finer regions where high-pressure gradients will be expected. The mesh is denser around the building and coarser further away from the building, see Figure 6.5. This is realised by refining the cells closer to the building. Refining is the number of times a cell is bisected, see Figure 6.6.

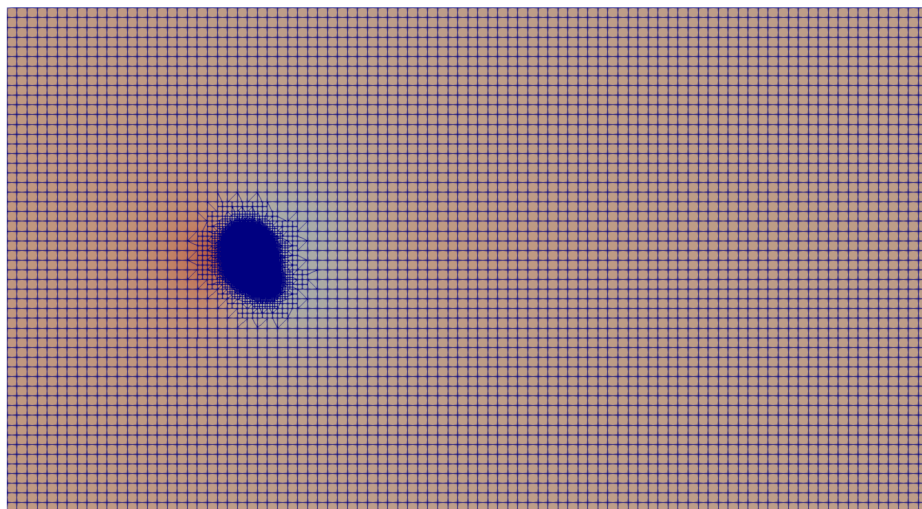


Figure 6.5: Top view of the mesh to simulate the wind force in a freeform structure, the wind flows from left to right

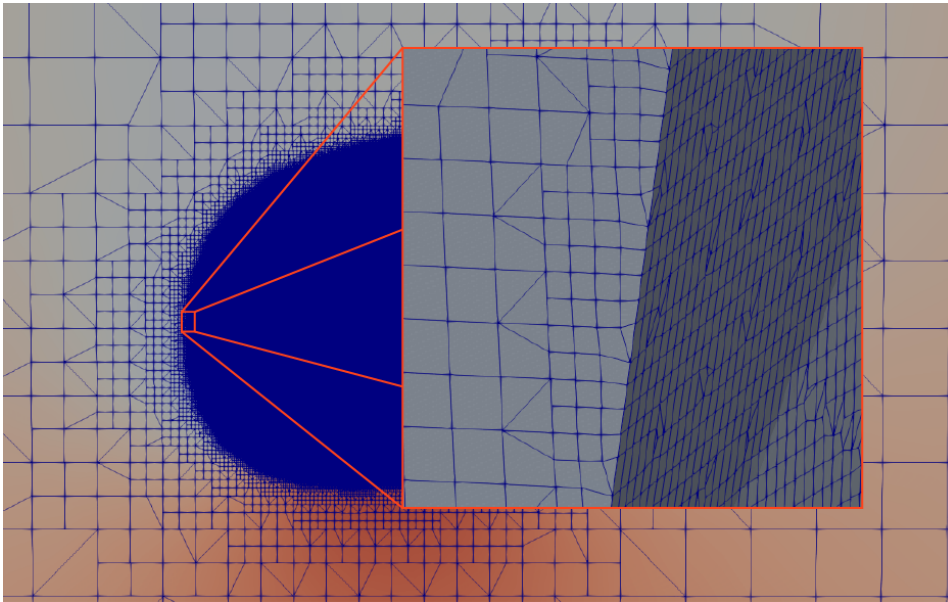


Figure 6.6: An example of a freeform structure with a cell refinement of 9

6.3.1. Mesh generation

It is straight forward to create a good match between a rectangular building and the mesh, but the match is less convenient for a freeform building. When creating a mesh, the first step is to create, a simple mesh of rectangles is, the background mesh (Figure 6.7a). Depending on the object, positioned in the virtual wind tunnel, the mesh is refined to fit the object as good as possible (Figure 6.7b). For a rectangular building, the mesh is done after cell removal, but in case of a freeform building, the cells are reshaped to match the object (Figure 6.7d).

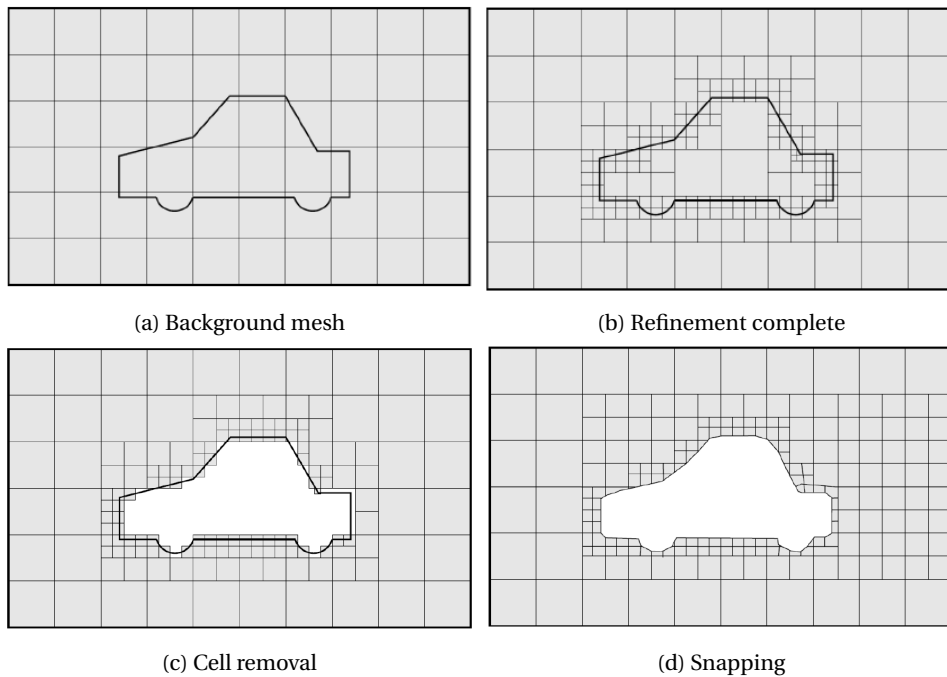


Figure 6.7: Intermediate steps to create a mesh [53]

6.4. Grid sensitivity

The size of the grid depends on the object which will be tested. A particular size may work for a rectangular building but perform badly for a freeform building. The cell size must be reduced until the results of the calculations are identical to check if a grid is suitable. Because freeform structures are tested in this thesis, rectangular buildings will be discussed only briefly.

6.4.1. Rectangular buildings

First, a rectangular building will be analysed, a highrise building of $30 \times 30 \times 120 \text{ m}^3$ similar to the highrise defined by Hunte [22]. At the height of 118 m, a slice of the building is made, and the cp-values are presented in a graph, see Figure 6.8. When looking at the graphs, the difference between the graphs R3 and R4 is very small at every point. Case R2 (refinement of level 6) is still quite good but deviates at the windward side. Case R1 (refinement of level 5) should not be used because it only has good results at the leeward side. When continuing with the calculations a refinement level of 7 would be the best option. The absolute cell size per refinement level is shown in Table 6.1. The number of cells, shown in the table, can be used as an indicator to estimate the amount of ram needed for a calculation. When running the CFD simulation, 1 million cells required roughly 1GB of ram in OpenFOAM.

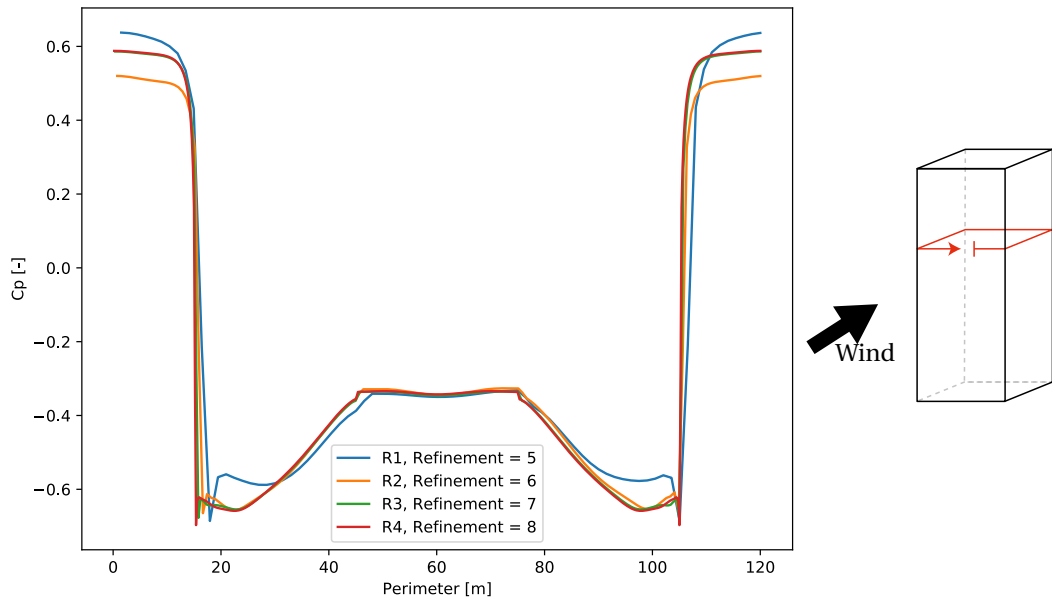


Figure 6.8: Cp-values at 118 m height for different refinement levels

| Case | Refinement | Largest cell [m] | Smallest cell [m] | Amount of cells |
|------|------------|------------------|-------------------|-------------------|
| R1 | 5 | 12.5 | 1.56 | 1.2×10^6 |
| R2 | 6 | 12.5 | 0.78 | 1.4×10^6 |
| R3 | 7 | 12.5 | 0.39 | 2.0×10^6 |
| R4 | 8 | 12.5 | 0.20 | 4.8×10^6 |

Table 6.1: Refinements details of rectangular building

6.4.2. Freeform buildings

A rectangular shape can be approximated easily even with a low amount of cells. A freeform shape can be approximated as well but with more cells. Again, the cp-values at the facade are computed for different cell

sizes, see Figure 6.9. Case F1 and F2 (refinement level 6 and 7) show very different results, here the bias can be addressed to the grid size which is just too large. That large is a relative term can be seen by the difference of the smallest cell size in Table 6.1 and 6.2. With a minimum cell of 0.117 m, this grid is already finer than the results of case R4 shown in Table 6.1. As discussed earlier, the cell size of case R3 and R4 are both adequate for a rectangular building. Case F3 and F4 (refinement 8 and 9) are comparable but do not have an exact match. Ideally a finer mesh should be used to check the difference between a refinement 9 and 10; however, this is not possible with my current resources. A refinement of level 10, with approximately 3.6×10^8 cells, would need around 36GB of ram for the CFD calculation alone and I have only 32GB available. Because this thesis addresses a preliminary design the results can be used, but for a final design more computer power is needed.

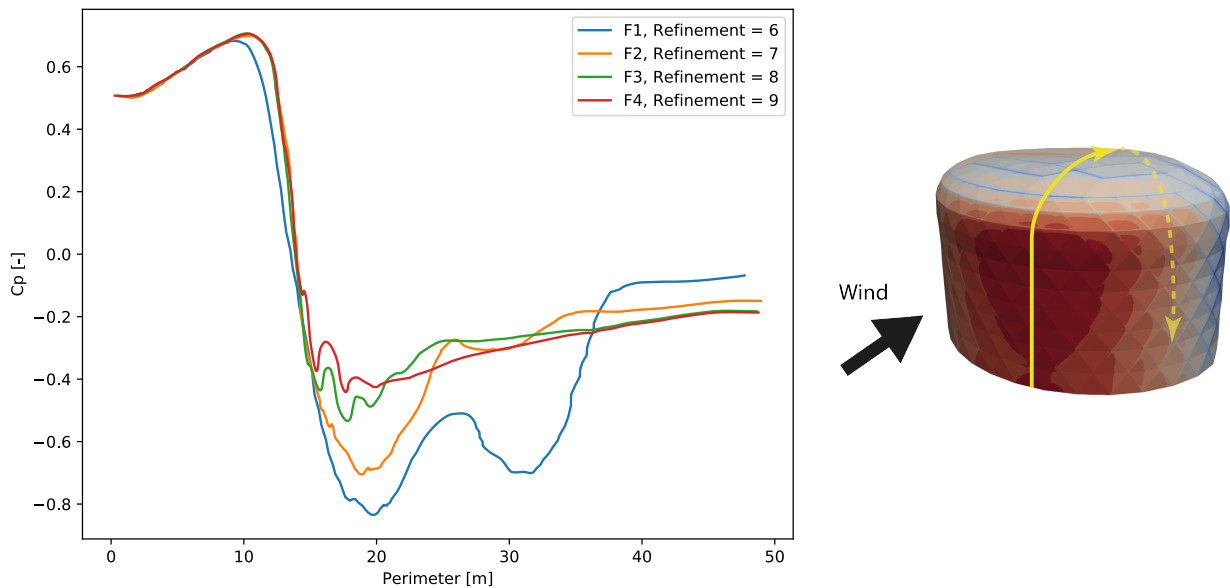


Figure 6.9: The c_p -values around the facade following the yellow line starting from the base of the structure

| Case | Refinement | Largest cell [m] | Smallest cell [m] | Amount of cells |
|------|------------|------------------|-------------------|-------------------|
| F1 | 6 | 3.75 | 0.234 | 4.6×10^5 |
| F2 | 7 | 3.75 | 0.117 | 1.3×10^6 |
| F3 | 8 | 3.75 | 0.059 | 4.8×10^6 |
| F4 | 9 | 3.75 | 0.029 | 1.8×10^7 |

Table 6.2: Refinements details

6.5. Residuals

The pressures and wind speeds are calculated with the Navier-Stokes which are based on three conservation rules, namely conservation of mass, energy and momentum. The computational domain is spatially discretised into different control volumes wherein each volume variables, such as wind speed in three directions and pressure, are defined. The Navier-Stokes equations are numerically discretised and set-up for every control volume to solve these variables. After discretisation, the differential equations are converted to a set of algebraic equations which have to be solved in each control volume. When solving the equations, the iterative numerical calculation will try to converge towards zero. This process can be monitored with the residuals. The residuals indicate the local imbalance of the variables defined inside the control volumes. The pressure and wind speeds are displayed in Figure 6.10 where the limit is set to 1×10^{-4} . The default limit is 1×10^{-5} but to speed up the process less strict limit is chosen.

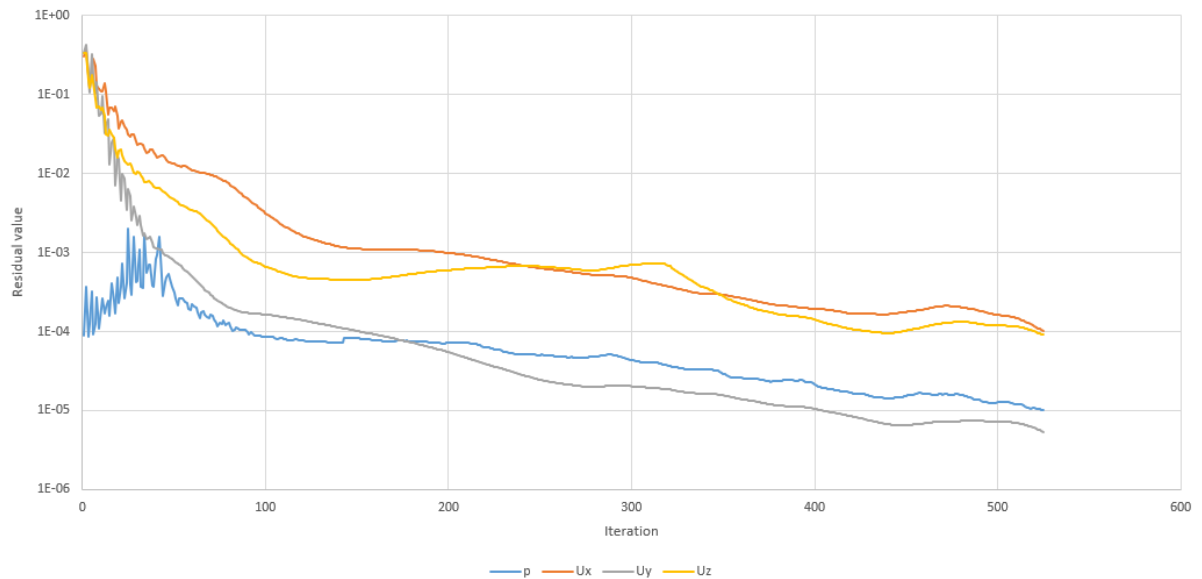


Figure 6.10: Residual values monitor, the y-axis has a logarithmic scale

6.6. Genetic algorithm

The principles of genetic algorithms are explained in Section 2.5. The following sections use that information.

6.6.1. Galapagos

Designs can be optimised with a Genetic Algorithm already discussed in 2.5. Grasshopper makes the usage of genetic algorithms straightforward with the plugins Galapagos and Octopus. The optimisations are single-objective which means there is only one performance indicator per problem. For this kind of problems Galapagos can be used, Octopus is for multi-objective problems. Galapagos works very intuitive and only requires a performance indicator and some inputs, see Figure 6.11.

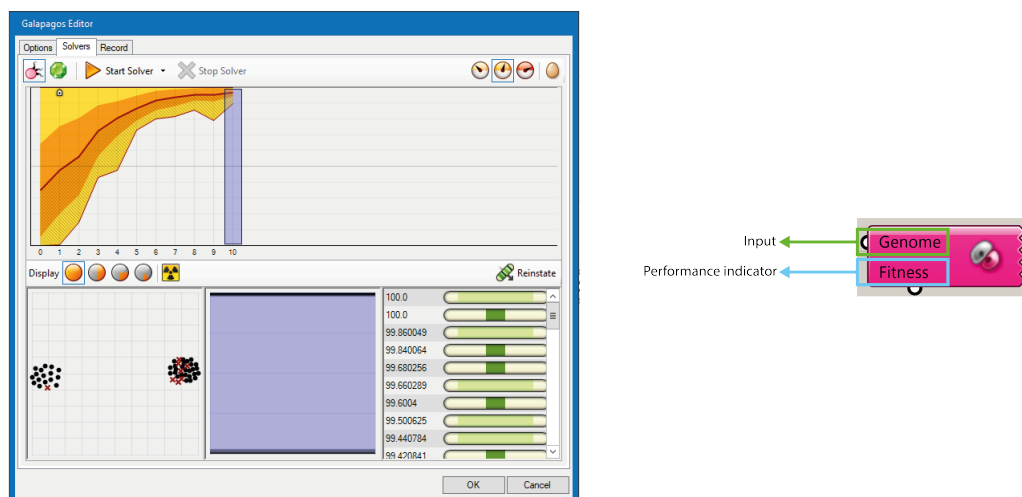


Figure 6.11: Setup of Galapagos, only the input (genomes) and the performance indicator (fitness) is needed.

The downside of Galapagos is that it gives one solution in the end, without good visualisation. The visualisation can be done with Colibri (grasshopper plugin to store the solutions) and DesignExplorer (visualisation).

Because the documentation on the usage of Colibri and Galapagos is limited and example is shown in Appendix G.

6.6.2. Genetic algorithm in Python

Galapagos can be used for different kind of problems so in theory it could be used in combination with CFD models. However, Galapagos cannot work with Butterfly, because one calculation in Butterfly takes a few hours. During a calculation, the canvas shows intermediate results which break Galapagos. Also, the results of Butterfly must be post-processed to become useful.

To solve this a problem a Python script is used to replace Galapagos. The Python determines the fitness or performance of the existing solutions and generates a new population based on best performing individuals. The script is based on a script of Larson Will [54], see Appendix A.

6.7. Shape optimisation

6.7.1. Design variable: Floor offset

Starting point

The structural floors are not a variable, but it is an important starting point of the second skin design. The shape of the structural floors and the floor heights are based on the drawing of the Mijnbouwstraat provided by B&D Architecten. The shape of the floors define the lower limit of the second skin, the skin cannot overlap with the structural floors, and the height of the structural floors determines the position of the support of the second skin.

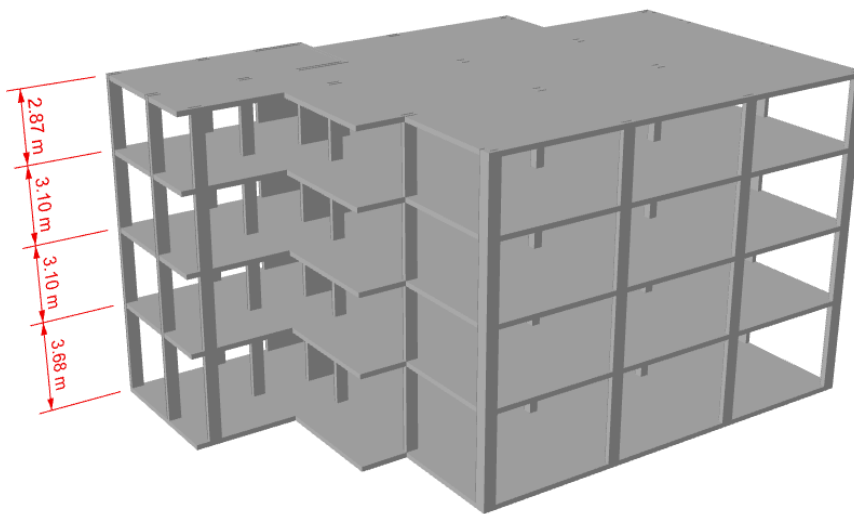


Figure 6.12: Structural floors heights of the building

Floor offset

The most important variable is the floor offset because it determines the shape of the second skin. In Figure 6.13a an offset-curve is shown, the shape of the offset-curve is smoothed to create an aerodynamic shape. To create this curve the distance between the curve and the structural floor is set at eight locations. If this is done for each of the five floors, 40 inputs are needed. With many inputs, it is more difficult to find an optimal solution because there are many solutions to investigate. The CFD model takes a few hours to finalise so the number of solutions to investigate must be limited.

The inputs are limited by reducing the eight floor-offsets to five (a-e), see Figure 6.13a. Also instead of specifying the offsets per floor a multiplication factor per floor is used (f-j), see Figure 6.13b. With this logic, the

offsets at the ground floor are $a \cdot f, b \cdot f, \dots, e \cdot f$ at the first floor and $a \cdot j, b \cdot j, \dots, e \cdot j$ on the last floor. The input k is the distance from the top floor to the highest point of the skin.

The limits for the input values:

- a - e can vary from 0.1 till 5.0 m
- f - j can vary from 0.1 till 2.0
- with the two limits stated above the limit of the multiplication factors $a \cdot f, b \cdot f, \dots, e \cdot j$ is 0.01-10 m
- After generating a few solutions k appears to be very dominant compared to the other inputs. The best performing solution is the solution with the smallest k . The process is speeded up by setting the value k to the lowest value possible, which is a floor height of ± 3 m.

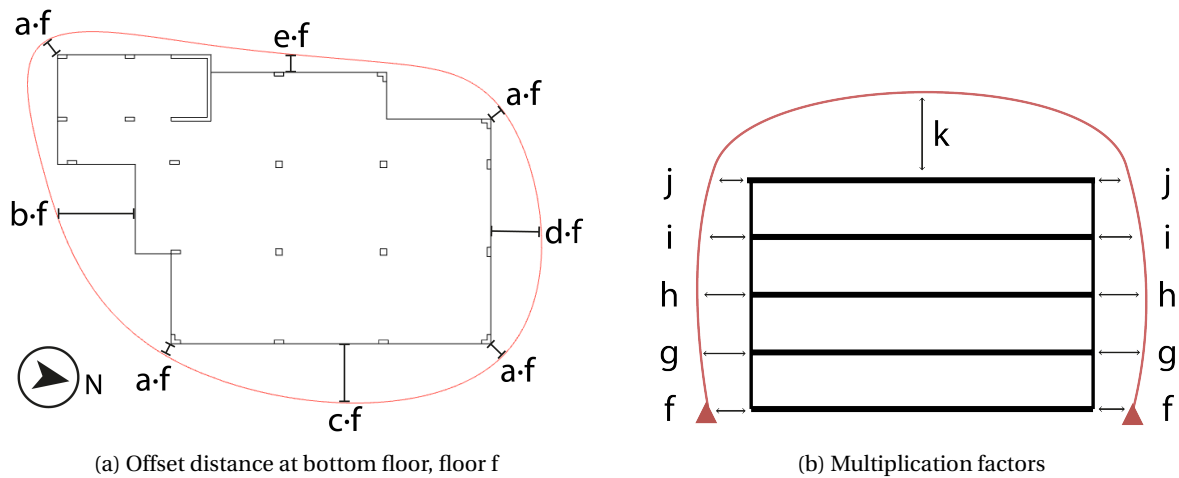


Figure 6.13: The definition of the eleven input parameters which define the shape of the structure

6.7.2. Performance indicator: Resultant wind force

When a car is subjected to a wind load, three forces can be distinguished, the lift force, side force and the drag force (Figure 6.14). Because a car is symmetrical the side force is small compared to the drag force. The Mijnbouwstraat is in some directions almost symmetrical but not in the direction of the dominant wind. Therefore the results of the drag force and the side force is taken into account. This resultant wind force is calculated by taking the sum of all the forces on the facade panels and ignoring the lift component (z -direction), see Figure 6.15.

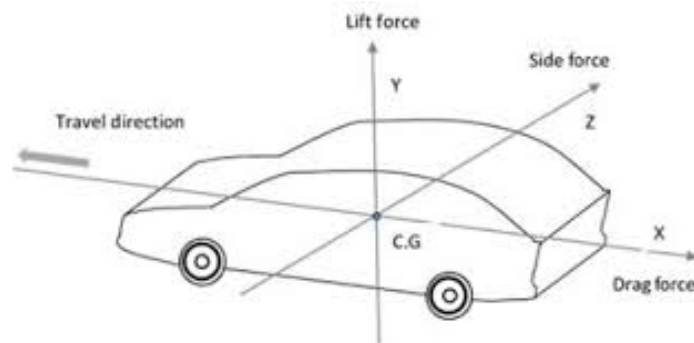


Figure 6.14: The lift, drag and side force subjected to a car in relation to its travel direction [55]

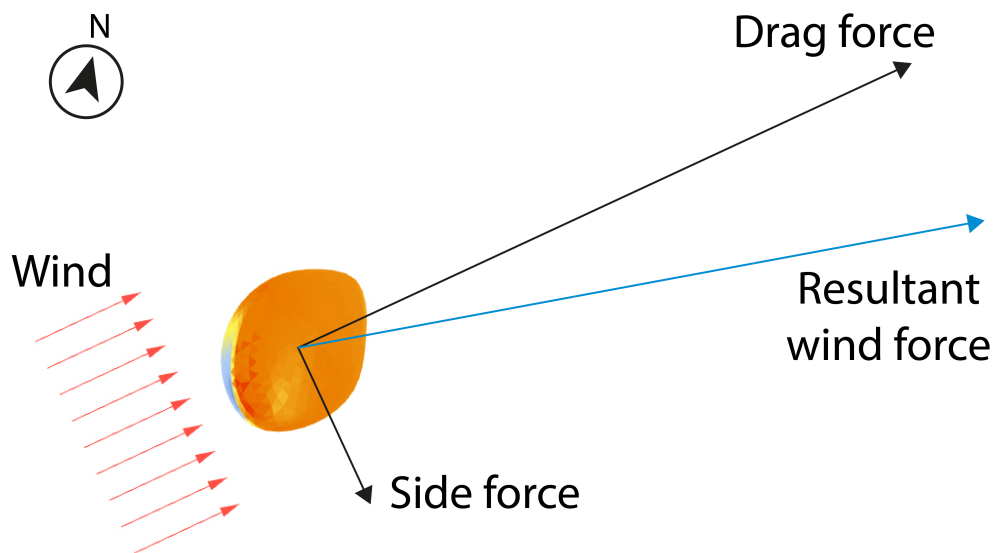


Figure 6.15: The sum of wind forces on each panel is the resultant wind force, this resultant wind force can be split in a drag force and a side force

The CFD calculations are time-consuming, so it takes too much time to perform a CFD calculation in four wind directions. As an alternative, the CFD simulations are performed on the best solutions after the optimisation, see Figure 6.16.

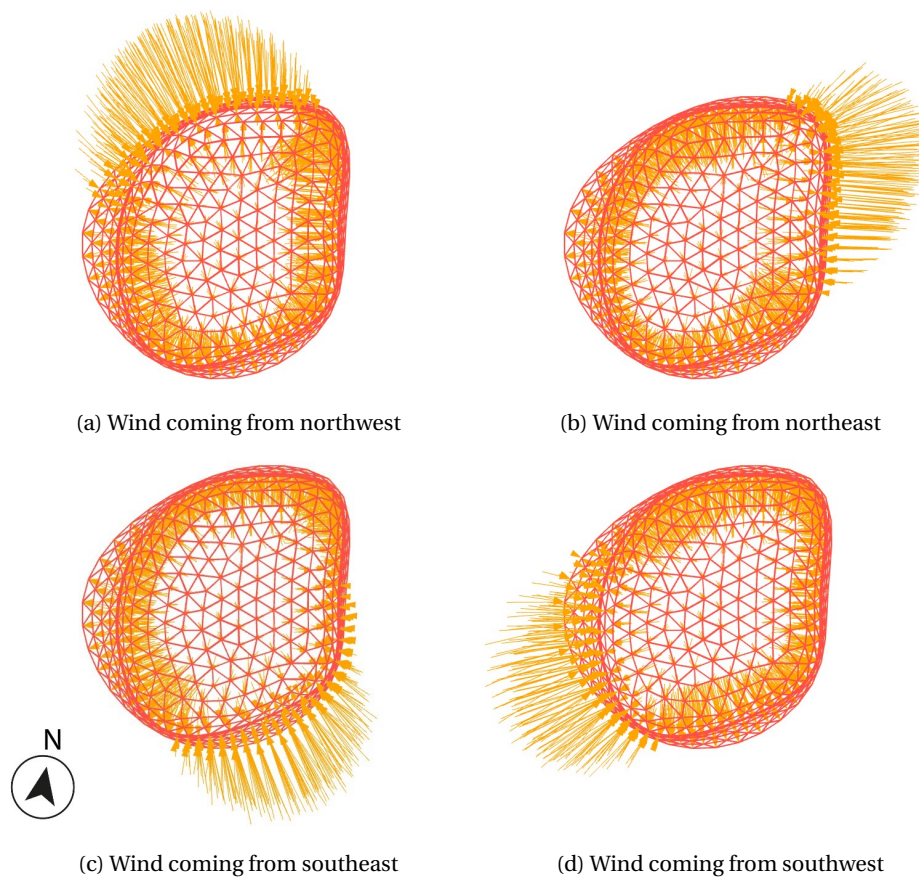


Figure 6.16: Windload from four directions

Reference case Mijnbouwstraat 106-112

To see the reduction of the wind force on the structure the results will be compared to the existing building at the Mijnbouwstraat. The residual wind force on the structure is determined with the Eurocode and the CFD model, see Section 7.4.1.

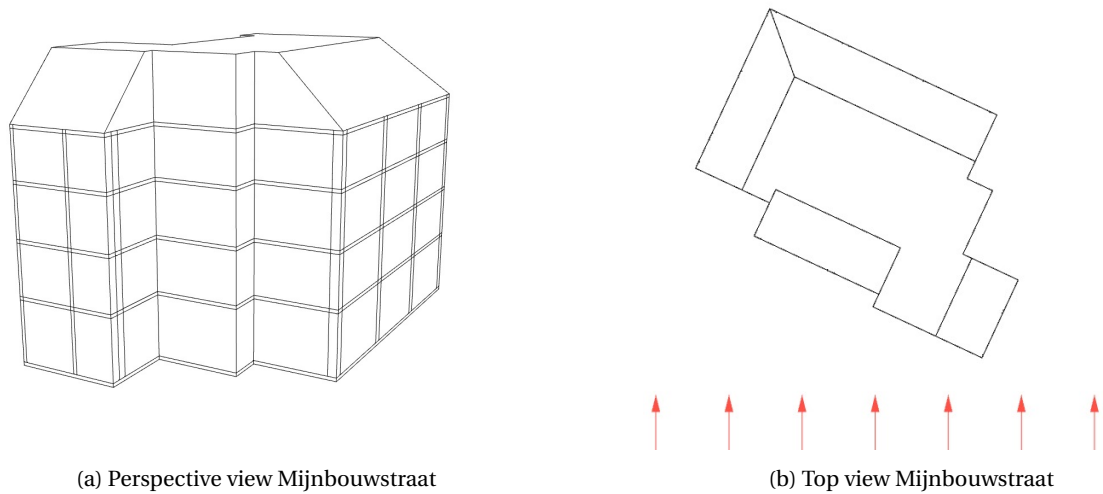


Figure 6.17: Two views of the Mijnbouwstraat 106-112

The Mijnbouwstraat 106-112 is analysed with Butterfly as it is today. The facade of the Mijnbouwstraat is divided into smaller rectangles, and for each sub-panel, the c_p -values are calculated, see Figure 6.18. With the c_p -values, the force on each sub-panel is calculated, and the sum of all the forces is the Resultant wind force. The component of the force in the z-direction is ignored. The resultant wind force in the xy-plane is 479 kN.

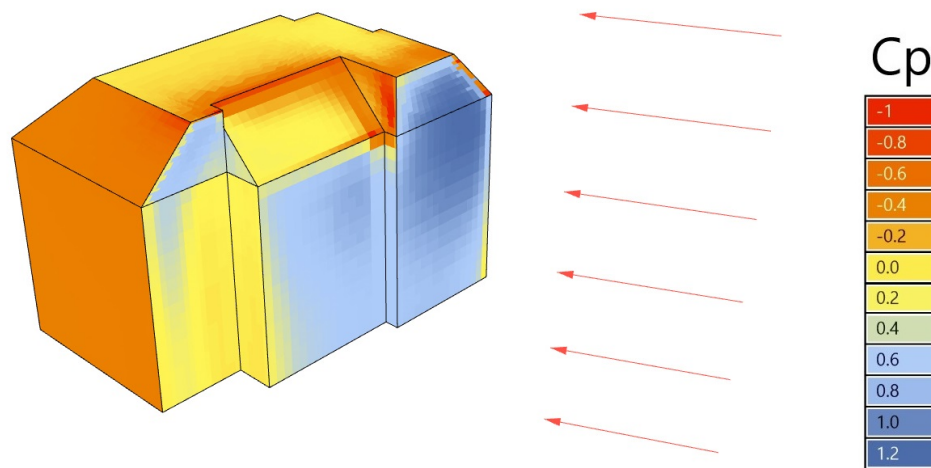


Figure 6.18: The c_p -values on the facade of the current building at the Mijnbouwstraat 106-112

The force on the building is compared with the Eurocode to check if the wind force is the same in Appendix F. The Residual wind force is 416 kN which is roughly the same as found with Butterfly. The calculation in the appendix is an estimation, so it can deviate from the CFD calculation.

6.7.3. Process

First population

The first population is created by choosing the input parameters a till j randomly. The random numbers are chosen between the limits, for example, a is chosen between 0.1 and 5.0. Some very unrealistic individuals were removed after creating the individuals. A structure with an offset of 5.0 m on the ground floor and second and an offset of 0.0 m on the first floor will be very removed. Each population has 16 individuals, see Figure 6.19.

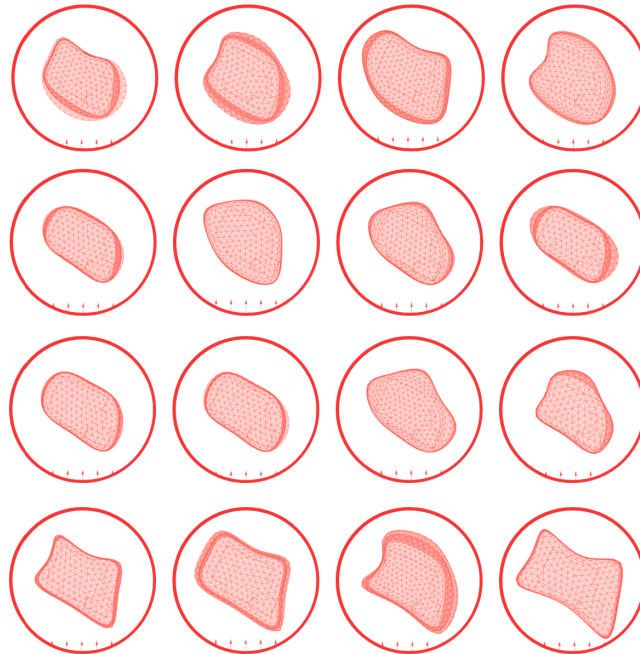


Figure 6.19: The top view of the first generation wind is flowing from bottom to top, the upper left has the lowest resistance and the lower right has the highest resistance against the wind

Next populations

The next iterations are generated with a Python script based on Larson Will [54]. The next generation is generated by selection, crossover and mutation, see Figure 6.20. After the mutation process, the selection process is repeated.

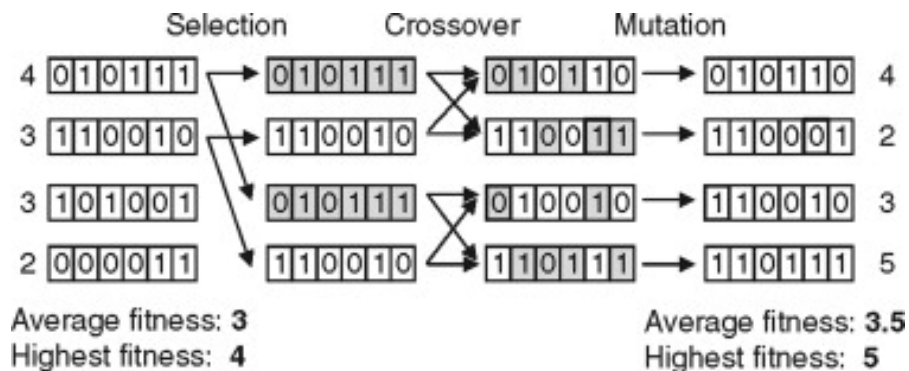


Figure 6.20: The three main processes of a genetic algorithm selection, crossover and mutation [56]

Selection The fitness of the current population must be known to perform a selection. The drag force of the structure determines the fitness. The individuals (lists of numbers) are transformed into actual geometry,

and that geometry is used to do a CFD model analysis. The outcome of the CFD analysis is used to calculate the resistance of the building against the wind, the drag force. The best individuals have a higher chance to be selected in the selection process. If an individual is chosen, a crossover will be performed on two individuals.

Crossover A crossover starts with two individuals, copies those individuals partially and merges the two. With this process a new individual (child) is created with properties of both of the parents. Because the best performing individuals get selected in the selection process the children will get perform over time. For this design an individual consists out of 11 numbers and a crossover looks like this:

$$[a_1, b_1, c_1, d_1, e_1, f_1, g_1, h_1, i_1, j_1, k_1] + [a_2, b_2, c_2, d_2, e_2, f_2, g_2, h_2, i_2, j_2, k_2]$$

becomes

$$[a_1, b_1, c_1, d_1, e_1, f_1, g_2, h_2, i_2, j_2, k_2]$$

Mutation To create more diversity in the population, mutations will be introduced. When a mutation happens a part of an individual changes. Some individuals will be mutated but not all of them. An example of a mutation can be seen below where the third value cannot be addressed to one of its parents because it is generated randomly:

$$[a_1, b_1, c_?, d_1, e_1, f_1, g_2, h_2, i_2, j_2, k_2]$$

Human interference Normally human interference is not included in a genetic algorithm. A genetic algorithm will run on its own and start again with the selection after the mutation process. The process will stop if there is no progress. It takes some time to find the optimal solution, especially if the creation of one individual takes a few hours. By creating some individuals with common sense, the processing time is reduced. When looking at the drag coefficients of different shapes the open sphere appear to perform the worst, and the streamlined half body performs the best, see Figure 6.21. To speed up the process individuals with the shape of a streamlined body will be inserted in the population.






| SHAPE | C_D |
|---|-------|
|  | 1.42 |
|  | 1.38 |
|  CUBE | 1.05 |
|  STING SUPPORT | 0.47 |
|  | 0.05 |

Figure 6.21: The drag coefficients of different shapes [57] [58]

6.7.4. Results

The progress over twenty-one generations with sixteen individuals is visualized in Figure 6.22. Three hundred thirty-six individuals are not much, so it is important to check if the input parameters are uniformly distributed. The input parameters can be compared with a parallel coordinates graph, see Figure 6.23. All the input parameters are scaled from 0% to 100%, where 0 is the lower limit, and 100 is the upper limit. The limits are defined in Section 6.7.1. The input parameters of the bottom and top floor will be discussed, the floors in between show similar results.

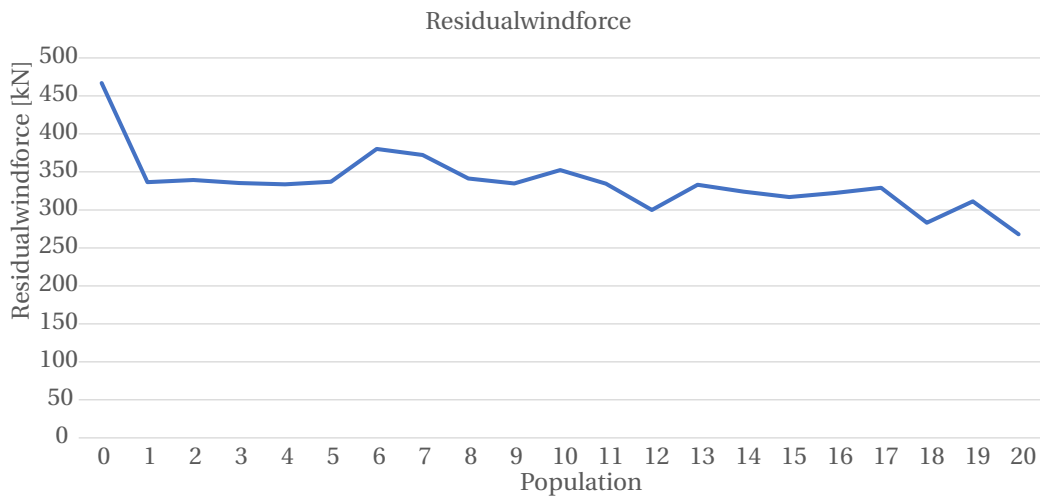


Figure 6.22: Progress of the twenty-one populations

Input parameters af-ef

All the input parameters of the 336 solutions are plotted in a parallel coordinate graph, see Figure 6.23. The letter f characterises the input parameters at the bottom floor. af is not uniformly distributed, because only solutions between 0-50% are analysed properly. The assumption is made that solutions with a large a perform badly, so only a few of these were tested. This is done by removing some solutions with a large a manually. Also, b is not uniformly distributed; the reason for this is that a small bf causes a collapse between the facade and the structural floors, see Figure 6.13a. The other input parameters are uniformly distributed.

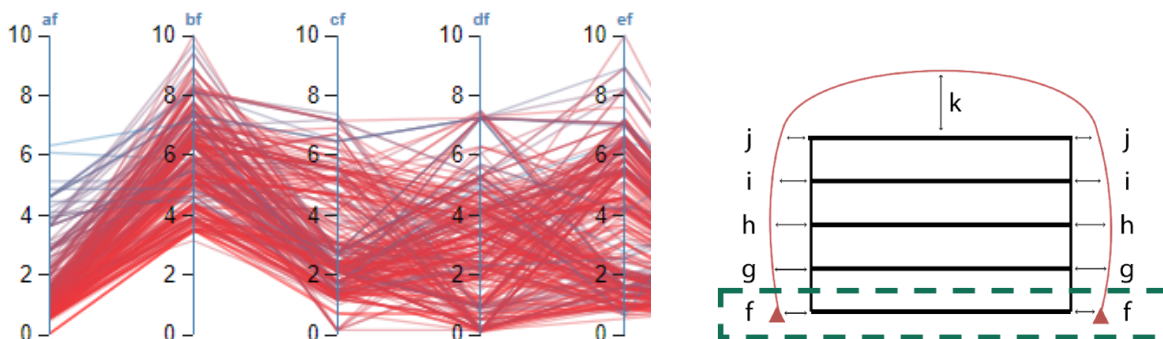


Figure 6.23: Parallel coordinate graph of the input parameters the figure on the right indicates the floor level

Input parameters aj - ej

The input parameters of the highest floor will be investigated, see Figure 6.24. The input parameters at the top floor are characterised by the letter j . The distribution on the top floor is similar to the distribution on the bottom floor. The inputs are limited to 8 m; larger values caused errors in the Grasshopper-script which created the structural grid.

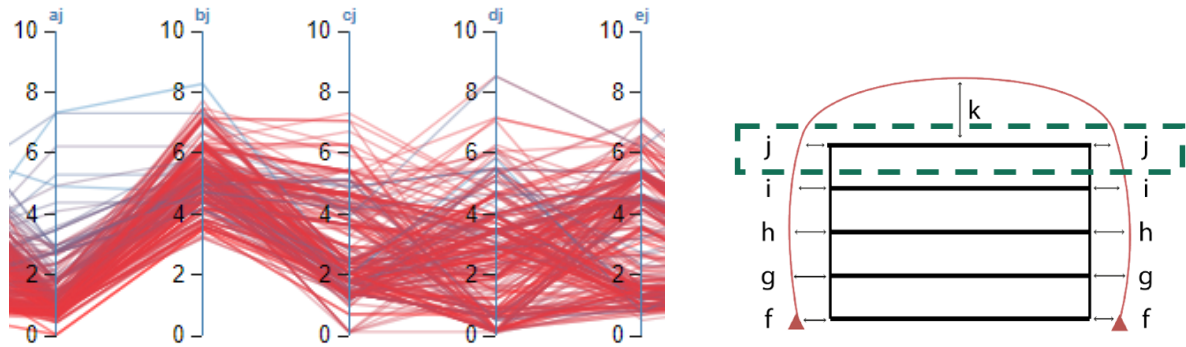


Figure 6.24: Parallel coordinate graph of the input parameters the figure on the right indicates the floor level

Some input parameters do not have a uniform distribution, but those can be explained. Overall it looks like the exploration of the designs space is good. In a future design, the limits can be smaller, to limit the design space and speed up the optimisation process.

The 10 best designs

The 10 best solutions are shown in Figure 6.25, the residual wind force of the ten best solutions varies from 245 to 260 kN.

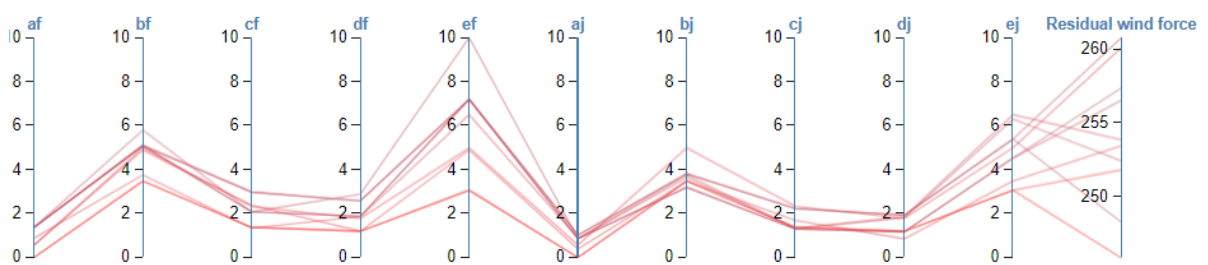


Figure 6.25

In Figure 6.26 the ten best solution are shown for the ground floor (6.26a) and for the fourth floor (6.26b). The input parameters are clustered which indicates that the best solutions have common properties. From the five parameters per floor, a is the most influential because it controls four offsets. Besides that, the inputs af and aj are most unanimous and vary from 0.83-1.4 m. On the top floor, the solutions are more clustered than on the ground floor which indicates that the offsets on the ground floor are less influential. For example, regardless of factor ef , which varies from 7.2-10 m, a residual wind force below 260 kN can be reached.

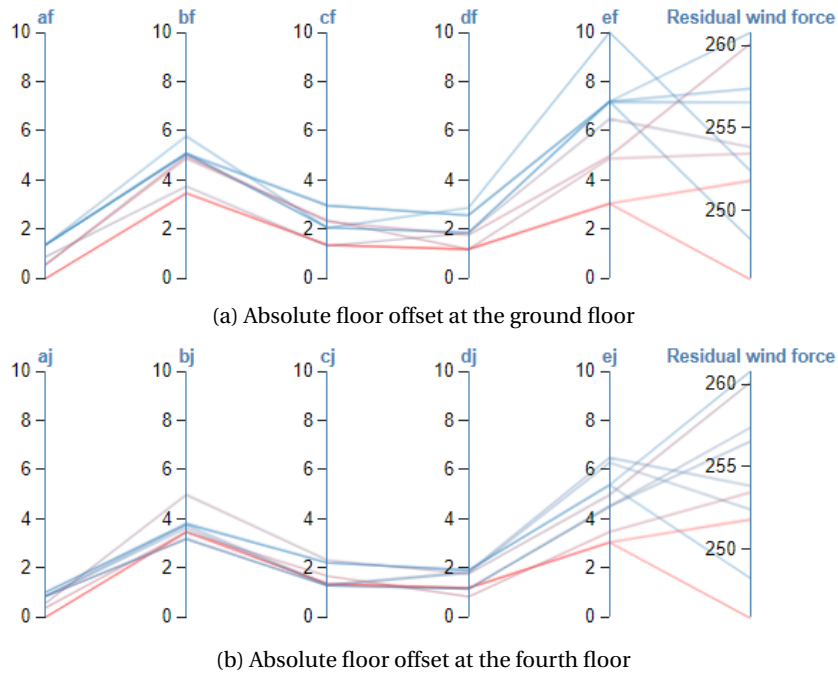


Figure 6.26: Floor offsets which determine the shape of the facade

A top view of the ten best individuals is shown in Figure 6.27. The wind flows from bottom to top. The designs have some similarity with the streamlined body (Figure 6.21). The shape is not exactly alike because the building must follow the shape of the structural floors. However, the windward side is more round and the leeward side is sharper just like the streamlined body.

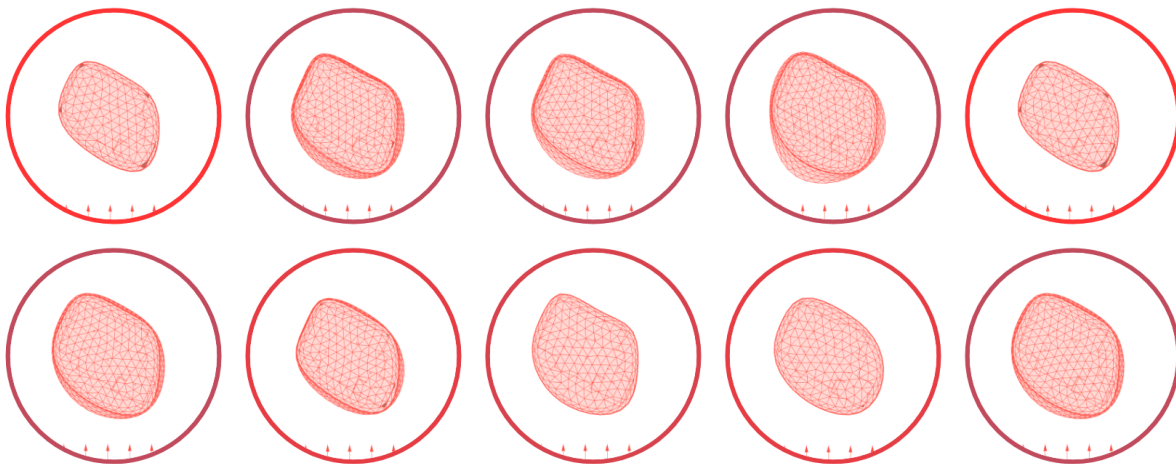


Figure 6.27: The top view of the best individuals wind is flowing from bottom to top, the upper left has the lowest resistance and the lower right has the highest resistance against the wind

An overview of the five best solutions is given in Table 6.3. Some solutions are discarded because the distance between the facade and the existing building is too small (0.035 m) for ventilation purposes. The solutions will be referred to as shape 1-3. The shapes 1 and 2 are visualised in Figure 6.28 and Figure 6.29.

| Name | Residual wind force [kN] | Note |
|----------|--------------------------|--|
| - | 245.87 | a = 0.035 m which is too small for ventilation |
| shape1 | 248.27 | |
| - | 251.76 | a = 0.035 m which is too small for ventilation |
| shape2 | 252.42 | |
| shape3 | 253.86 | |
| original | 454.19 | Original Mijnbouwstraat Building |

Table 6.3: The residual wind force of the five best solutions

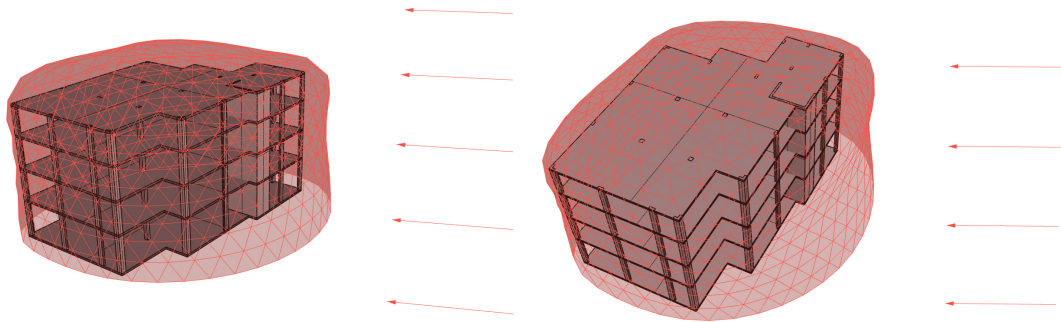


Figure 6.28: Optimised shape 1, 248.27 kN

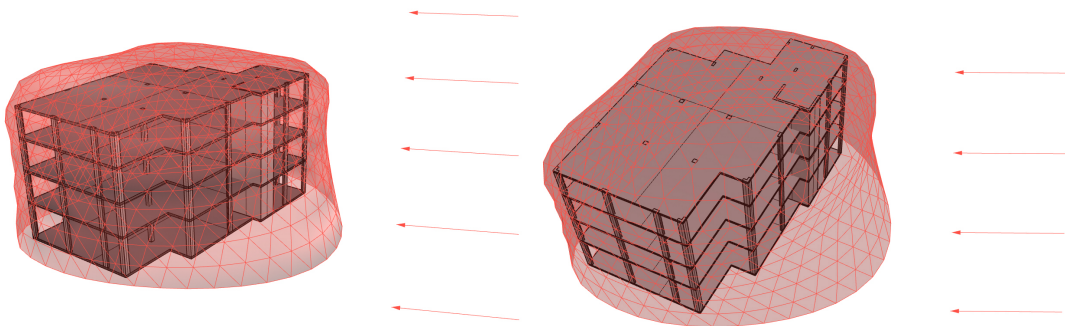


Figure 6.29: Optimised shape 2, 252.42 kN

7

Structural model set-up and optimisations

In this chapter will focus on the second sub question: "What is the effect of integrating a structural optimisation with a shape optimisation?". The first section continues with the shapes 1-3 found in Chapter 6 and creates multiple structures based on these shapes. In Section 7.2 - 7.5 the structural model is explained by discussing the supports, connections, materials, loads and structural requirements. After the set-up of the structural model the optimisation itself will be discussed. Section 7.6 goes into the structural optimisation itself and Section 7.7 combines the structural optimisation with the shape optimisation. In this section the effect of the combination of a structural optimisation with a shape optimisation is discussed, by comparing the following two approaches:

Approach 1 (Section 7.6 Structural optimisation)

1. performing a shape optimisation
2. process the results
3. perform a structural optimisation
4. process the results

Approach 2 (Section 7.7 Structural and shape optimisation)

1. performing a shape and structural optimisation simultaneously
2. process the results

7.1. Freeform gridshell

7.1.1. Optimal grid

The first step is to determine the optimal grid. In Section 4.1 several existing structures are reviewed, and different gridtypes can be found. To make an educated guess for the grid, we can look at a cylindrical shell under axial compression. In the paper of Lai et al. [59] six grid patterns are compared. The conclusion is that the triangle grid and the rotated triangle grid are most efficient under axial compression and pure bending, see Figure 7.1. A benefit of the triangular grid is that the beams can be aligned with the structural floors. Accordingly, the view to the outside is cleaner compared to the rotated triangular grid. If a gridshell will be used for the facade, the triangular grid is the preferred option.

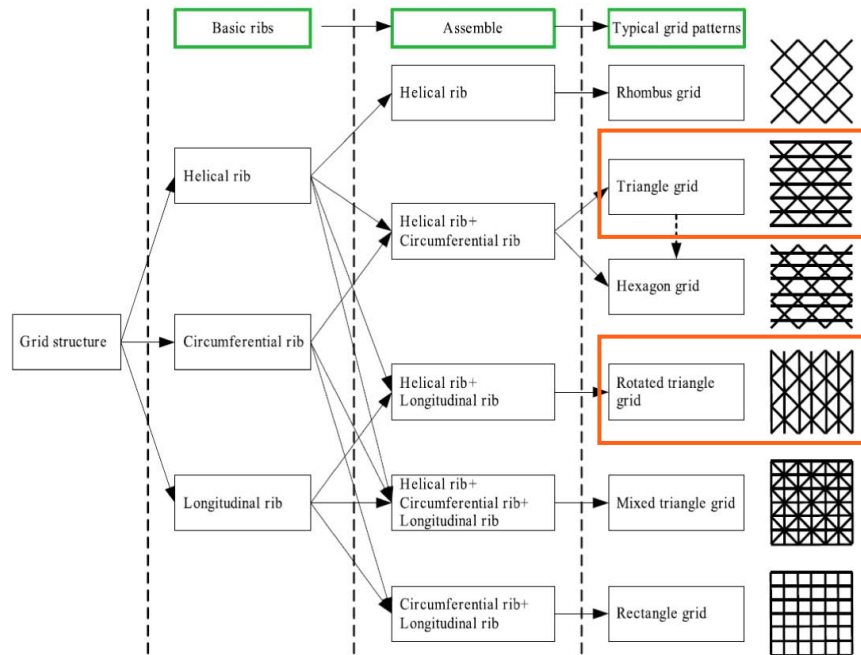


Figure 7.1: Cylindrical shell grid patterns [59]

7.1.2. Translation of a freeform facade to a gridshell

The shapes found in Chapter 6 are the basis of the structural grid. The shape is split in a top (roof) and a bottom part (facade), this section discusses the facade part of the gridshell. The starting point is the optimal shape found in the shape optimisation and the existing structural floors (Figure 7.2a).

Step 1: creating support points

Step 1 is to create the support points at each floor level (Figure 7.2b). The amount of supports matches the horizontal grid size as good as possible. For example, seven supports will be created when the perimeter of the floor is 20 m, and the grid size is 3 m.

Step 2: interpolating

Step 2 creates points between the floors to match the vertical grid size (Figure 7.2c). If the vertical grid size is 1 m and the distance between the floors is 4 m, three rows of points will be created between the floors.

Step 3: connecting the points

After the creation of all the points the mesh is created (Figure 7.2d). The creation of the roof part of the structure is discussed in the next section.

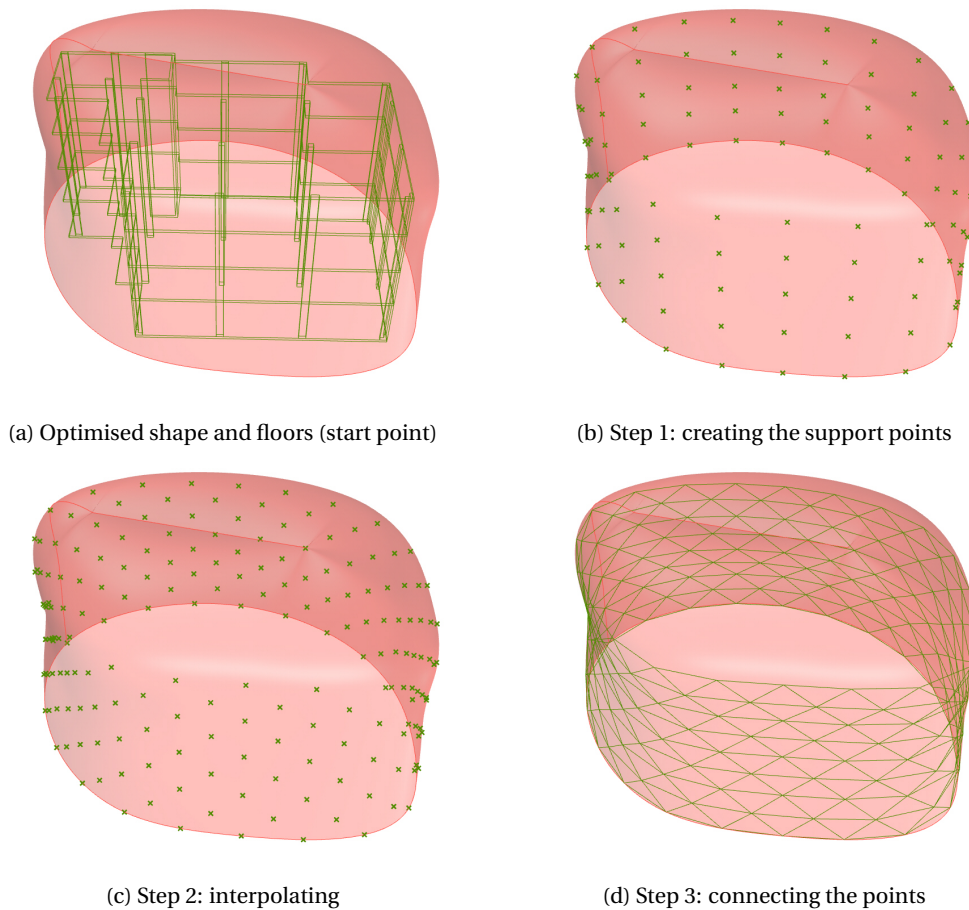


Figure 7.2: Steps to create the bottom half of the mesh

7.1.3. Translation of a freeform roof to a gridshell

With the chosen grid-pattern the facade and roof can be constructed. Creating the roof requires more attention because the pattern must be adjusted to close off the space. In Figure 7.3a triangular and quadrilateral shapes alternate to create a closed shape. Another possibility is to remove bars closer to the centre of the roof like at King's Cross in London, see Figure 7.3b. Both are good solutions when the roof is supported by a regular shape; when the support conditions are very irregular, a different approach is needed.



(a) Irregular gridshell roof [60]



(b) King's Cross station [61]

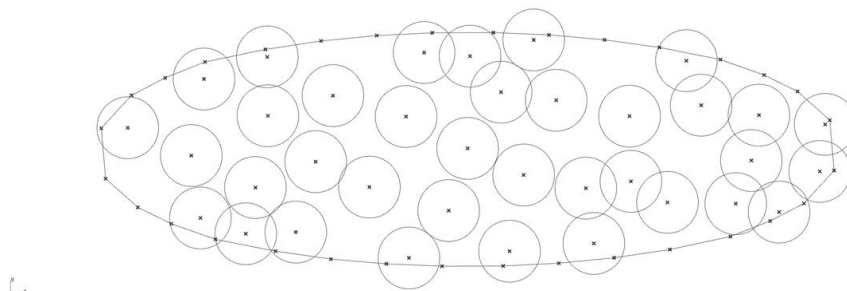
Figure 7.3: Two gridshell roof structures

Sphere collision

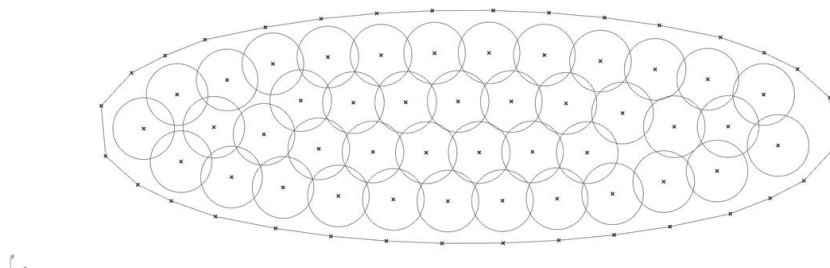
Another approach is to use sphere collision to create an equally distributed triangular grid. The idea is to position a certain amount of spheres on a surface and let the spheres repel each other, quantified by a certain force. When minimizing the sum of forces the distribution can be optimized, because the closer the spheres get, the more they repel each other. After several iterations, the optimal solution is found, and the spheres are equally distributed.

The steps a-c are illustrated in Figure 7.4.

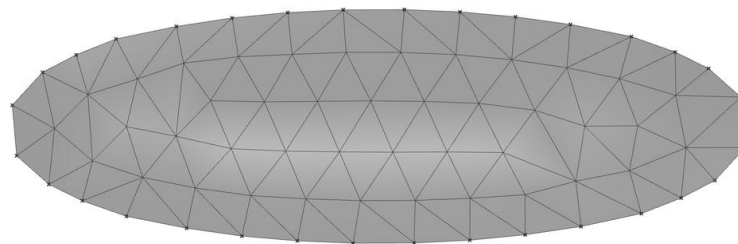
- (a) Determine the number of nodes based on the area of the roof and position that amount of nodes on the surface.
- (b) Move the nodes to distribute the nodes equally over the surface. Each iteration the nodes are better distributed. Stop the iterations if there is no progress.
- (c) Create a grid with the last iteration.



(a) Starting point: random distribution of points



(b) Last iteration: points equally distributed



(c) Last iteration used for the grid.

Figure 7.4: Sphere collide

In Figure 7.4 a grid is created with an oval as a starting point, but the method also works with irregular shapes. For example in Figure 7.5 a roof is made for an irregular building and the panels are either transparent or glass.

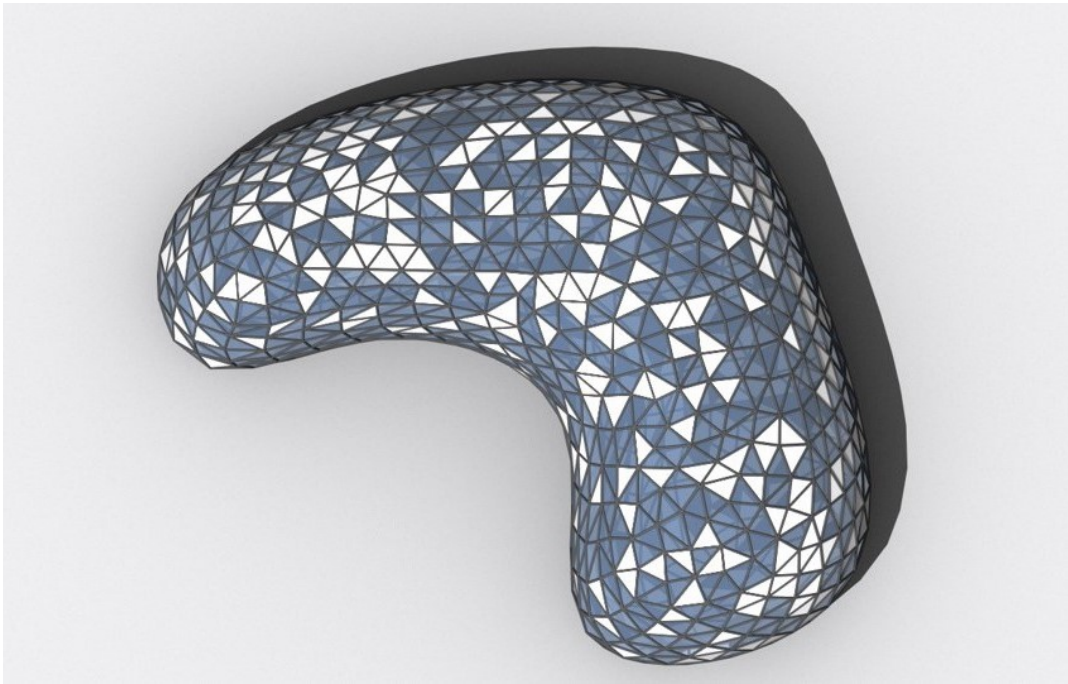


Figure 7.5: Example of a freeform roof

7.2. Supports and connections

7.2.1. Supports types

Four support conditions are shown in Figure 7.6:

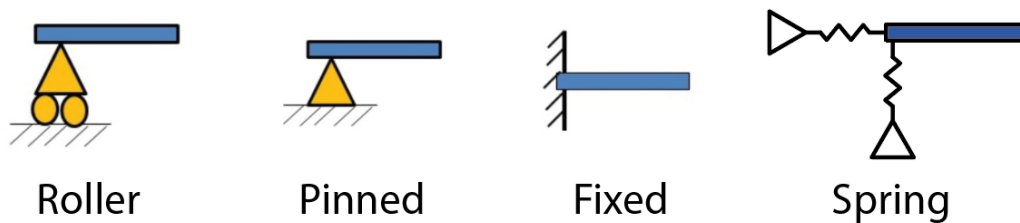


Figure 7.6: Different type of supports

Roller supports A roller support is free to translate and rotate on the surface upon which the roller sets. The resulting reaction force is a single force that is perpendicular to the surface. Roller supports allow the structure to expand and contract with temperature change.

Pinned supports A pinned support can resist both horizontal and vertical forces but not a moment. As a result, a structural member can rotate, but not translate. Many connections are assumed to be pinned even though they might resist a small amount of moment in reality.

Fixed supports Fixed supports can resist moments and forces in the horizontal and vertical direction. A structural member needs only one fixed support in order to be stable; in that situation, the three equations of equilibrium can be satisfied.

Spring Spring supports can be used to create more realistic models. In reality, a support moves a little when a certain amount of force is applied. This is the behaviour of a spring. The movement is related to the spring stiffness k (kN/m). When a spring stiffness is very low (≈ 0), the support will almost move freely, and when the spring stiffness is very high ($= \infty$) the spring will behave like a pinned support.

7.2.2. Supports

Pinned supports are the easiest to implement, but a pinned support is not realistic, especially when attaching a structure to an existing building. Karamba has only rollers, pinned and fixed supports, but there is a workaround. In Karamba spring elements can be connected to a rigid support to mimic the spring support. In GSA spring supports can be defined which is more convenient. Because the spring supports have a minor effect, they will be discussed separately, see Section 7.10. For the calculations in Karamba pinned supports will be used at the bottom and pendulum (roller) supports at each floor level.

The roller supports have a local axis with z_{loc} perpendicular to the facade. The pinned supports at the bottom follow the global axes, see Figure 7.7a. A similar structure is the Peek and Cloppenburg department store in Cologne, where pendulums are used, see Figure 7.7b. Pendulums behave the same as rollers.

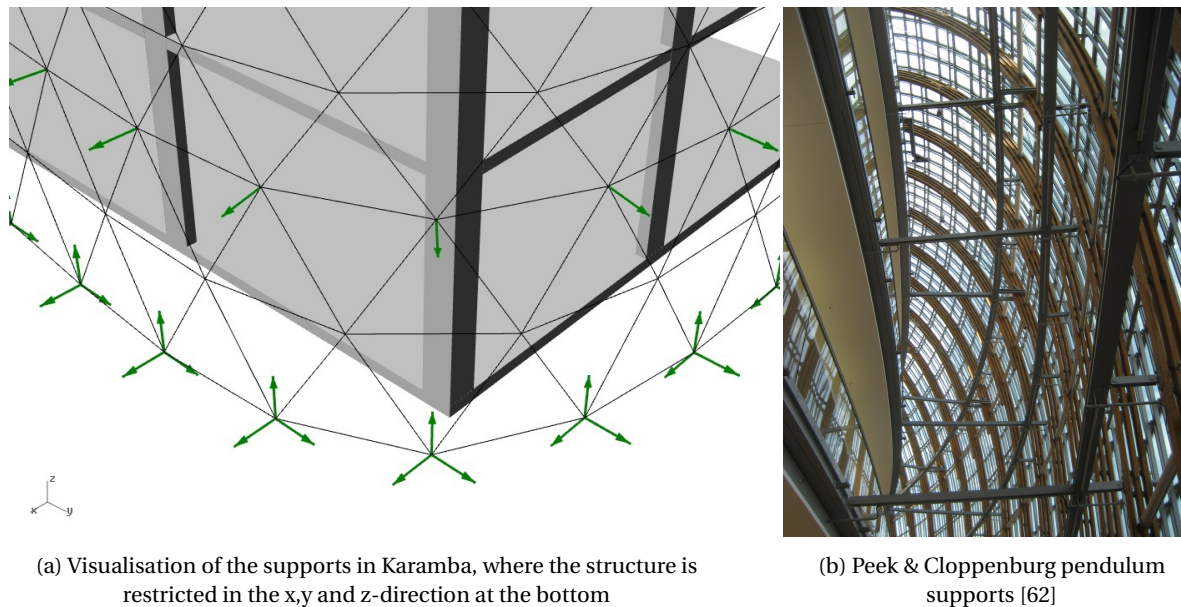


Figure 7.7: The support conditions of the second skin

7.2.3. Mechanic scheme

The building at the Mijnbouwstraat is designed to withstand the wind load. Once the second skin is positioned the second skin can withstand the wind load and distribute it to the existing structure. The assumption is made that the second skin will make the structure more aerodynamic so the wind load will be reduced. The existing structure is capable to withstand the wind load in the new situation. In contrast to that, the vertical loads like dead load will increase by the second skin. One can strengthen the existing structure or make the second skin bear its own vertical loads. The later is chosen because it is easier to implement. In the model, this is translated to pendulum supports at each floor and pinned supports at the bottom, see Figure 7.8.

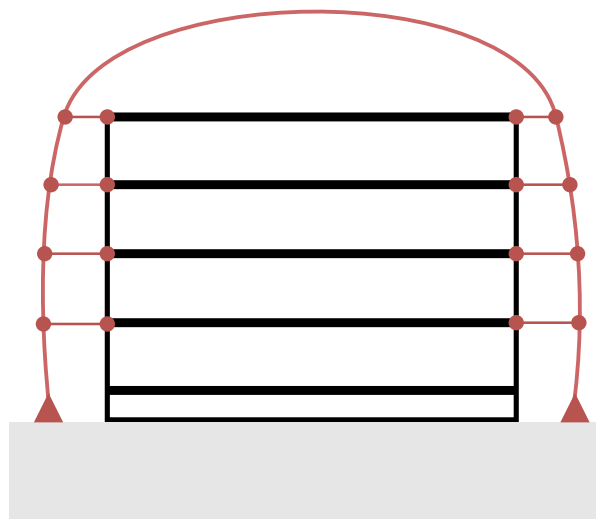


Figure 7.8: Mechanic scheme second skin

7.2.4. Stiffness supports

Ground supports

The stiffness of the support depends on the foundation and the current building because this is a preliminary design; the calculation can be simple. A few assumptions are made to determine the stiffness of the supports at the bottom. For example, the assumption is made that the structure will be supported by piles (200mm) with a strength class of C45/55. To calculate the stiffness of a pile a method described by Braam [63] will be used. The stiffness of a pile foundation is the combined stiffness of the pile and the tip, see Equation 7.1. That formula can be rewritten to calculate the stiffness of the pile foundation directly based on the stiffness of the concrete pile, see Equation 7.3. The factor β is the influence of the tip, the longer the pile, the smaller the influence. Also, the soil layers influence the factor β . The vertical stiffness of the supports is assumed to be 23 MN/m. For the full calculation see appendix E.

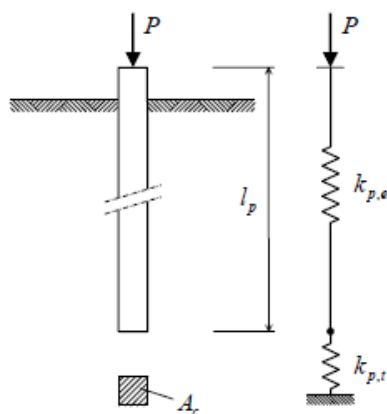


Figure 7.9: Scheme for the determination of the spring stiffness of the pile

$$\frac{1}{k_p} = \frac{1}{k_{p,el}} + \frac{1}{k_{p,t}} = \frac{1}{k_{p,el}} + \frac{\beta}{k_{p,el}} \quad (7.1)$$

$$k_{p,el} = \frac{E_c A_c}{l_p} \quad (7.2)$$

$$k_p = \frac{k_{p,el}}{1 + \beta} = \frac{E_c A_c}{(1 + \beta) l_p} \quad (7.3)$$

Building supports

For the support at each floor level, the stiffness is calculated by assuming a certain deformation and load. The deformations are determined with the help of NEN6702, Belastingen en vervormingen and the loads are the wind loads (NEN-EN 1991-1-4). The position of each spring is visualized in Figure 7.10. The stiffness of the supports can be found in Table 7.1. The stiffness is calculated in appendix E.

| Support | h [m] | k [MN/m] |
|---------|--------|----------|
| S0v | -0.17 | 22.9 |
| S1h | 3.68 | 0.30 |
| S2h | 6.78 | 0.15 |
| S3h | 9.88 | 0.10 |
| S4h | 12.745 | 0.09 |

Table 7.1: Stiffness of the supports

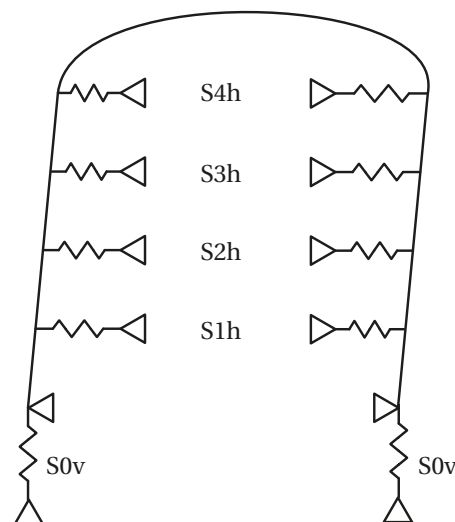


Figure 7.10: Names of the supports, h for horizontal and v for vertical

7.2.5. Connections

The connections are welded so they will be modelled as fixed. Because a triangular grid is used the moments in plane will be very low, so welded connections are not necessary. However, at the roof the out of plane the moments are indeed present, so bolted connections could be critical.

7.3. Materials and elements

7.3.1. Materials

The impact on the environment of high strength steel is often lower compared to ordinary steel. One of the reasons is that less material is needed to fulfil a specific function [64]. Therefore steel of at least quality S355 is used for the gridshell structure. The thickness of the glass panels must be determined as well so the

- Young's modulus $E: 210000 \text{ [N/mm}^2\text{]}$
- Shear modulus $G: 80760 \text{ [N/mm}^2\text{]}$

- Density Gamma: 78.5 [kN/m³]
- Thermal expansion, alphaT: 1.2E-5 [1/C°]
- Steel yield strength, fy:360 [N/mm²]

To determine the thickness of the glass panels a structural calculation is performed. The material properties of float glass are given below:

- Young's modulus E:72000 [N/mm²]
- Shear modulus G:29250 [N/mm²]
- Density Gamma: 25.0 [kN/m³]
- Strength, $f_{m;t;u;d} = 15.25$ [N/mm²]

The design strength of glass is calculated in appendix D

7.3.2. Cross section

Sizing optimisation is applied to the structure to minimize material usage. A family of cross sections is specified to keep the structure buildable. The Rectangular hollow section and the Square hollow section are compared (Figure 7.11).

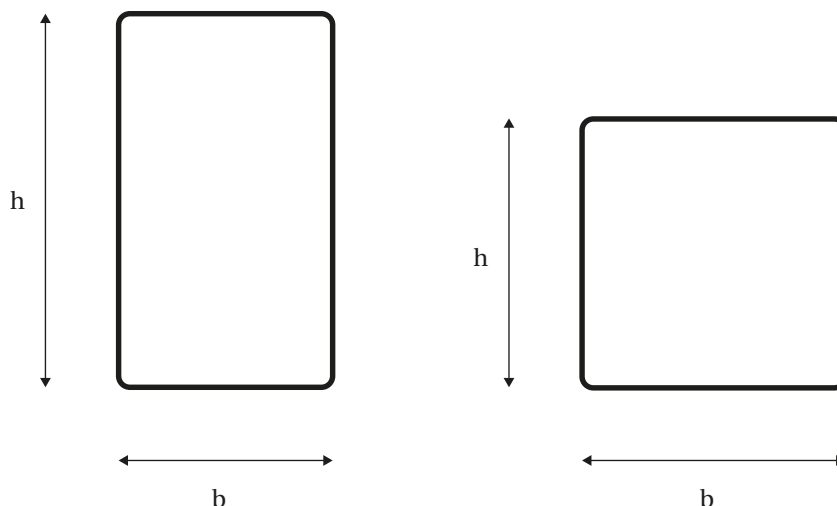


Figure 7.11: Rectangular hollow section or RHS on the left and the Square hollow section or SHS on the right

7.4. Loads

7.4.1. Load cases

Dead load (G)

The self-weight of the steel structure and the self-weight of the glass elements will be added in each load case.

- Specific weight of glass 25.0 kN/m³ SentryGlas 6.6.2 is used in the calculations [65]
- Specific weight of steel 78.5 kN/m³

Wind load (Q_w)

The wind load will be calculated with formula 7.4 which is a combination of equation 5.1 and 5.5 from NEN-EN 1991-1-4.

$$F_{w,e} = c_s c_d \cdot \sum_{elements} q_p(z_e) \cdot c_{pe} \cdot A_{ref} \quad (7.4)$$

- $c_s c_d$ is 1 in this calculation
- $q_p(z_e)$ is the peak velocity pressure at reference height z_e . The peak velocity pressure $q_p(z_e)$ is defined in the Dutch National Annex. The Mijnbouwstraat 106-112 is located in area II and for a building in urban Area with a height of 16.5m $q_p(z_e) = 0.83 \text{ kN/m}^2$
- c_{pe} is the pressure coefficient is determined with a CFD model made with Butterfly (Section 3.3.4)
- A_{ref} is the reference area on the structure, for this thesis the reference area is a facade panel. For each facade panel the cp-value is determined with the pressures from Butterfly and Equation 3.3. The cp-value is calculated for each facade panel, see Figure 7.12.

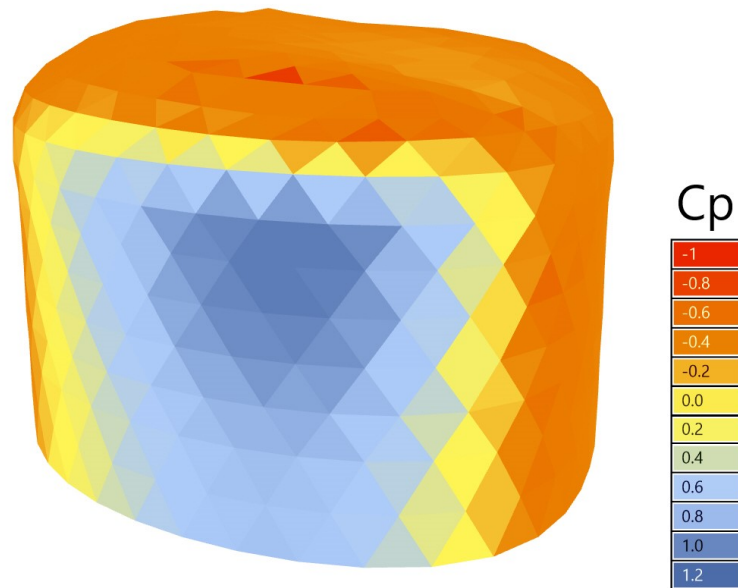


Figure 7.12: The cp-values of each facade panel in Butterfly including a safety factor of 1.45 for the uncertainty in the CFD model

Snow load (Q_{sn})

The snow load is defined by equation 7.5 (NEN-EN 1991-1-3), where the characteristic value of the snow load (s_k) is 0.7 kN/m^2 in the Netherlands and $C_e \cdot C_t$ can be 1.0 for this case. The shape coefficient is depended on the angle α (Figure 7.13a) and α is the angle between the normal of a facade panel and the global z direction (Figure 7.13b). The asymmetric snow load ($Q_{sn,asym}$) is of the same magnitude as the regular snow load only applied on half of the roof.

Snow accumulation cannot occur, because the round shape of the roof.

$$s = \mu_i \cdot C_e \cdot C_t \cdot s_k \quad (7.5)$$

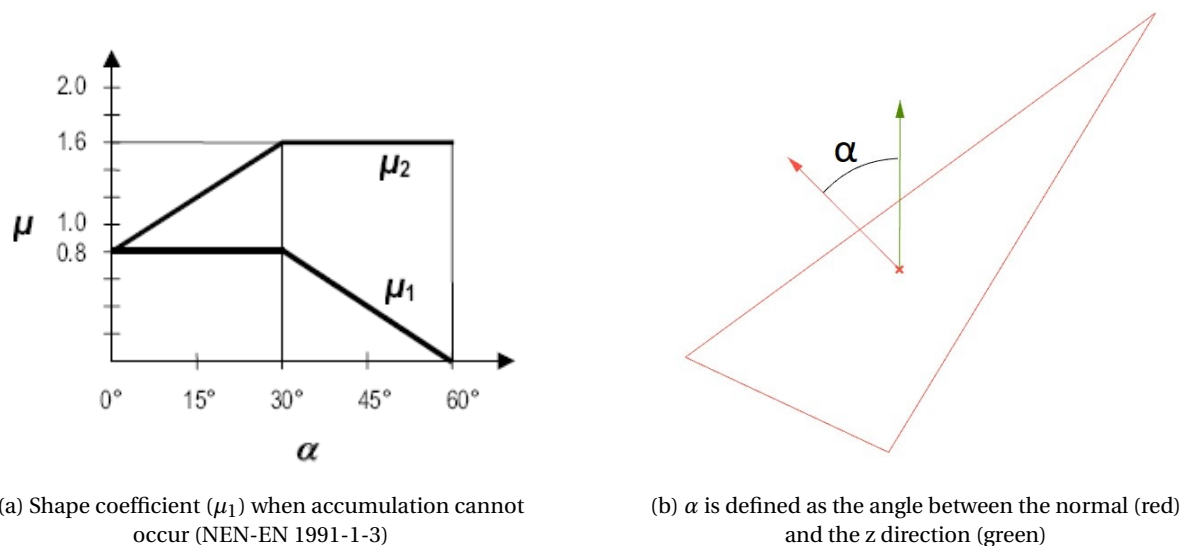


Figure 7.13: Snow load on a triangular facade panel

Maintenance load

The maintenance loading will be ignored in this preliminary calculation.

7.4.2. Load combinations

The construction will be tested on the basis of different load case either in ultimate limit state (ULS) or in serviceability limit state (SLS). A distinction between permanent load, which is mainly dead load of the glass and the steel beams, and variable loads like wind-, snow- and maintenance loading. The wind and snow load will be applied on the structure, and because a gridshell is sensitive for asymmetric loads, the snow load will also be applied asymmetrically ($Q_{sn,asym}$). Various load cases will be defined to check the structure. The safety factors will change depending on the dominant load. For example in load case 1 the dead load is dominant.

ULS

- 1) $1.35 * G$
- 2) $1.2 * G + 1.5 * Q_{sn}$
- 3) $1.2 * G + 1.5 * Q_{sn,asym}$
- 4) $1.2 * G + 1.5 * Q_w$

SLS

- 5) $1.0 * G$
- 6) $1.0 * G + 1.0 * Q_{sn}$
- 7) $1.0 * G + 1.0 * Q_{sn,asym}$
- 8) $1.0 * G + 1.0 * Q_w$

7.5. Structural requirements

The structural requirements are similar to the performance indicators because they determine which structures are valid, but the requirements cannot be used as performance indicators. A performance indicator gives a certain rating to a design, and the structural requirements determine if a structure is safe or not safe, nothing in between.

7.5.1. Displacement

To create a valid construction the maximum global displacement must be limited. In NEN 6702 Belastingen en vervormingen the limit is set to $w_{max} = 0.004 \cdot l$ where w_{max} is defined as the deflection under variable actions + permanent actions.

7.5.2. Strength

The strength will be checked by checking the utilization of the steel. The utilization of the steel will be tested with Karamba, and the limit of the utilization will be set to 80%.

7.5.3. Buckling

In Karamba local buckling of a single member will be tested. The best performing designs will be also be tested for global buckling in GSA.

7.6. Structural optimisation

In this section, the structural optimisation alone is performed. In the next section, structural optimisation and shape optimisation is discussed.

7.6.1. Design variables

Grid size

Based on the paper of Lai et al. [59] the assumption is made that a triangular grid is the most optimal grid. The type of the grid is determined but the size of the grid variable. The grid size is defined by two variables namely the height and the width, see Figure 7.14. Here the width is unrestricted, but the height is linked to the floors. Height of the grid is chosen so that at least one row of joints can be connected to the structural floor behind it. After testing

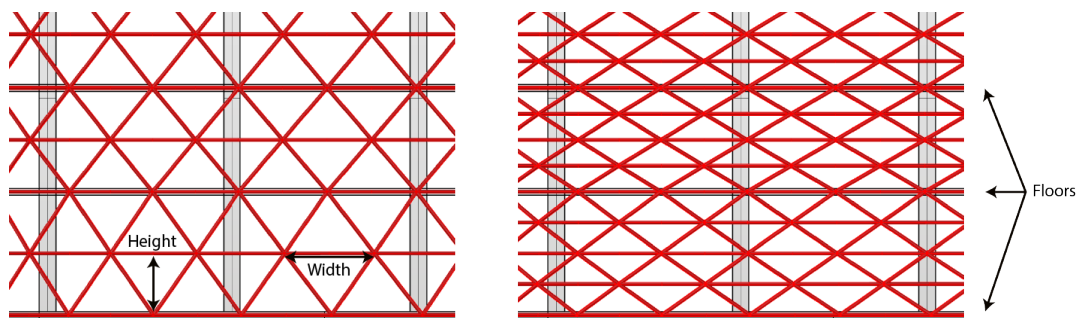


Figure 7.14: Two different grid configurations defined by the variables width and height

Cross section

The cross sections are variable to minimize material usage. Two cross-sections are compared namely rectangular hollow section (RHS) and the square hollow section (SHS). The RHS varies from 20x20x2.0mm to 400x400x8.0mm and the SHS varies from 50x30x3.2mm to 500x300x8.0mm. Besides that, the cross sections are grouped over the height and in the lateral direction to avoid many unique cross-sections. A top view of these sectors is shown in Figure 7.15.

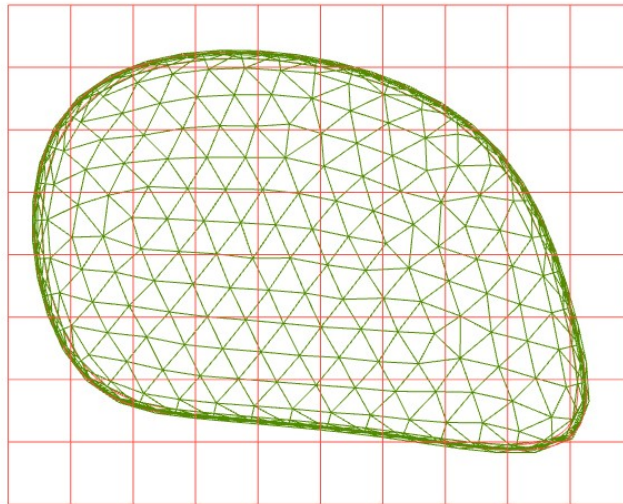


Figure 7.15: Top view of the structure with sectors

7.6.2. Performance indicator: Material usage

When a building consists of various materials, the embodied energy of a material can be used to quantify the environmental impact. By determining the life cycle energy, a building's environmental performance can be quantified. The total life-cycle energy of a building is the combination of embodied and operational energy. The embodied energy is the amount of energy consumed during production, renovation and demolition, whereas the operational energy is the energy required for heating, cooling and lighting [66], [67]. The operational energy is a relatively large portion of the total life cycle energy [68], but recent research shows the significance of embodied energy, which proportion is increasing due to the creation of more energy efficient buildings [69], [70]. A notable performance indicator is the amount of material applied in the structure. In this thesis comparing the mass of steel will suffice because that is the only material which is optimised. When comparing different buildings, the mass of steel per m^2 can be used.

The performance of the gridshell in this thesis can be compared to existing structures. For example The Great Court at The British Museum has a total steel mass of 478 ton and an area of 6700 m^2 ; the structure weighs 72 kg/m^2 [71]. The structure of Zlote Tarasy weighs 800 ton with an area of 10200 m^2 [72]. The structural weight is 78 kg/m^2 .

7.6.3. Process

The grid size and the cross-sections are both adjustable.

Grid size

The first process is very straight forward. The grid size (height and width) will be altered and the material used will be monitored. The best solutions will be investigated further. Because the design is parametric, it is possible to adjust the grid size. The process will be controlled with Galapagos.

OptiCroSec

Karamba is used for the structural calculations. Karamba has a component OptiCroSec (Figure 7.16) which can choose the smallest cross-section which is capable of transferring the loads. OptiCroSec chooses the optimal cross-section from a list of cross-sections (family) which must be given. Karamba uses the following procedure to determine which cross-section is suitable [73]:

1. Determining the section forces (moment, normal and shear) at three test points along the beam. At the two ends and in the middle

2. Check if buckling will appear.
3. Select the first entry from the family of cross-sections which can withstand the loads.
4. If all the beams are sufficient the algorithm stops.

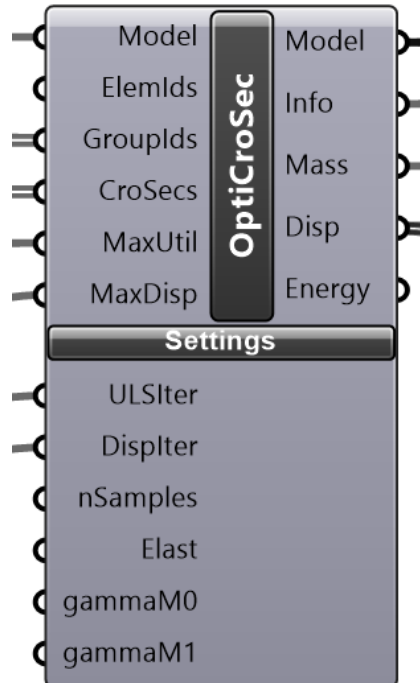


Figure 7.16: The OptiCroSec component can choose the appropriate cross-sections to withstand the loads

The options of OptiCroSec are:

- Model: the model to be optimized
- ElemIds: elements (beams) to include, by default all elements are included
- GroupIds: All the separate group names, each element is part of one of the groups, elements in the same group get the same cross-section
- CrosSecs: The family of cross-sections to choose from.
- MaxUtil: the maximum utility allowed, it is set to 0.8. If the utility is overstepped a heavier beam will be selected
- MaxDisp: the maximum utility for the displacement, is set to 1.0
- For the other inputs see the documentation [73].

A different buckling length is used in plane and out of plane to calculate local buckling. The gridshell is a single layer triangular gridshell, so the stiffness in plane is higher than the stiffness out of plane. Depending on the stiffness of the nodes, the buckling length in plane can vary between $0.5L_{sys}$ and L_{sys} , see situation one and three in Figure 7.17. The nodes are welded but not infinitely stiff, so the buckling length is set to $0.7L_{sys}$. The stiffness of out of plane is set to $2L_{sys}$. When the buckling length is set to $2L_{sys}$, the requirements for global buckling in GSA are met as well.

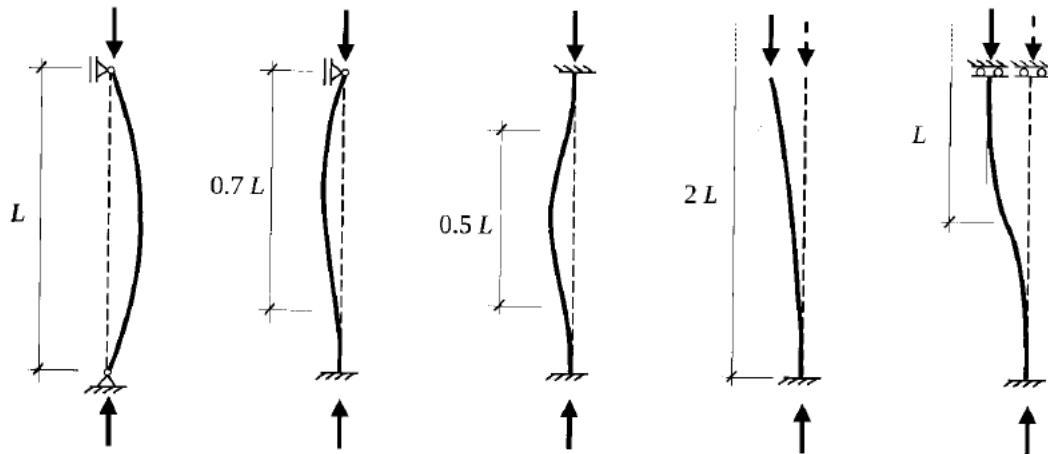


Figure 7.17: Buckling length as a function of the real length L_{sys} of the column

Grouping

OptiCroSec has an option to group beam. If the option is not used Karamba considers each beam as an individual and very unrealistic nodes can be created. OptiCroSec iterates a few times to find the optimal configuration, but it tends to converge to an unrealistic situation like a beam of 400x400mm connected to a 20x20mm beam, see Figure 7.18. To avoid connections like these grouping will be used. Roughly a dozen groups will be created, which increases the buildability of the structure.

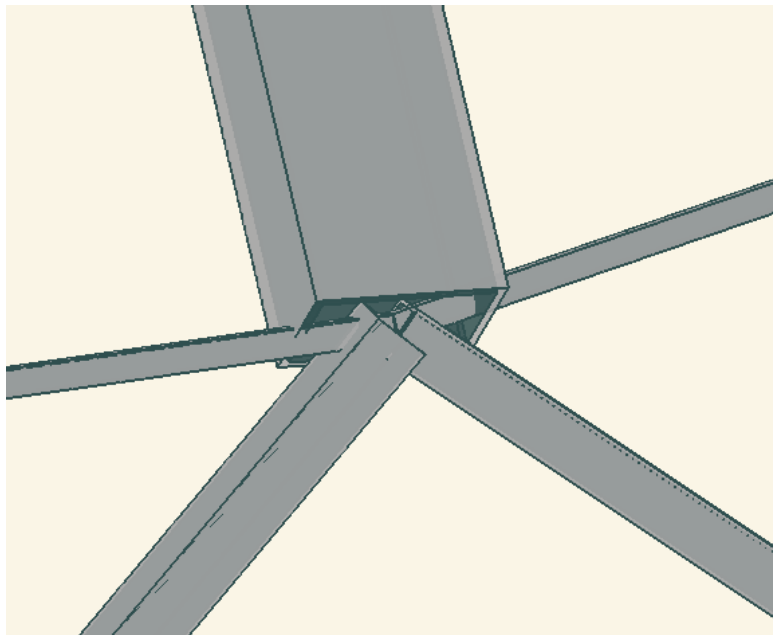


Figure 7.18: Example of a challenging connection, largest beam is RHS350x250x16.0mm and the smallest beam is RHS50x25x2.5mm

7.6.4. Results

Three best designs of the shape optimisation will be used (shape 1-3). These three designs are analysed with different cross-sections (RHS and SHS) and different grid sizes. The structure is stiff in plane because a triangular grid is used. Therefore one can expect that RHS profiles would perform better. Indeed there is a big difference in performance, the five best results all contain the RHS profile. To rank the structures the steel mass per area is used. The lightest structure weighs 15.42 kg/m^2 , is based on shape 1 and weighs 25350 kg in total, see Figure 7.2. The second best weighs 15.45 kg/m^2 , is based on shape 3 and weighs 24950 kg in

total. The total weight is less, but the facade area is smaller, so the structural performance per m^2 is worse. The vertical grid size is linked to the structural floors, so the amount of options is limited. The size is either 3.8, 1.9 or 0.95 m, 1.9 m appears to be the most optimal solution. The best solution (15.42 kg/m^2) will be checked more thoroughly in the next section.

| CFD | Design variables | | | performance indicator | |
|--------|---------------------|-------------------|---------|-----------------------|--------------------------------|
| | Grid horizontal [m] | Grid vertical [m] | Section | Steel mass [kg] | Steel mass [kg/m^2] |
| shape1 | 2.2 | 1.9 | RHS | 25350 | 15.42 |
| shape3 | 2.1 | 1.9 | RHS | 24950 | 15.45 |
| shape1 | 2.6 | 1.9 | RHS | 25200 | 15.47 |
| shape1 | 2.7 | 1.9 | RHS | 25450 | 15.63 |
| shape1 | 2.4 | 1.9 | RHS | 26000 | 15.83 |
| shape3 | 2.4 | 1.9 | RHS | 25800 | 15.99 |
| shape1 | 2.2 | 1.9 | SHS | 29580 | 18.15 |
| shape1 | 2.1 | 1.9 | SHS | 29990 | 18.40 |
| shape1 | 2.5 | 1.9 | SHS | 30860 | 18.79 |
| shape1 | 2.1 | 1.9 | SHS | 31430 | 19.18 |
| shape3 | 2.1 | 1.9 | SHS | 31320 | 19.39 |
| shape3 | 2.2 | 1.9 | SHS | 32500 | 20.12 |

Table 7.2: Comparison of multiple designs with different shapes sorted by steel mass [kg/m^2]

Displacement

The displacement is checked in SLS, and the displacements stay within limits, see Table 7.3. The maximum displacement is present in the middle of the roof.

| Load Combination | Limit state | U [m] | Umax [m] | Check |
|------------------|-------------|-------|----------|-------|
| LC1 | ULS | 0.066 | - | - |
| LC2 | ULS | 0.119 | - | - |
| LC3 | ULS | 0.077 | - | - |
| LC4 | ULS | 0.009 | - | - |
| LC5 | SLS | 0.049 | 0.108 | OK |
| LC6 | SLS | 0.089 | 0.108 | OK |
| LC7 | SLS | 0.061 | 0.108 | OK |
| LC8 | SLS | 0.009 | 0.108 | OK |

Table 7.3: Maximum deflections according to Karamba

Strength and Buckling

Only the ten cross-sections with the highest utilisation grades are shown in Table 7.4. The average utilisation is 0.33 and the cross-sections vary from RHS50x25x2.5 till SHS150x100x10.0. The maximum utilisation for local buckling is 0.79. Global buckling will be checked in GSA, see Section 7.9.

| Beam id | Cross-section | Length [m] | Util all | Util Buckling | N max [kN] | M Resultant[kNm] |
|---------|-------------------|------------|----------|---------------|------------|------------------|
| 75 | RHSH60x40x6.3 | 1.44 | 0.86 | 0.79 | -38.89 | 0.24 |
| 665 | RHSH60x40x6.0 | 1.33 | 0.84 | 0.74 | -41.71 | 0.32 |
| 73 | RHSH60x40x6.3 | 1.44 | 0.80 | 0.73 | -35.99 | 0.23 |
| 186 | RHSH60x40x6.3 | 1.66 | 0.75 | 0.68 | -25.40 | 0.22 |
| 189 | RHSH60x40x6.3 | 1.41 | 0.74 | 0.66 | -34.01 | 0.30 |
| 185 | RHSH60x40x6.3 | 1.42 | 0.74 | 0.66 | -33.13 | 0.25 |
| 187 | RHSH60x40x6.3 | 1.42 | 0.73 | 0.66 | -33.20 | 0.26 |
| 553 | RHSH60x40x6.0 | 1.33 | 0.73 | 0.69 | -38.47 | 0.14 |
| 106 | RHSH76.2x50.8x3.2 | 1.53 | 0.71 | 0.66 | -21.47 | 0.11 |
| 1425 | RHSH90x50x8.0 | 1.43 | 0.71 | 0.43 | -80.53 | 3.03 |

Table 7.4: Utilisation, normal forces and moments according to Karamba

7.7. Structural and shape optimisation

At this stage the shape optimisation and structural optimisation are executed separately, and the results are known (Section 6.7.4 and 7.6.4). With the help of those results, the effect of integrating a structural optimisation with a shape optimisation can be quantified. The estimation is that height has a big influence on the efficiency, and by separating the structural and shape optimisation a suboptimal solution is found. Because the shape optimisation was done beforehand, the roof height converged to the smallest height possible. This behaviour is logical because the smaller the object, the smaller the resistance against the wind. It is good to check what the effect is of this split and see if the structure performs better if the height increases.

After the structural optimisation the lightest structure is 15.42 kg/m² (25350 kg in total). The CFD analysis takes much time and so the number of input parameters must be reduced, therefore, the input parameter k¹ was set to 3 m in the shape optimisation. However, a low k can perform well in the shape optimisation and bad in the structural optimisation. To see how important the input parameter k is the structural optimisation and shape optimisation will be done at the same time.

The importance of the shape in the structural analysis is visible in Figure 7.19. The wind forces are determined with a CFD analysis when the roof height is 3.0 m, when the height increases the wind forces are extrapolated. Because of this extrapolation, the results are an estimation. In the previous optimisation, the roof height (k) was set at 3.0 m, and the lightest solution weighted 15.42 kg/m². When including the roof height (k) as variable, the mass might be reduced by 43%, see Table 7.5.

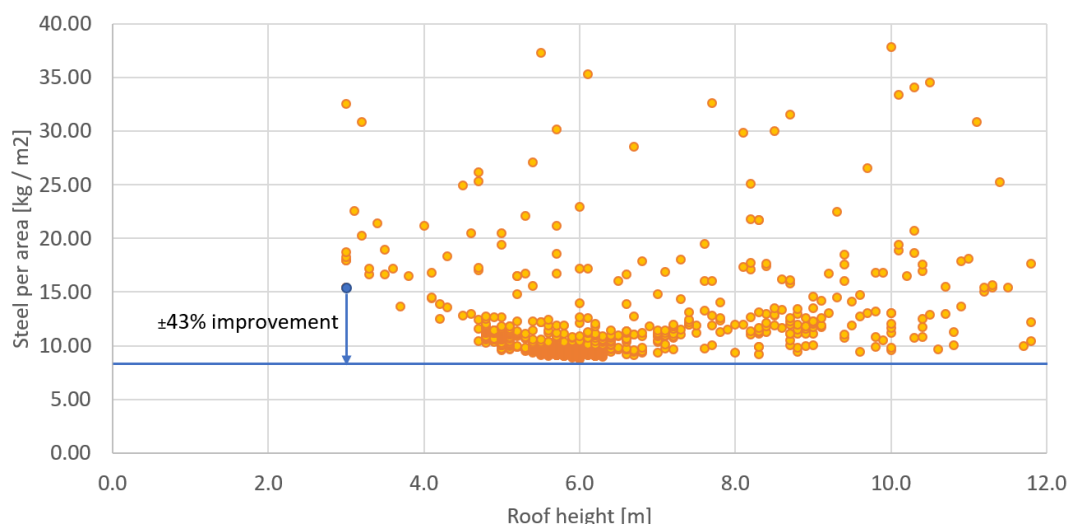


Figure 7.19: The relation between the roof height (input k) [m] and the mass of steel per area [kg/m²]. The orange dots present possible solutions for the gridshell with varying grid sizes. The blue dot is the solution mentioned in the previous section.

¹The factor k is discussed and visualised in a Section 6.7.1, see Figure 6.12.

| Design variables | | | | performance indicator | |
|------------------|---------------------|-------------------|---------|----------------------------|-------------|
| Roof height [m] | Grid horizontal [m] | Grid vertical [m] | Section | Steel [kg/m ²] | Improvement |
| 3.0 | 2.2 | 1.9 | RHS | 15.42 | - |
| 6.0 | 1.8 | 1.9 | RHS | 8.75 | 43.3% |
| 8.0 | 1.6 | 1.9 | RHS | 9.33 | 39.5% |
| 10.0 | 1.7 | 1.9 | RHS | 9.82 | 36.3% |

Table 7.5: This table highlights some of the best solutions presented in Figure 7.19. The blue dot is the starting point and by changing the roof height the mass per meter area can be reduced.

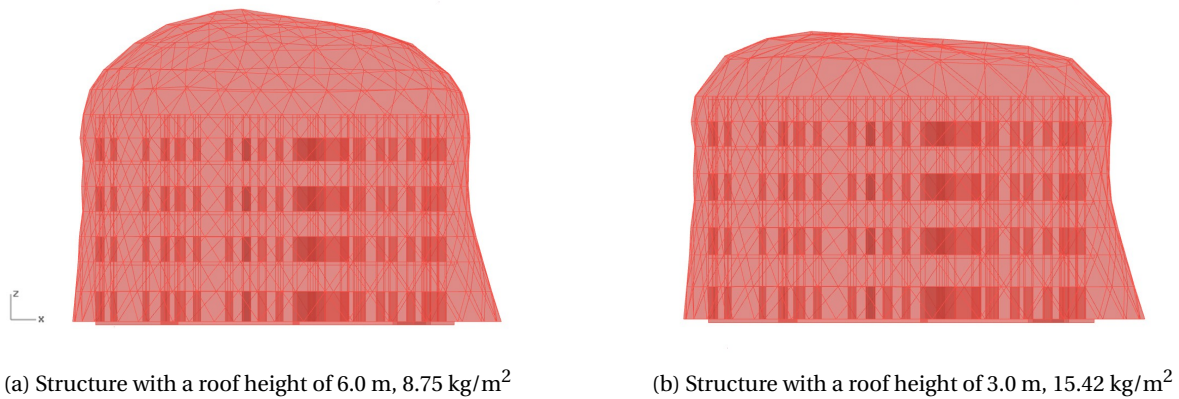


Figure 7.20: Two cases of structural optimisation with a roof height of 3.0m or 6.0m

7.8. Benchmark: Karamba and GSA

In this section, the results of Karamba and GSA are compared.

7.8.1. Displacement

The maximum displacements in Karamba are very similar to GSA. Worst case scenario (in SLS) there is a difference of 3.14%. The deflections are determined per load case and displayed in Table 7.6.

| Load Combination | Limit state | Karamba: U [m] | GSA: U [m] | Umax | Check |
|------------------|-------------|------------------|--------------|-------|-------|
| LC1 | ULS | 0.066 | 0.065 | - | - |
| LC2 | ULS | 0.119 | 0.116 | - | - |
| LC3 | ULS | 0.077 | 0.075 | - | - |
| LC4 | ULS | 0.009 | 0.008 | - | - |
| LC5 | SLS | 0.049 | 0.048 | 0.108 | OK |
| LC6 | SLS | 0.089 | 0.087 | 0.108 | OK |
| LC7 | SLS | 0.061 | 0.059 | 0.108 | OK |
| LC8 | SLS | 0.009 | 0.009 | 0.108 | OK |

Table 7.6: The maximum deflections in Karamba and GSA

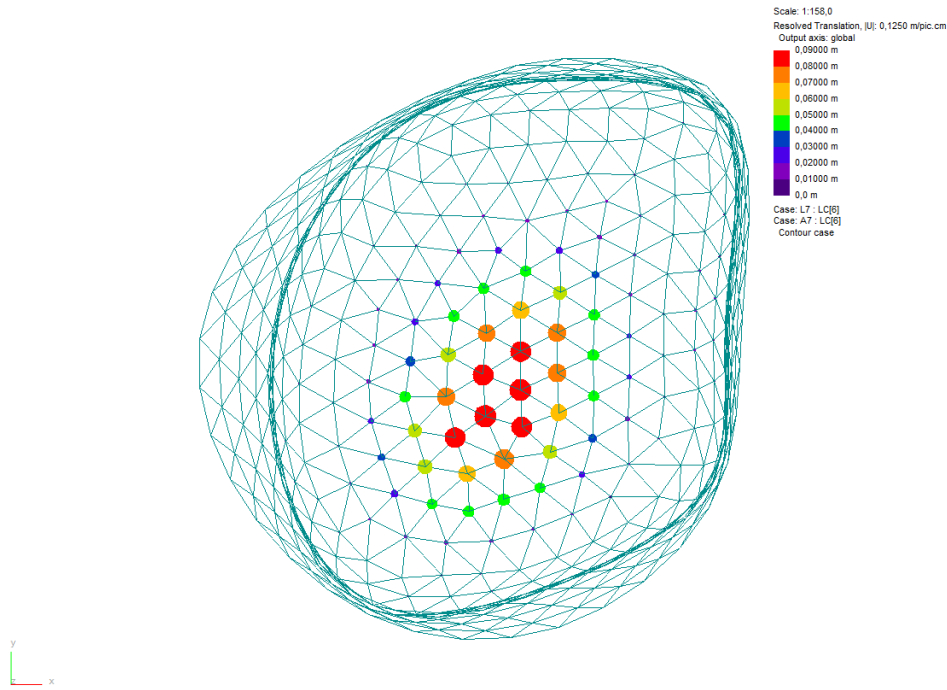
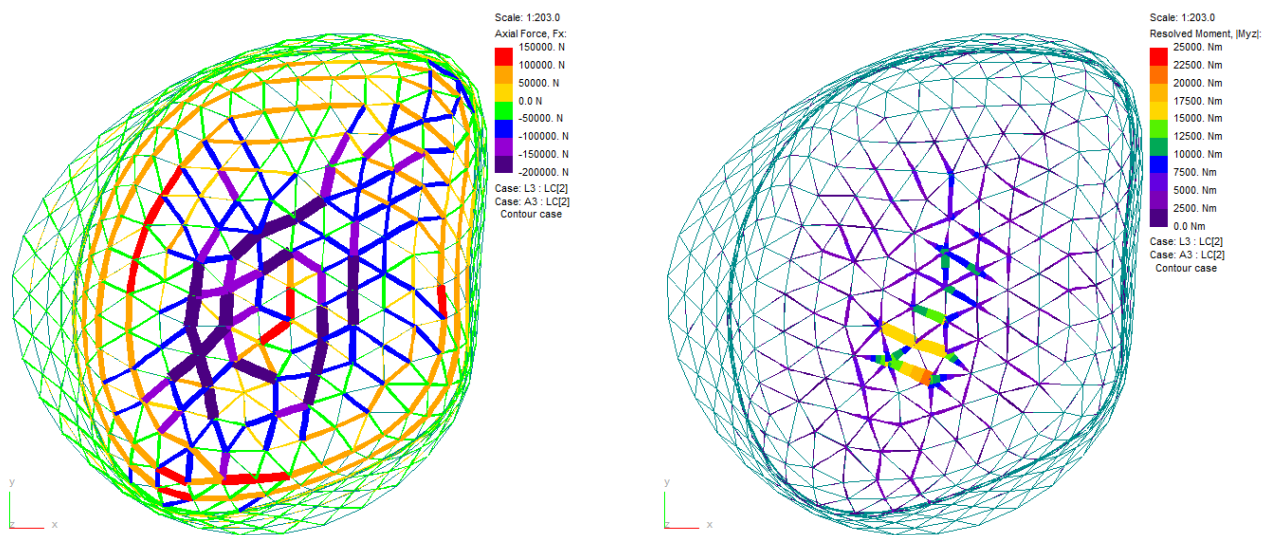


Figure 7.21: Topview of the deflection in SLS: LC6 snow is dominant

7.8.2. Forces and Moments

The difference between the forces and moments is small. The absolute difference in the normal force is 2.1 kN at maximum and the difference between the moments is 0.13 kNm, see Table 7.7. The fifteen beams with the largest Von Mises stresses are shown. The axial stresses and resolved moments are displayed in Figure 7.22.



(a) Topview of the axial forces, F_x in ULS: LC2 snow is dominant

(b) Topview of the resolved moment, $|M_{yz}|$ in ULS: LC2 snow is dominant

Figure 7.22

| element | Cross-section | Length [m] | Karamba LC 2 | | | | GSA LC 2 | | | | Difference | |
|----------------|-------------------|------------|--------------|---------|------------|---------|------------|--------------------------------|---------|------------|------------|------------|
| | | | Util all | Fx [kN] | Myz [kNm] | Fx [kN] | Myz [kNm] | Von Mises [N/mm ²] | Fx [kN] | Myz [kNm] | Fx [kN] | Myz [kNm] |
| 71 | RHSH60x40x6.3 | 2.39 | 0.54 | -19.00 | 0.08 | -18.83 | 0.09 | 236.90 | -0.01 | 0.05 | | |
| 137 | RHSH50x25x2.5 | 2.33 | 0.11 | 10.57 | 0.02 | 10.47 | 0.02 | 214.30 | -0.01 | 0.01 | | |
| 444 | RHSH60x40x6.0 | 1.91 | 0.69 | -35.72 | 0.13 | -35.77 | 0.14 | 204.80 | 0.00 | 0.06 | | |
| 51 | RHSH60x40x6.3 | 2.19 | 0.40 | -16.75 | 0.06 | -16.73 | 0.06 | 198.90 | 0.00 | 0.05 | | |
| 256 | RHSH76.2x50.8x3.0 | 2.27 | 0.06 | 0.17 | 0.05 | 0.18 | 0.05 | 194.30 | 0.04 | 0.01 | | |
| 268 | RHSH60x40x2.5 | 1.97 | 0.52 | -12.45 | 0.17 | -12.38 | 0.17 | 187.10 | -0.01 | 0.02 | | |
| 348 | RHSH50x25x2.5 | 2.23 | 0.08 | -0.33 | 0.05 | -0.42 | 0.05 | 186.10 | 0.28 | 0.02 | | |
| 423 | RHSH60x40x3.0 | 2.16 | 0.56 | -12.90 | 0.09 | -12.87 | 0.09 | 181.80 | 0.00 | 0.02 | | |
| 49 | RHSH60x40x6.3 | 2.22 | 0.38 | -15.80 | 0.03 | -15.82 | 0.04 | 179.80 | 0.00 | 0.05 | | |
| 410 | RHSH76.2x50.8x3.0 | 1.78 | 0.37 | -25.22 | 0.21 | -25.48 | 0.22 | 179.40 | 0.01 | 0.01 | | |
| 253 | RHSH60x40x4.0 | 2.27 | 0.06 | 3.41 | 0.03 | 3.43 | 0.03 | 177.60 | 0.01 | 0.03 | | |
| 263 | RHSH76.2x50.8x3.0 | 1.94 | 0.38 | -23.67 | 0.13 | -23.67 | 0.13 | 174.30 | 0.00 | 0.00 | | |
| 85 | RHSH76.2x50.8x3.0 | 2.49 | 0.40 | -15.23 | 0.21 | -15.20 | 0.22 | 171.10 | 0.00 | 0.02 | | |
| 486 | SHSH50x5.0 | 2.40 | 0.72 | -29.97 | 1.19 | -30.13 | 1.232 | 160 | 0.2 | 0.04 | | |
| 595 | SHSH90x8.0 | 4.80 | 0.74 | -75.66 | 8.19 | -75.83 | 8.388 | 159.7 | 0.2 | 0.20 | | |
| Average | | 2.01 | 0.33 | -9.99 | 0.88 | -9.99 | 0.90 | 50.11 | 0.00 | 0.02 | | |
| Max | | 2.65 | 0.86 | 142.93 | 21.88 | 143.30 | 22.02 | 236.90 | 0.49 | 0.13 | | |
| Min | | 1.02 | 0.01 | -194.00 | 0.01 | -194.70 | 0.01 | 3.44 | -2.07 | -0.13 | | |

Table 7.7: Difference between the forces and moments in Karamba and GSA. The beam are sorted by the Von Mises stress from large to small and only the first ten elements are shown. The average, maximum and minimum values of all the elements are displayed at the bottom.

7.9. Global buckling

The stability of a gridshell is influenced by the shape of the structure and the type of structure. The paper of Cai et al. [74] is used as a reference because it has several similarities with this thesis, namely the load combination (dead load and snow load) and the type of grid. A single layer gridshell with quadrangular mesh (Figure 7.23), as described in the paper of Cai et al. [74], has a buckling load factor of 0.63. In this case, the critical load is smaller than the design-load, because the buckling load factor is defined as the ratio of the critical load to the design load. With braces, the buckling load factor increases to 6.0, which is more reasonable for a design. The paper of Cai et al. [74] does not give guidelines for the design of a gridshell but the critical load for a shell structure, which is sensitive to imperfections, must be larger than $6 \cdot$ design load [75].

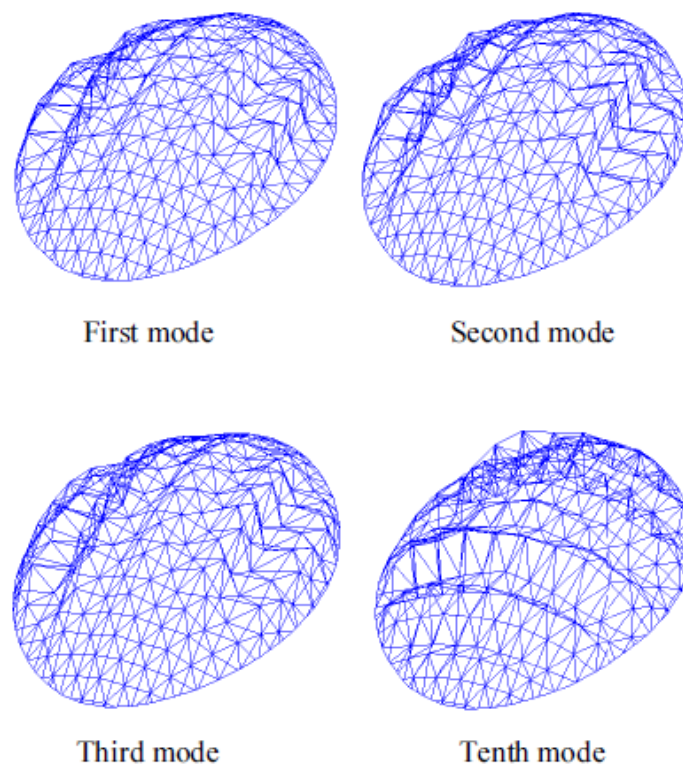


Figure 7.23: Four buckling modes of a single layer gridshell under a symmetric loading [74]

In Karamba single members are checked for local buckling. In GSA a global buckling analysis is executed to check for weak spots. This is done with the modal buckling analysis. The buckling is tested for all the load combinations in ULS LC1-4, and LC2 appears to be dominant. When testing the structure with LC2, the structure buckles when $5.1x$ the load is applied. The structure buckles at the bottom of the grid, see Figure 7.24. To increase the safety factor, the members will increase from RSH60x40x6.0mm to RSH76.2x50.8x3.0mm. After the increase, the safety factor is 6.1.

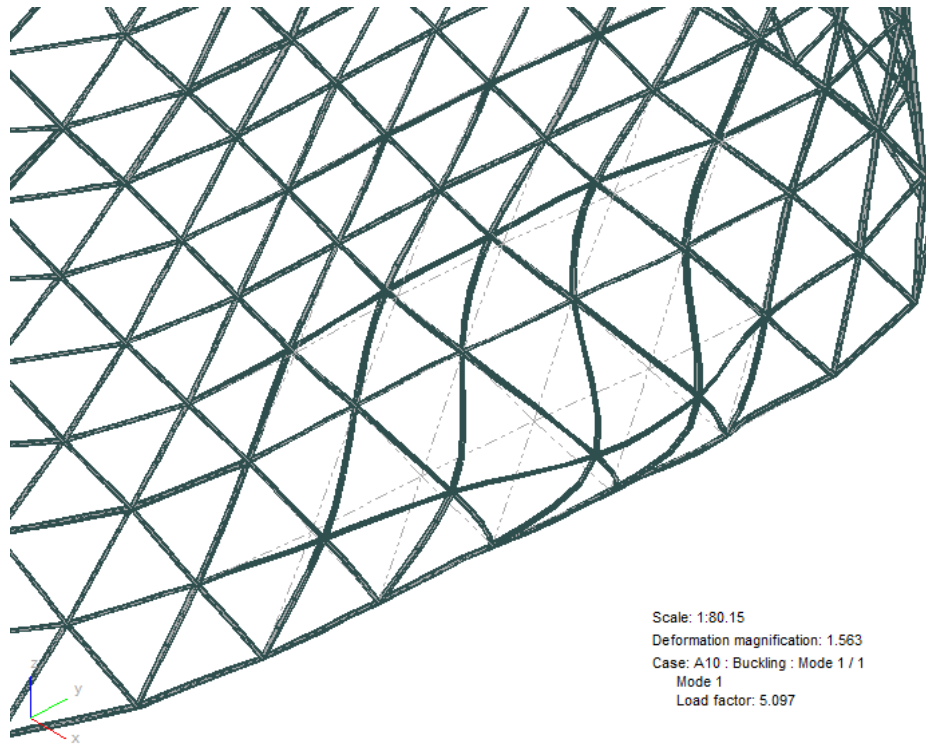


Figure 7.24: The buckling load factor is 5.1x LC2 (ULS) snow load is dominant

7.10. Testing spring supports

Because the structure is attached to an existing building, it is not accurate to assume that the supports are infinitely stiff. Therefore spring supports will be tested, to see the influence on the support reactions. Two problems which will be discussed are negative support reactions and high support reactions. The negative support reactions arise when spring supports are used, and fixed supports are a remedy for high support reactions. Multiple gridshell designs can be used, to test the support reactions. The gridshell used in this section has the following specifications:

- Horizontal grid size = 3.9 m
- Vertical grid size = 1.9 m
- Profiles: SHS
- Shape 2 is used for the shape of the structure

Also, the building will move when a load is applied, and at higher levels more deflection is present. A simple model is made where each floor level has a certain stiffness. The stiffness is calculated in Figure E. The springs can be divided into two groups, one at ground floor level ($z = -0.17$) and one is attached to the building ($z > -0.17$ m). The supports at the ground floor level are assumed to be supported by pile foundation, the supports in the z -direction are spring supports, and in x - y -direction, they are pinned. The supports attached to the building have a local axis where the z -direction is aligned with the normal of the facade, see Figure 7.25.

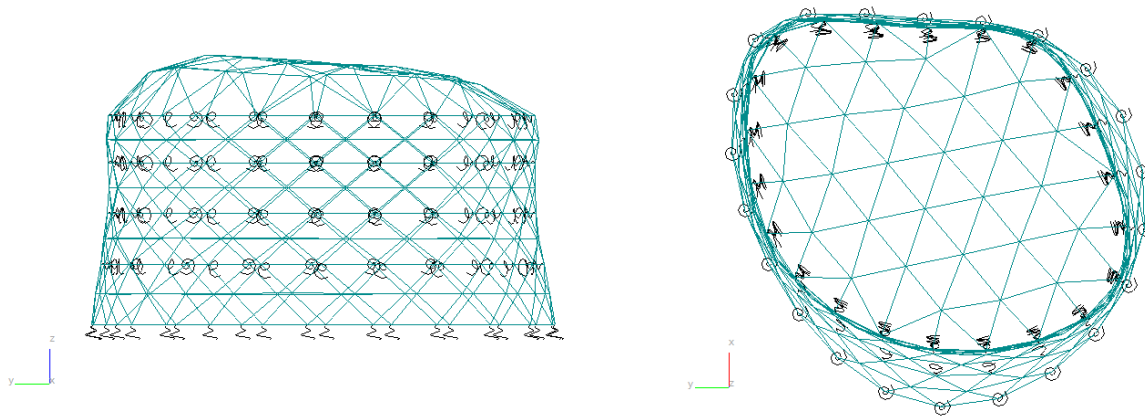


Figure 7.25: Visualisation of the spring supports (left) and pinned supports (right) in GSA.

In the tables the supports are named G or B, where G stands for ground support and B is a connection to the building.

7.10.1. Negative support reactions

At the bottom, there are 22 supports. Overall the support reactions (F_z) reduce or increase slightly when using spring supports, see Table 7.8. The slight increase in forces will not be a problem for the foundation. However in load combination 4 (wind) there are negative support reactions, see node 222 and 223. This requires extra attention; the foundation must be able to take up the negative forces. Also, the stiffness of the supports is estimated so that the actual forces might differ.

| Support | Pinned support | | | | Spring support | | | | Change (max) [N] |
|---------|----------------|------|------------|------------|----------------|------|------------|------------|------------------|
| | Node | Case | Fz min [N] | Fz max [N] | Node | Case | Fz min [N] | Fz max [N] | |
| G1 | 429 | LC2 | 28260 | 67030 | 204 | LC8 | 34610 | 76420 | 9390 |
| G2 | 430 | LC2 | 23110 | 57490 | 205 | LC8 | 30460 | 60270 | 2780 |
| G3 | 431 | LC2 | 27880 | 63470 | 206 | LC5 | 22700 | 40380 | -23090 |
| G4 | 432 | LC2 | 26820 | 61990 | 207 | LC5 | 21950 | 38760 | -23230 |
| G5 | 433 | LC2 | 23730 | 60290 | 208 | LC8 | 23020 | 63020 | 2730 |
| G6 | 434 | LC2 | 26810 | 67570 | 209 | LC8 | 28290 | 77490 | 9920 |
| G7 | 435 | LC2 | 23580 | 57670 | 210 | LC8 | 29290 | 63950 | 6280 |
| G8 | 436 | LC2 | 30610 | 74620 | 211 | LC8 | 30660 | 66650 | -7970 |
| G9 | 437 | LC2 | 32840 | 71400 | 212 | LC8 | 34780 | 59890 | -11510 |
| G10 | 438 | LC2 | 26110 | 61110 | 213 | LC8 | 32220 | 56450 | -4660 |
| G11 | 439 | LC2 | 24540 | 58410 | 214 | LC8 | 25310 | 58080 | -330 |
| G12 | 440 | LC2 | 23690 | 56800 | 215 | LC8 | 21140 | 46660 | -10140 |
| G13 | 441 | LC2 | 26030 | 59520 | 216 | LC8 | 25800 | 52250 | -7270 |
| G14 | 442 | LC2 | 23750 | 58540 | 217 | LC8 | 27270 | 60930 | 2390 |
| G15 | 443 | LC2 | 20700 | 57640 | 218 | LC8 | 31530 | 66930 | 9290 |
| G16 | 444 | LC2 | 23990 | 61160 | 219 | LC8 | 40380 | 70880 | 9720 |
| G17 | 445 | LC2 | 29600 | 66700 | 220 | LC5 | 38850 | 67740 | 1040 |
| G18 | 446 | LC2 | 27300 | 60000 | 221 | LC5 | 24160 | 42760 | -17240 |
| G19 | 447 | LC2 | 21000 | 56390 | 222 | LC4 | -21780 | 21000 | -35390 |
| G20 | 448 | LC2 | 21210 | 58240 | 223 | LC4 | -22400 | 38420 | -19820 |
| G21 | 449 | LC2 | 25790 | 61990 | 224 | LC4 | 11720 | 58700 | -3290 |
| G22 | 450 | LC2 | 25410 | 59350 | 225 | LC8 | 28150 | 69610 | 10260 |

Table 7.8: Support reactions in F_z

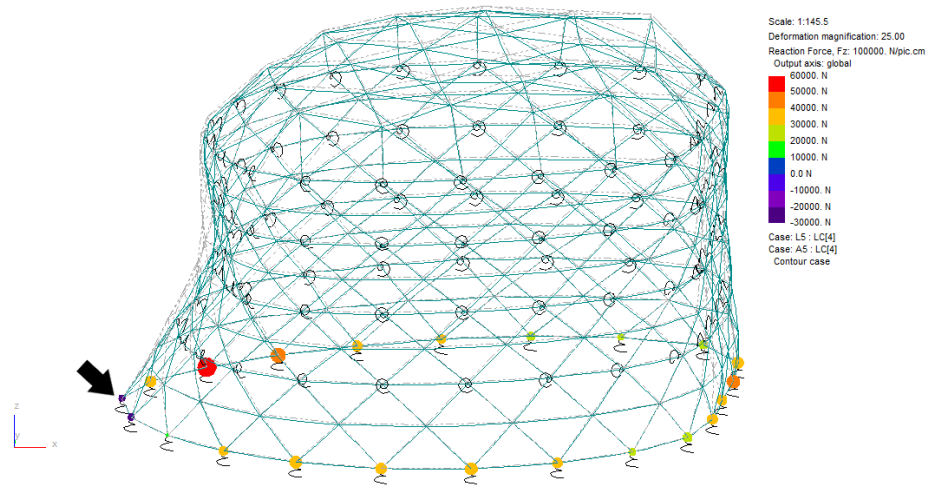


Figure 7.26: Visualisation of the support reactions F_z in GSA. Load combination 4 (dominant wind load) causes negative support reactions which are indicated with a black arrow

7.10.2. Relation between support stiffness and support reactions

The issue mentioned above arises when spring supports are used. When pinned supports are used the connections at the top, have to endure high forces. The forces at these connections are higher than the forces at the ground supports, see Figure 7.27. When spring supports are used the forces reduce in general. The ten highest supports reactions are shown in Table 7.9, all the support reactions are shown in Appendix E Section E.3. For a detailed design, the stiffness of the supports must be known to determine the magnitude of support reactions, because the stiffness has a large impact on the support reactions.

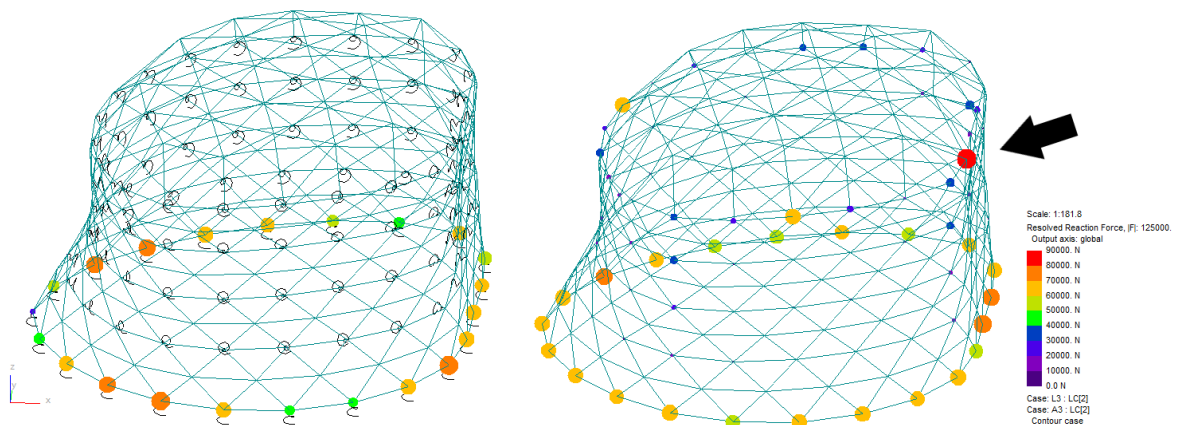
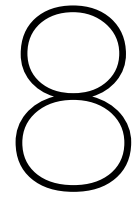


Figure 7.27: Visualisation of the support reactions $|F|$ in GSA (load combination two dominant snow load). The structure on the left has spring supports, and the structure on the right has pinned supports. The highest load is marked with a black arrow and present at the top right of the building.

| Support | Pinned support | | | Spring support | | | Change |
|---------|----------------|------|--------|----------------|------|--------|----------|
| | Node | Case | F [N] | Node | Case | F [N] | |
| B73 | 386 | LC2 | 81790 | 161 | LC2 | 1130 | ● -80660 |
| B69 | 382 | LC2 | 65510 | 157 | LC2 | 455.4 | ● -65055 |
| B84 | 397 | LC2 | 65470 | 172 | LC2 | 201.2 | ● -65269 |
| B55 | 346 | LC2 | 38090 | 121 | LC2 | 1559 | ● -36531 |
| B72 | 385 | LC2 | 37210 | 160 | LC2 | 123.3 | ● -37087 |
| B86 | 399 | LC2 | 34970 | 174 | LC4 | 544.5 | ● -34426 |
| B50 | 341 | LC2 | 33810 | 116 | LC2 | 1183 | ● -32627 |
| B45 | 336 | LC2 | 32610 | 111 | LC2 | 814.5 | ● -31796 |
| B79 | 392 | LC2 | 31750 | 167 | LC2 | 749.6 | ● -31000 |
| B67 | 380 | LC2 | 30760 | 155 | LC3 | 181.9 | ● -30578 |

Table 7.9: The largest forces (|F|) in the connections attached to the building.



Ventilation concept

This chapter will answer the question: "How to integrate a low energy ventilation system in the design and what can be achieved?". The first part of the question is answered in Section 8.1 to 8.5. Here ventilation system is explained, and the integration with the facade is clarified. Section 8.6 to 8.7 substantiate what can be achieved in terms of uptime of the ventilation system.

8.1. Ventilation concept: mean idea

The ventilation concept is a combination of multiple ventilation types, see Figure 8.1. The ventilation types are discussed in Section 5.3. Due to the floor plan of $23.7 \times 16 \text{ m}^2$, single-sided ventilation and cross ventilation are difficult to realise. A rule of thumb for single-sided ventilation is $\text{width}_{\text{room}} \leq 2 \cdot \text{height}_{\text{room}}$ and for cross ventilation $\text{width}_{\text{room}} \leq 5 \cdot \text{height}_{\text{room}}$ [42] [33]. With a height of 2.5m, no room is suitable for these types of ventilation. Moreover, contamination originated from inside the building can spread from one room to another when cross ventilation is used. To avoid these problems, a shaft is positioned in the building and is connected to a central outlet. The position of the shaft does not necessarily have to be in the middle of the building; it can be shifted to the sides. There are multiple inlets around the facade which open or close depending on the wind direction to provide a pressure difference between the inlet and the outlet. The second skin will be essential to establish a constant wind flow, and this will be explained in Section 8.4.

The calculations for the ventilation system are influenced by the position of the main insulating layer. The second skin can function as a thermal barrier, but the thermal barrier can also be positioned inside the building near the existing facade. The later is chosen because the cavity will not be accessible for occupants, so it is not useful to insulate that area. Also, the second skin itself would be more complicated if it is a thermal barrier.

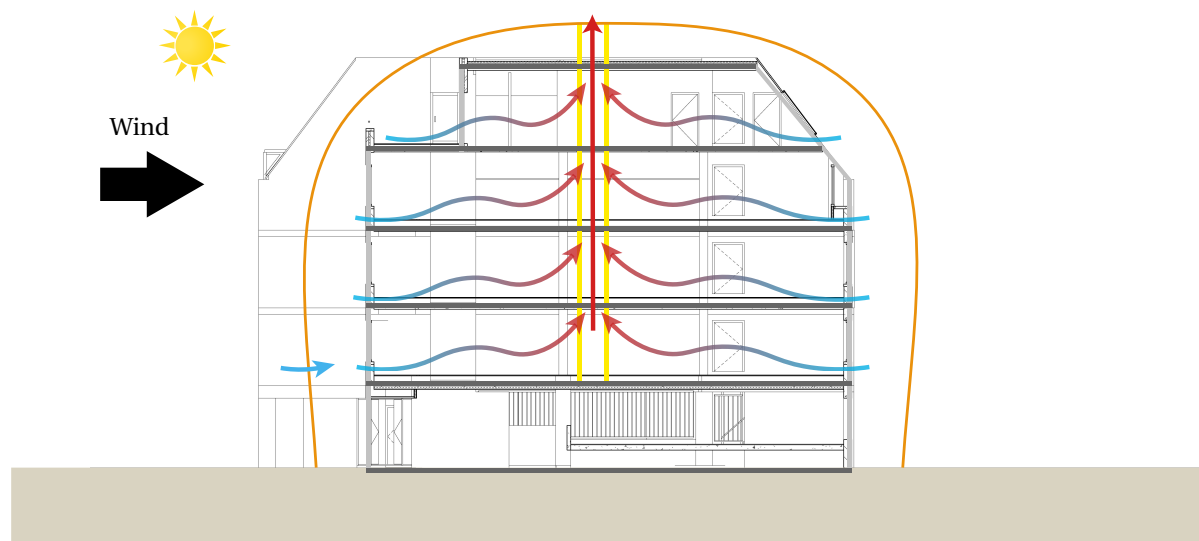


Figure 8.1: Ventilation concept with a central shaft

8.2. Ventilation demand

Two regulations of the Bouwbesluit 2012 are important for ventilation. Firstly, the required amount of ventilation is $6.5 \text{ dm}^3/\text{s}$ per person for an office building. Secondly, the number of persons per m^2 area must be higher than 0.05 which is 20 m^2 per person. In the NEN 1824:2010 is stated that each workplace must have a minimum area of 4 m^2 excluding meeting rooms or closet space. To avoid an under-dimensioned ventilation system, the ventilation system will be designed with 12 m^2 per person including meeting rooms or closet space. Each floor of the Mijnbouwstraat is 325 m^2 , enough for 27 people. The required amount of ventilation per floor is $175 \text{ dm}^3/\text{s}$.

8.3. Behaviour of the openings

With fixed openings, the wind can contribute or counteract the stack effect depending on the pressure difference at the inlet and outlet. By creating movable openings wind always contribute regardless of the wind direction. In a simple 2d situation the wind can come from the left side or the right side of the building, and the openings react to the wind direction, see Figure 8.2. The assumption is made that the wind pressure coefficient on the roof is always negative, so the wind flows from the inlet to the roof. For the actual building

the openings are positioned all around the facade and which of them are open or closed is determined by the wind direction. The next section will discuss this behaviour in more detail.

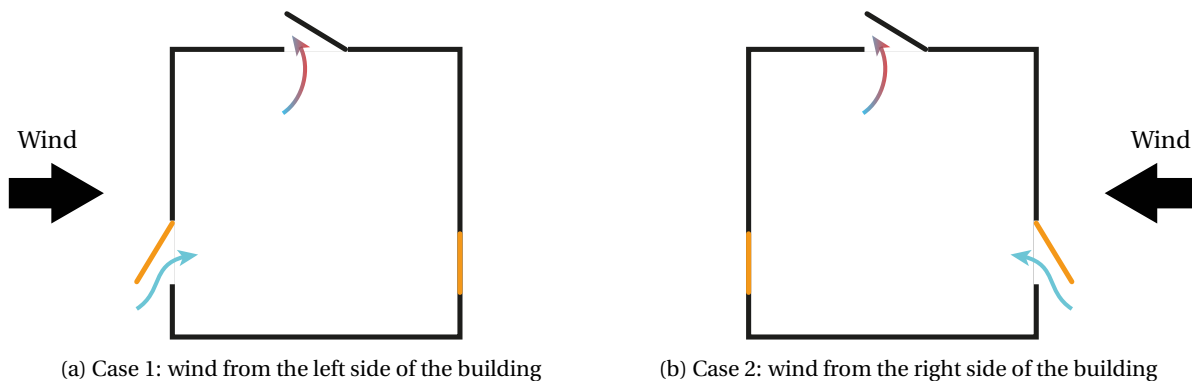


Figure 8.2: The inlets are open if the wind is pointed towards the opening, at the outlet a lower pressure is present

8.4. Position openings

There must be a pressure difference between the inlet and the outlet to establish a wind flow. The pressure difference between the inlet and outlet must be maximised to increase the uptime of the ventilation system.

8.4.1. Stack-effect

The stack-effect is influenced by the temperature difference between inside and outside but also by the position of the openings. To maximise the airflow the height difference between the inlet and the outlet must be as large as possible. The downside of positioning the inlet close to ground level is easier access for unauthorised people and animals. Therefore the inlet must be positioned a few meters above ground level. When the openings is positioned 3 m above the ground it is not accessible people without tools. At 3.7 the structural floors are positioned and when the operable windows are positioned near the structural floors the electronics can be hidden. The openings will be positioned at the height of 3.7 m.

8.4.2. Wind

The best position regarding the wind depends on the c_p -values. In Figure 8.3 the c_p -values for two wind directions are visualised where the red areas indicate the zones with a positive pressure coefficient and the blue zones indicate a negative pressure coefficient. One of the assumptions made previously is that the wind pressure coefficient on the roof is always negative. Only if it is windless, the assumption is not completely correct; if the wind speed is 0, the pressure coefficient is meaningless. In all other situations, the pressure coefficient is indeed negative and positioning the outlet on the roof is a logical option.

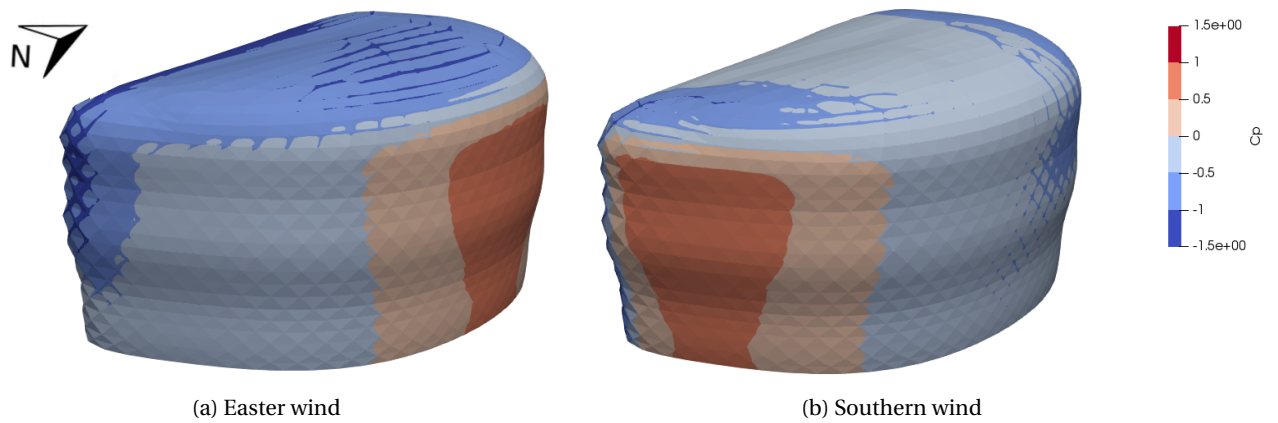


Figure 8.3: The magnitude and sign of the cp-values depend on the wind direction

The position of the inlet is not that simple. Because of the changing wind direction, the pressure coefficient can either be positive or negative. The simplest solution is to position the openings in the dominant wind direction but the operational time of the system would still be low. To increase the operational time, electric ventilation grills of windows can be positioned all around the facade and open when a positive wind pressure coefficient occurs. The pressure can be monitored near an opening to determine if it should be opened or not. Another option is to attach a weather station to the roof and measure the wind speed and direction. The relation between the wind direction and the pressures at the opening can be found theoretically but also experimentally. By monitoring the pressures at the openings over a certain period the relationship between the wind direction and the pressures at the openings can be established. The relation can be used to control the openings. Lastly, the wind flow inside the building can be monitored and used to control the ventilation openings.

To show the behaviour in more detail a slice of the building at 3.7 m is made, see Figure 8.4. Here the positive and negative pressure coefficients are indicated with a plus and minus sign and by the colour. When the electric grills are opened at the position of the green dashed line, an overpressure will be created everywhere inside the skin. This overpressure in combination with the pressure on the roof will establish an airflow.



Figure 8.4: Horizontal slice at 3.7 m above ground level of Figure 8.3b showing the cp-values

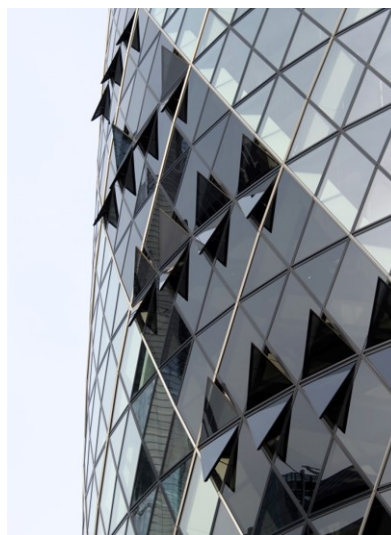
8.5. Design ventilation openings

8.5.1. Type of opening

An important difference between natural ventilation and mechanical ventilation is the size of the openings. When mechanical ventilation is used ventilation grills with sound dampening is applicable (see Figure 8.5a). For natural ventilation these openings would be too small, Duco offers grills with a maximum opening of 25 mm [76]. Besides that, Duco offers larger night-ventilation grills without sound dampening. Openable windows are also an option when using natural ventilation, see Figure 8.5b. These project openings similar to the Gherkin in London will be used in the design.



(a) Duco electronic ventilation grill [76]



(b) Openable windows of the Gherkin in London [77]

Figure 8.5: Two different types of openings in the facade

8.6. Calculation procedure

Two calculation programs will be discussed namely the CIBSE spreadsheet and Contam. Both programs work with the same equations. The CIBSE spreadsheet will be the starting point to calculate the initial opening size, and Contam will be used for fine-tuning those results. The reason for this is that CIBSE spreadsheet is good for a quick calculation but is limited. Only a few specific building configurations can be calculated. Also, Contam cannot calculate the ventilation openings directly. The size of the openings is an input, and the airflows are the outcome.

8.6.1. Equations

To calculate the size of the ventilation openings only a few formulas are needed. The first formula uses the principle of mass conservation of a fixed volume defined by the envelope and gives the relation between the flow rates of the openings, see Equation 8.1. For the context of a ventilation design, the difference between the densities can be ignored so the equation can be simplified to $\sum q_i = 0$.

$$\sum \rho_i q_i = 0 \quad (8.1)$$

- ρ_i is the density of the air at height i [kg/m^3]
- q_i is the flow rate through opening i [m^3/s]

Secondly, the flow rate through an opening and a pressure difference across it can be calculated with Expression 8.2 where i identifies the opening [33].

$$q_i = C_{di} \cdot A_i \cdot \sqrt{\frac{2|\Delta p_i|}{\rho_0}} \quad (8.2)$$

- A_i is the size of opening i [m²]
- C_{di} is the discharge coefficient (usually around 0.6)
- Δp_i is the pressure difference [Pa]
- ρ_0 is the air density [1.225 kg/m³]

Lastly, the pressure difference at opening i relative to the neutral height can be calculated with expression 8.3. $\Delta\rho_0 g z_i$ is the pressure difference due to the buoyancy forces at a height z_i above the reference level, and $0.5\rho_0 U^2 C_{pi}$ is the pressure difference induced by the wind [33].

$$\Delta p_i = \Delta p_0 - \Delta\rho_0 g z_i + 0.5\rho_0 U^2 C_{pi} \quad (8.3)$$

- Δp_0 is the pressure difference at the reference level
- g is the gravity constant [9.81 m/s²]
- z_i is the height of opening i [m]
- U is the wind speed [m/s]
- C_{pi} is the pressure coefficient

8.6.2. CIBSE spreadsheet

These expressions are put into work in a spreadsheet to calculate the size of the ventilation openings. The spreadsheet of CIBSE¹ is used as a basis and is adjusted to fit the Mijnbouwstraat as good as possible. The building has four inlets and one central outlet, in contrast to the concept mentioned at the begin of this chapter there is no second skin and an atrium instead of a shaft, see Figure 8.6.

As a starting point, the ventilation will be designed with buoyancy forces alone and will operate if the difference between the inside (T_{in}) and outside (T_{out}) temperature is 3 K. The other variables used for this calculation are: inlets heights (related to the floor heights of Mijnbouwstraat), an inlet flow of 175 dm³/s per floor, $T_{in} = 21\text{C}^\circ$ and a Cd value of 0.6. The variables are shown in Table 8.1 together with the results. The details of the calculation of the ventilation openings can be found in appendix B.

| Opening number | Height [m] | Cp [-] | Flow [m ³ /s] | Cd [-] | A [m ²] |
|----------------|------------|--------|--------------------------|--------|---------------------|
| 1 | 3.68 | 0.45 | 0.175 | 0.60 | 0.198 |
| 2 | 6.78 | 0.55 | 0.175 | 0.60 | 0.234 |
| 3 | 9.88 | 0.60 | 0.175 | 0.60 | 0.302 |
| 4 | 12.745 | 0.40 | 0.175 | 0.60 | 0.487 |
| Outlet | 16.33 | -0.20 | -0.700 | 0.60 | 1.948 |

Table 8.1: Results of the sizes of the openings

¹this spreadsheet may be downloaded from the CIBSE website (www.cibse.org/venttool)

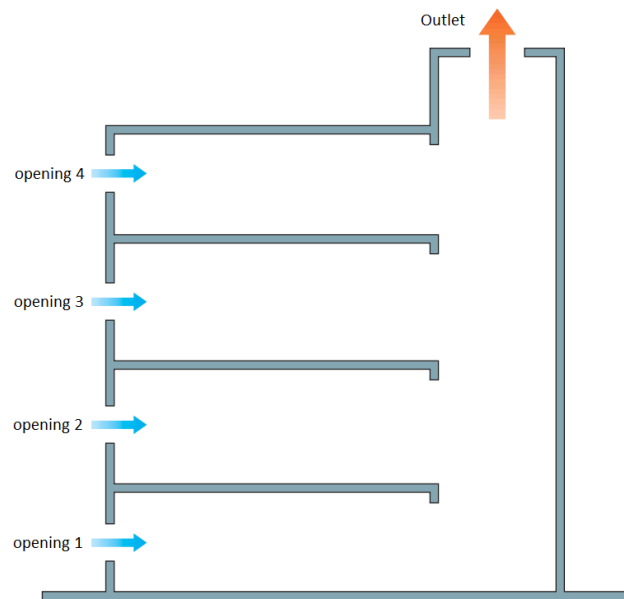


Figure 8.6: Simplification of the ventilation concept

8.6.3. Contam

The main issue with the spreadsheet is that the resistance of the shaft is missing. In Figure 8.6 the rooms are connected with a shaft, and the shaft is connected to the outside. The resistance between the rooms and the shaft is neglected in this example. In reality, there is some resistance, and this cannot be neglected. With Contam this resistance can be added.

Contam version 3.2 released in 2015-06-08 is used for the calculation. Contam, short for contamination, is a multizone air quality and ventilation analysis program. Setting up a project is a bit cumbersome because the software is dated, but the documentation [78] is very extended which makes the input, output and the processes very understandable. Two examples of Irving et al. [33] are verified with Contam to make sure the program is used correctly, see appendix C. The results conclude that Contam is accurate.

Also, the second skin is tested in Contam, and the influence is nil if the temperature of the cavity is identical to the outside temperature. If there is a difference in temperature, the results will differ. In a good model, the temperature of the cavity depends on T_{in} , T_{out} and the other heat sources like the sun. This is not possible in Contam so the assumption is made that $T_{cavity} = T_{out}$.

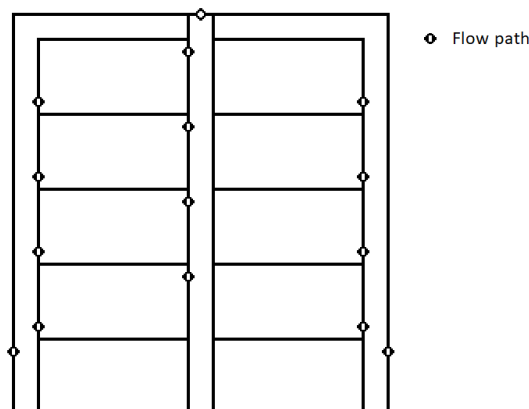


Figure 8.7: 2d-view of the project in Contam, the ground floor is the garage and does not contain any flow paths

8.6.4. Contam result

With the proper settings, the error between the CIBSE spreadsheet and Contam is <1%. The benefit of Contam is that the shaft resistance can be added. For now, the room-shaft connection is defined as an opening of 1x1 m². If there is no resistance, the airflow will be 0.175 m/s at all floor levels, when the resistance is added the results drop to 0.161 m/s, see Table 8.2. Even though the airflow is below the requirements, the size of the openings are kept the same because an outlet >2 m² would not be convenient. This means that the ventilation will be provided by stack-effect if the temperature difference is higher than 3.6 K; this value is determined with Contam. If the availability throughout the year will be meagre, the size can be increased.

T_{in} : 21 °C
 T_{out} : 18 °C
 ρ : 1.212 kg/m³
 Wind: 0 m/s

| Opening: | z_i [m] | C_p | C_{di} | A_i [m] | q_i [m/s] |
|----------|-----------|-------|----------|-----------|-------------|
| 1 | 3.68 | 0.45 | 0.6 | 0.198 | 0.1723 |
| 2 | 6.78 | 0.55 | 0.6 | 0.234 | 0.1713 |
| 3 | 9.88 | 0.60 | 0.6 | 0.302 | 0.1691 |
| 4 | 12.745 | 0.40 | 0.6 | 0.487 | 0.1609 |
| outlet | 16.33 | -0.20 | 0.6 | 1.948 | 0.6736 |

Table 8.2: Results Contam, no wind and $T_{in} - T_{out} = 3$ K

The results shown in the table above are the results of a single calculation. Weather data can be imported to get an idea of the ventilation throughout the year, and a calculation can be done for each hour of the day, 365 days a year. In the next section, this feature will be used to check the uptime of the ventilation system.

8.7. The uptime of the ventilation system

An important aspect of a hybrid ventilation system is to check the availability of natural ventilation. The availability of the wind is already discussed Section 3.5 *Wind availability*, but the driving force for the ventilation system is not wind alone. The system will be driven by wind, buoyancy or a mechanical system, where mechanical ventilation can be considered as "downtime". This is not completely correct because ventilation is up and running but it does not work on natural resources. The ventilation based on buoyancy is the main driving force if that is not available the wind will be used as a backup. If the required amount of wind is not available than mechanical ventilation is needed. This process is visualized with a flowchart in Figure 8.8.

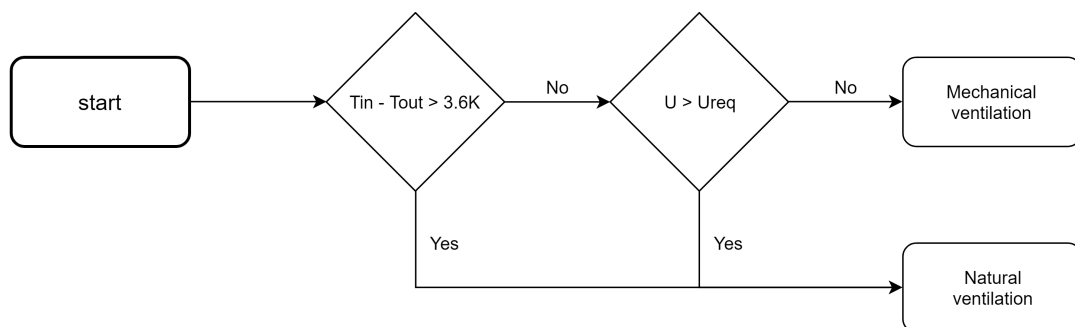


Figure 8.8: Flowchart hybrid ventilation

The inside temperature is 21°C during office hours and when the outside temperature is lower than 18°C the ventilation is provided by the stack effect. At a higher temperature, a certain amount of wind is required to let the ventilation system work without mechanic ventilation. For example, at an outside temperature of 19°C a meteorologic wind speed of at least 2.74 m/s (see cell B11 in appendix B on page 117) is required to provide

a flow of $175 \text{ dm}^3/\text{s}$ at each floor. The value of 2.74 m/s is found by increasing the meteorologic wind speed (B11) until all the ventilation openings meet the requirements. Instead of checking the results manually per hour Contam can process multiple time steps in a sequence.

The historical weather data of the KNMI over the period 2000-2017 is imported in Contam, and for each hour the appropriate type of ventilation will be calculated and stored. The appropriate type of ventilation is determined in accordance with the flowchart (Figure 8.8). Lastly, the results are grouped per month and visualised in a flowchart, see Figure 8.9. The chart can be read as follows, in May 75.7% of the time the stack effect can provide the required amount of ventilation, 18.1% of the time wind can be used as a backup and 6.2% of the time mechanical ventilation is needed. Yearly, the ventilation systems use 93.5% of the time natural sources for the ventilation.

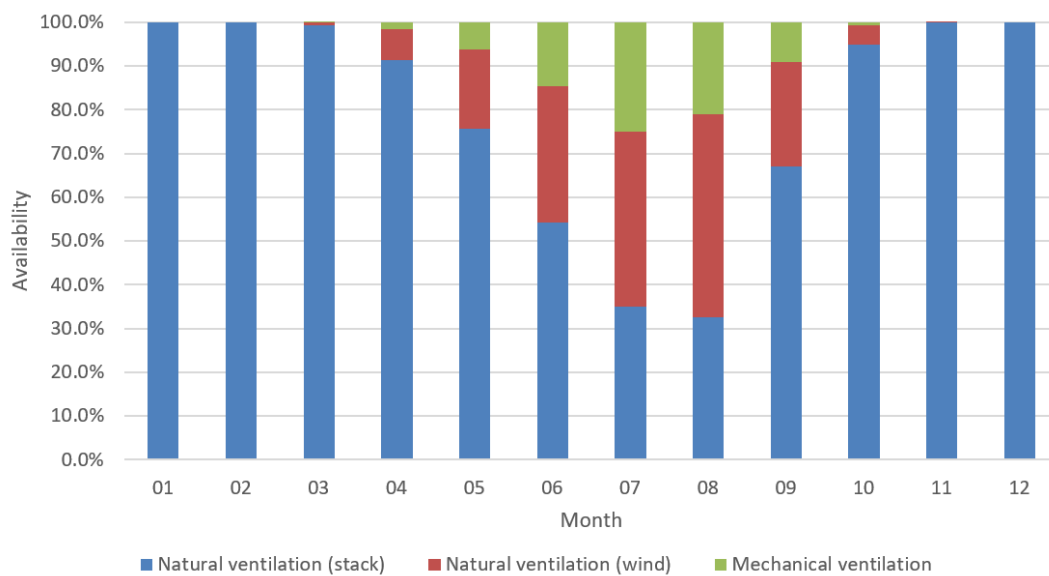


Figure 8.9: The availability of different types of ventilation based on historical data of the KNMI over the period 2000-2017

III

Conclusion & Reflection

9

Conclusion & Reflection

9.1. Conclusion

"What can be achieved - in terms of structural and building physics performance - when an existing skin of a building is removed and replaced by a new facade?"

The answer to the research question will be given by answering the three subquestions. The following three subquestions will be discussed:

- How to perform a shape optimisation of a facade to reduce the wind load by making the building more aerodynamic?
- What is the effect of integrating a structural optimisation with a shape optimisation?
- How to integrate a low energy ventilation system in the design and what can be achieved?

9.1.1. Shape optimisation

How to perform a shape optimisation of a facade to reduce the wind load by making the building more aerodynamic?

This question can be answered by setting up a plan with different steps to perform a shape optimisation. The objective or performance indicator of the optimisation is to reduce the wind load on the structure. For an optimisation four steps must be followed (Figure 2.3):

1. the input
2. the simulation
3. the output
4. the optimisation program (including an objective, optimisation settings and the stop criterion)

1. Input or design variable

When using CFD models in an optimisation process, time is scarce. However, time is needed to explore the design space with many individual calculations. The design space can be limited by reducing the number of inputs or adjust the boundaries of the input values. The input must be chosen with care because with a too strict limit; possible solutions might be left out. To check if the inputs are good, different set-ups can be tested. In this thesis, the input is the shape of the facade. The shape of the facade must be simplified to a string containing genes (Figure 2.6) to use the shape in the optimisation process. The string can contain digits, and with a parametric program like Grasshopper, these digits can represent a shape. An example of how a set of digits define a shape is presented in Section 6.7.1 Design variable: Floor offset.

2. The CFD simulation

The first step is to set-up the CFD simulation. To set-up the CFD simulation some background information is needed, which is given in Chapter 3 Wind engineering. The set-up of the model is done in Butterfly; this is a Grasshopper plugin which can perform CFD analysis. The engine for the CDF analysis is OpenFOAM. After setting up the geometry, the computational domain, the mesh and the boundary conditions, the model must be verified. Most literature investigates standard, rectangular buildings. The background information about these simple buildings is pervasive and great to use for calibration. For example, the work of Richards et al. [32] and Wright and Easom [30] can be used to verify the simulation by means of a simple 6m cube, see 6.2 Comparing Butterfly with existing research. If the buildings are freeform, extra information is welcome. This can be gathered from research but only for specific buildings. Another option is to use state of the art software like ANSYS to verify Butterfly. The results are more reliable when Butterfly is compared with other software. Butterfly itself is not mature and under development, but the engine (OpenFOAM) is reliable so with the right settings the results are also reliable. The last step to set-up the model is the grid sensitivity analysis (Section 6.4), which indicates whether the results are reliable.

3. Output or performance indicator

When optimising a problem, the output determines the fitness of the simulation. Moreover, by maximising or minimising the fitness, the best solution can be found. In this case, the output is the wind load on the building, more specific, the resultant wind force, see Figure 6.15. The resultant wind force is found, with the help of Butterfly. When the simulation is complete, the cp-values around the facade are calculated. With the help of the Eurocode (Equation 7.4) the cp-values are used to calculate the wind load. The resultant wind force is defined as the summation of the wind load on the facade.

4. Optimisation program

Most Grasshopper users are familiar with Galapagos, but Galapagos does not work with Butterfly. Another optimisation program is needed, to perform an optimisation with Butterfly. For this thesis, a Python script is used as optimisation program, see Appendix A. The objective of this program is to minimise the resultant wind force. After each generation, the fitness is determined and based on the fitness a new generation is created. The program generates twenty-one generations of solutions, and the progress can be seen in Figure 6.22.

Reflection

In this thesis, a low-rise building is considered. This is done because a high-rise building is more difficult to analyse with a CFD program. The size of the computational domain is influenced by the height of the building, and a larger computational domain takes more time to analyse. Doing this thesis with a high-rise building and with the same resources was not possible. Nevertheless, it would be interesting to scale-up and investigate a high-rise building. In case of a high-rise structure, a reduction of the wind load would have more value compared to a low-rise building. When investigating a high-rise building, arranging the resources like a supercomputer becomes part of the project. This thesis was about exploring and visualising the possibilities of an optimisation driven by a CFD analysis, but since the results show the added value, it can be taken a step further. Currently, the maximum drag force and side force acting on the building at the Mijnbouwstraat is 454kN. With the shape optimisation, this residual wind force is reduced by 40-45% to 247kN.

9.1.2. Structural optimisation

What is the effect of integrating a structural optimisation with a shape optimisation?

To answer this question, the difference between two optimisations will be quantified, namely a separate shape and structural optimisation and a combined shape and structural optimisation. First, the separate shape and structural calculation will be discussed.

Performance of a separate shape and structural optimisation

In this thesis, the shape optimisation and the structural optimisation are executed separately. First the optimal shape is found using CFD analysis, and secondly, the structure is optimised based on that shape.

The set-up is an important part of the of structural model and is discussed in Section 7.1.1 to 7.5. The set-up determines the behaviour of Karamba and Karamba is used for structural calculations. The structure is optimised by altering the grid size and cross-sections, and the shape of the structure is set. When performing the optimisations separately the best solution is a gridshell with a steel weight of 15.42 m², see Section 7.6.4.

Performance of a combined optimisation

The structure is also optimised while altering the roof height, to see the influence of the shape on the structure. The shape is defined by 11 offsets (a-k), and the offsets a-j are kept the same while the offset k (roof height) can be altered. When adding the roof height to the design variables the mass of the structure can be reduced by 36-43%. For followup research, it is better to integrate the shape and the structural analysis because the shape has a significant influence on structural performance.

Reflection

The structural optimisation is driven by Karamba. The differences between Karamba and GSA are small when comparing the two. The difference in deflection is 4 mm (<5%), the difference in the forces is < 2.1 kN and the difference in moments is < 0.13 kNm. This indicates that Karamba gives reliable answers if set-up correctly.

Forces, moments and buckling resistance are used to determine the cross-section with OptiCrosSec. Karamba has an option to calculate local buckling besides the forces and moments. If a certain profile fails, the cross-section is increased. This is great for a first design, but a gridshell like this must be tested for global buckling as well. By default, the buckling length is identical to the system length, and with that setting, the structure has a buckling load factor which is too low¹. Therefore the local buckling length is increased, see Figure 7.6.3 Process. After a check with GSA, the safety factor is still too low, so the cross-section of a few elements is increased. After the increase, the requirements are met. In conclusion, global buckling must be checked to assure a safe structure.

The stiffness of the supports is adjusted to investigate the effect on the support reactions. With the chosen support stiffness negative support reactions appear. It is not problematic if the foundation can take-up the force. Nevertheless, in the final design, a calculation must be executed to determine if the foundation is structurally safe, also regarding negative support reactions. As a side-note, the stiffness is based on a number of assumptions, see Appendix E, so it is a rough estimation of the support stiffness.

9.1.3. Ventilation

How to integrate a low energy ventilation system in the design and what can be achieved?

First of all, a completely natural ventilation system is not possible for an office building. Therefore only mechanical and hybrid ventilation systems will be discussed. Throughout the year there is always a period without wind and temperature difference between inside and outside. It is not acceptable to have no ventilation during these periods so a form of mechanical ventilation must be installed. This can be accomplished by installing a separate mechanical ventilation system as a backup or simple vents integrated into the natural ventilation system. The latter is simpler and easier to install.

There are many examples of successfully hybrid ventilation systems, but those solutions are not implemented on a big scale. The incentive to use mechanical ventilation cannot be purely economic, because hybrid ventilation can induce substantial energy saving if the adaptive thermal comfort is encountered in the design [45]. The main idea behind adaptive thermal comfort is that people habituate to higher outside temperatures (only in the long term), which means that the inside temperatures can be higher as well [43]. The adaptive thermal comfort is applicable for buildings with operable windows, without dress-code and without active cooling. The energy savings can also be assigned to the absence of electrical energy for the ventilators.

¹The buckling load factor is set to 6.0, this is discussed in Section 7.9

The main reasons to choose for mechanical ventilation is that it is much simpler to install and the designers are familiar with the solution. Also, the lack of knowledge about the benefits of hybrid ventilation can be an issue. Because hybrid ventilation is uncommon, there is a certain risk that the energy savings are not as predicted. Also, the designer must encounter more aspects like the climate and the occupants' behaviour. On top of that, dimensioning the ducts and openings is more crucial. If a hybrid ventilation system is constructed with the wrong dimensions, it is more difficult to solve the problems compared to a mechanical ventilation system.

It is vital for a designer to integrate a hybrid ventilation system into the structural design. Integration with the ventilation system is essential when the dimensions of the ducts and openings are large, like in a natural ventilation system. This thesis is an example of how structural design and building physics can support each other. The outcome of the CFD analysis is used in the structural design and for the ventilation system. Besides that, the position of the facade is altered to accommodate the hybrid ventilation. If the cavity of the second skin is too narrow the solution is discarded.

The ventilation concept of the Mijnbouwstraat achieves high availability of natural ventilation. This is accomplished by using electrical openings which catch wind from every direction. Multiple ventilation concepts have been compared, and the concept with a central shaft is chosen. The ventilation system has been thought out by integrating the ventilation system in the structural design and calculating the ventilation openings with multiple programs. The largest opening is positioned at the roof (2 m^2), and a shaft of the same size is connected to the opening. Due to the combination of stack-effect and wind, the availability of the system is 93.5%. A few percentages increase is possible, but the system with 93.5% availability is designed with reasonable dimensions.

9.2. Further research

Add surrounding

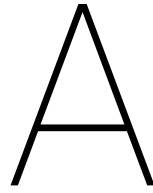
For further research, some of the assumptions made in this thesis can be analysed. The surroundings are neglected in this thesis to make it comprehensible. Nevertheless, the surroundings do influence the wind around the structure. The main pattern will be a reduction in wind load because the surrounding is full of obstacles, but locally the wind load can increase. The reduction is also important for ventilation because the system can be under-dimensioned.

Investigate high-rise buildings

The research has shown the potential of shape optimisation. However, the true potential of the shape optimisation lies with high-rise buildings. The wind load is more important and minimising it translates directly to a lighter structure. Also optimising the structure can be economically feasible. There is more money involved when building a high-rise building, so there is more money available for structural optimisation. There is more potential to reduce the amount of material and make the optimisation feasible, because the number of profiles and material is higher.

IV

Appendix



Python code highlights

Galapagos has the ability to adjust sliders which is necessary to investigate different designs with a genetic algorithm. Galapagos is very useful for optimisations but Galapagos is not compatible with Butterfly (CFD analysis). Butterfly shows intermediate results and one solution takes a few hours, which breaks Galapagos. With the Python code below panels can be adjusted to mimic the behaviour of Galapagos, see Section A.1. The genetic algorithm properties of Galapagos are replaced with the code in Section A.2.

A.1. Python code to adjust panels

```
import Grasshopper as gh
ghObjects = ghenv.Component.OnPingDocument().Objects

def panel_updater(PanelNames, Values):
    if PanelNames != [] and Values != []:
        global ghObjects

        # Iterate the GH objects
        for obj in ghObjects:
            if obj.NickName in PanelNames:
                if type(obj) is gh.Kernel.Special.GH_Panel:
                    # Set value
                    obj.SetUserText(Values[PanelNames.index(obj.NickName)])

                    # Update Panel
                    obj.ExpireSolution(True)

PanelNames = ['Demo_panel']
Values = ['usefull info']
panel_updater(PanelNames, Values)
```

A.2. Genetic algorithm in Python

It would be time consuming to create a Genetic algorithms. Also there are many open source algoritms available online like the one of Larson Will [54].

```
"""
Code from https://lethain.com/genetic-algorithms-cool-name-damn-simple

```

```

"""

from random import randint, random
from operator import add

def individual(length, min, max):
    'Create a member of the population.'
    return [randint(min, max) for x in xrange(length)]

def population(count, length, min, max):
    """
    Create a number of individuals (i.e. a population).
    count: the number of individuals in the population
    length: the number of values per individual
    min: the minimum possible value in an individual's list of values
    max: the maximum possible value in an individual's list of values
    """
    return [individual(length, min, max) for x in xrange(count)]

def fitness(individual, target):
    """
    Determine the fitness of an individual. Higher is better.
    individual: the individual to evaluate
    target: the target number individuals are aiming for
    """
    sum = reduce(add, individual, 0)
    return abs(target - sum)

def grade(pop, target):
    'Find average fitness for a population.'
    summed = reduce(add, (fitness(x, target) for x in pop))
    return summed / (len(pop) * 1.0)

def evolve(pop, target, retain=0.2, random_select=0.05, mutate=0.01):
    graded = [(fitness(x, target), x) for x in pop]
    graded = [x[1] for x in sorted(graded)]
    retain_length = int(len(graded) * retain)
    parents = graded[:retain_length]
    # randomly add other individuals to
    # promote genetic diversity
    for individual in graded[retain_length:]:
        if random_select > random():
            parents.append(individual)
    # mutate some individuals
    for individual in parents:
        if mutate > random():
            pos_to_mutate = randint(0, len(individual) - 1)
            # this mutation is not ideal, because it
            # restricts the range of possible values,
            # but the function is unaware of the min/max
            # values used to create the individuals,

```

```
        individual[pos_to_mutate] = randint(
            min(individual), max(individual))
    # crossover parents to create children
    parents_length = len(parents)
    desired_length = len(pop) - parents_length
    children = []
    while len(children) < desired_length:
        male = randint(0, parents_length - 1)
        female = randint(0, parents_length - 1)
        if male != female:
            male = parents[male]
            female = parents[female]
            half = len(male) / 2
            child = male[:half] + female[half:]
            children.append(child)
    parents.extend(children)
    return parents

if __name__ == '__main__':
    target = 371
    p_count = 100
    i_length = 6
    i_min = 0
    i_max = 100
    p = population(p_count, i_length, i_min, i_max)
    fitness_history = [grade(p, target)]
    for i in xrange(100):
        p = evolve(p, target)
        fitness_history.append(grade(p, target))

    for datum in fitness_history:
        print datum
```


B

Ventilation excel tool

B.1. Basis formulas

Conservation of mass

$$\sum \rho_i q_i = 0 \quad (\text{B.1})$$

Flow through a ventilation opening

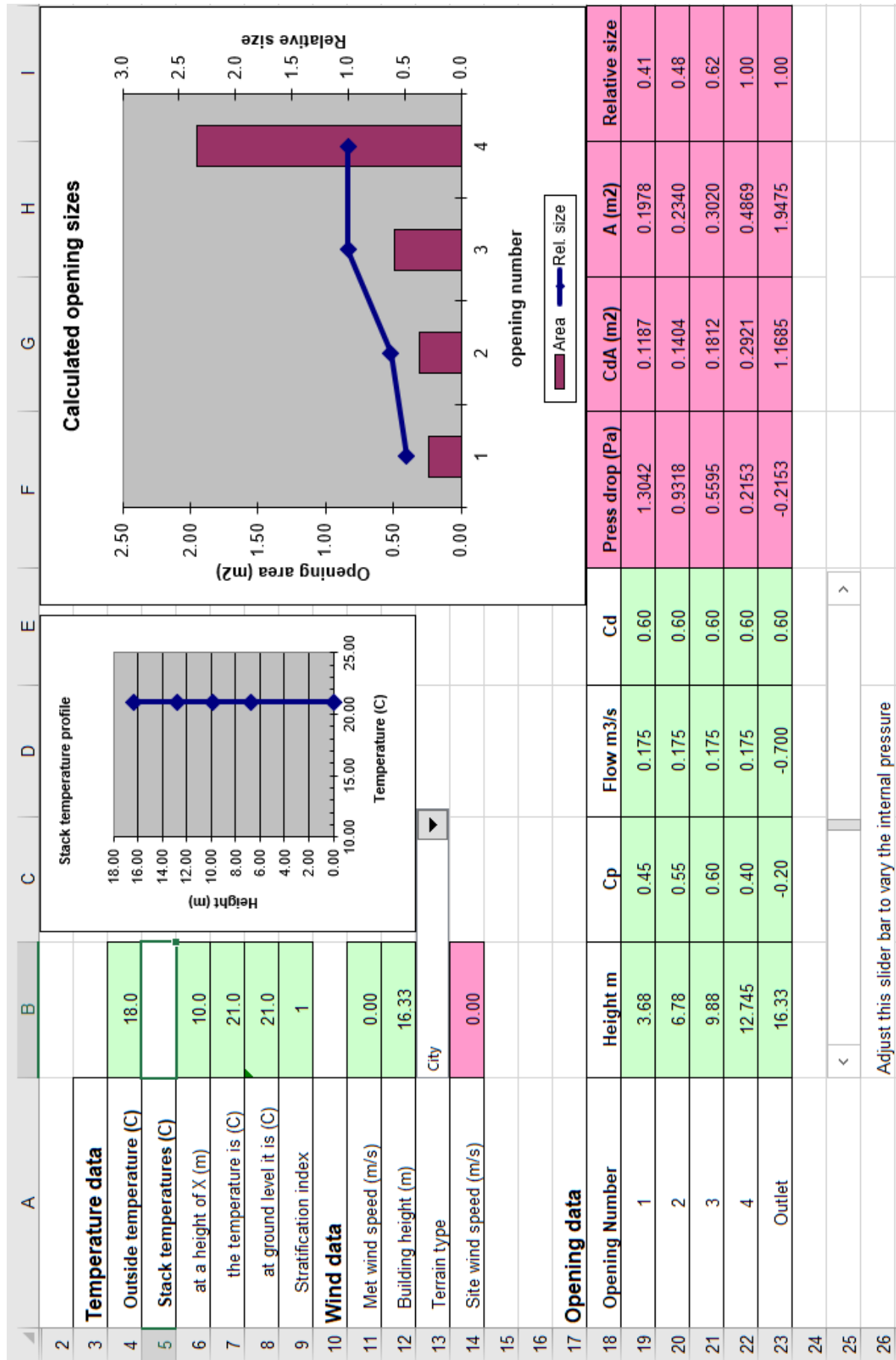
$$q_i = C_{di} \cdot A_i \cdot \sqrt{\frac{2|\Delta p_i|}{\rho_0}} \quad (\text{B.2})$$

The pressure difference at opening i relative to the neutral height

$$\Delta p_i = \Delta p_0 - \Delta \rho_0 g z_i + 0.5 \rho_0 U^2 C_{pi} \quad (\text{B.3})$$

It is assumed that the inside temperature is the same at all heights. However, in the spreadsheet stratification is also taken into account, but this is ignored by using the same temperature at a height of X and at ground level. The stratification index can be ignored as well. For background information about see paragraph 4.3.3 of Natural ventilation in non-domestic buildings [33].

The neutral height is chosen so the pressure difference between inlet 3 and the outlet is equal but with an opposite sign.



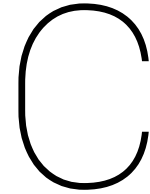
| | A | B | C | D | E | F | G | H | I | |
|----|--|----------|-------|-----------|------|-----------------|----------|--------|---------------|---|
| 2 | | | | | | | | | | |
| 3 | Temperature data | | | | | | | | | |
| 4 | Outside temperature (C) | 19.0 | | | | | | | | |
| 5 | Stack temperatures (C) | | | | | | | | | |
| 6 | at a height of X (m) | 10.0 | | | | | | | | |
| 7 | the temperature is (C) | 21.0 | | | | | | | | |
| 8 | at ground level it is (C) | 21.0 | | | | | | | | |
| 9 | Stratification index | 1 | | | | | | | | |
| 10 | Wind data | | | | | | | | | |
| 11 | Met wind speed (m/s) | 2.74 | | | | | | | | |
| 12 | Building height (m) | 16.33 | | | | | | | | |
| 13 | Terrain type | City | | | | | | | | |
| 14 | Site wind speed (m/s) | 1.45 | | | | | | | | |
| 15 | | | | | | | | | | |
| 16 | | | | | | | | | | |
| 17 | Opening data | | | | | | | | | |
| 18 | Opening Number | Height m | Cp | Flow m3/s | Cd | Press drop (Pa) | CdA (m2) | A (m2) | Relative size | |
| 19 | 1 | 3.68 | 0.45 | 0.175 | 0.60 | 1.3043 | 0.1185 | 0.1975 | 0.63 | |
| 20 | 2 | 6.78 | 0.55 | 0.175 | 0.60 | 1.1819 | 0.1245 | 0.2075 | 0.66 | |
| 21 | 3 | 9.88 | 0.60 | 0.175 | 0.60 | 0.9971 | 0.1355 | 0.2259 | 0.72 | |
| 22 | 4 | 12.745 | 0.40 | 0.175 | 0.60 | 0.5183 | 0.1880 | 0.3133 | 1.00 | |
| 23 | Outlet | 16.33 | -0.20 | -0.700 | 0.60 | -0.5183 | 0.7519 | 1.2531 | 1.00 | |
| 24 | | | | | | | | | | |
| 25 | | < | | | | | | | | > |
| 26 | Adjust this slider bar to vary the internal pressure | | | | | | | | | |

Stack temperature profile

| Height (m) | Temperature (C) |
|------------|-----------------|
| 0.00 | 21.00 |
| 2.00 | 21.00 |
| 4.00 | 21.00 |
| 6.00 | 21.00 |
| 8.00 | 21.00 |
| 10.00 | 21.00 |
| 12.00 | 21.00 |
| 14.00 | 21.00 |
| 16.00 | 21.00 |
| 16.33 | 19.00 |

Calculated opening sizes

| Opening number | Opening area (m2) | Relative size |
|----------------|-------------------|---------------|
| 1 | 0.1975 | 0.63 |
| 2 | 0.2075 | 0.66 |
| 3 | 0.2259 | 0.72 |
| 4 | 0.3133 | 1.00 |



Contam verification

The main driving forces for natural air-flows are wind and buoyancy. Contam will be verified with two examples from literature, one focusing on wind and the other on buoyancy.

C.1. Example Wind

In Contam the windpressure is defined with the second formula in Figure C.1. Ideally, a C_p value can be defined for each opening, but this is not possible in Contam. However, the value C_h and $f(\theta)$ can be manipulated in such a manner that it behaves the same as a predefined C_p value. The main issue is that the factor C_h depends on the height in contrast to the C_p value. More in detail, C_h is defined with the last formula in Figure C.1. When A_o is set to 1 and $\frac{H}{H_{ref}} = 1$ then the factor $C_h = 1$ ¹. When $C_h = 1$ regardless of the height $f(\theta)$ can be misused as C_p .

¹Setting A_o to 1 and a to 0 could also do the trick but a must be larger than 0.1 in Contam.

The equation for wind pressure on the building surface is

$$P_w = \frac{\rho V_H^2}{2} C_p$$

where

V_H Approach wind speed at the upwind wall height (usually the height of the building)

C_p Wind pressure coefficient

The wind pressure coefficient can be further generalized in terms of a local terrain effects coefficient and the direction of the wind relative to the wall under consideration. The following equation is that used by CONTAM when calculating wind pressures on the building.

$$P_w = \frac{\rho V_{met}^2}{2} C_k f(\theta)$$

where

ρ ambient air density

V_{met} wind speed measured at meteorological station

C_k wind speed modifier coefficient accounting for terrain and elevation effects

$f(\theta)$ coefficient that is a function of the relative wind direction. CONTAM refers to this function as the *wind pressure profile*.

$$C_k = \frac{V_H^2}{V_{met}^2} = A_o^2 \left(\frac{H}{H_{ref}} \right)^{2a} \quad (1)$$

where H is the wall height and A_o and a depend on the terrain around the building [ASHRAE 1993, p 14.3]:

| Terrain Type | Coefficient (A_o) | Exponent (a) |
|--------------|-----------------------|------------------|
| Urban | 0.35 | 0.40 |
| Suburban | 0.60 | 0.28 |
| Airport | 1.00 | 0.15 |

Figure C.1: A section of the Contam guideline describing the procedure to calculate the wind pressure [78]

Cross flow ventilation occurs when there are openings on two sides of a space. The flows in on one side of the building and out on the other side, see Figure C.2a. According Irving et al. [33] crossflow ventilation can be described with formula C.1. A is the area of the opening, C_d is the discharge coefficient, U is the wind speed and ΔC_p is the difference between the C_p values of the openings. The same conditions can be created in Contam, with an inflow on the left and an outflow on the right, see C.2b.

$$q = A \cdot C_d \cdot U \cdot \sqrt{\frac{\Delta C_p}{2}} \quad (C.1)$$

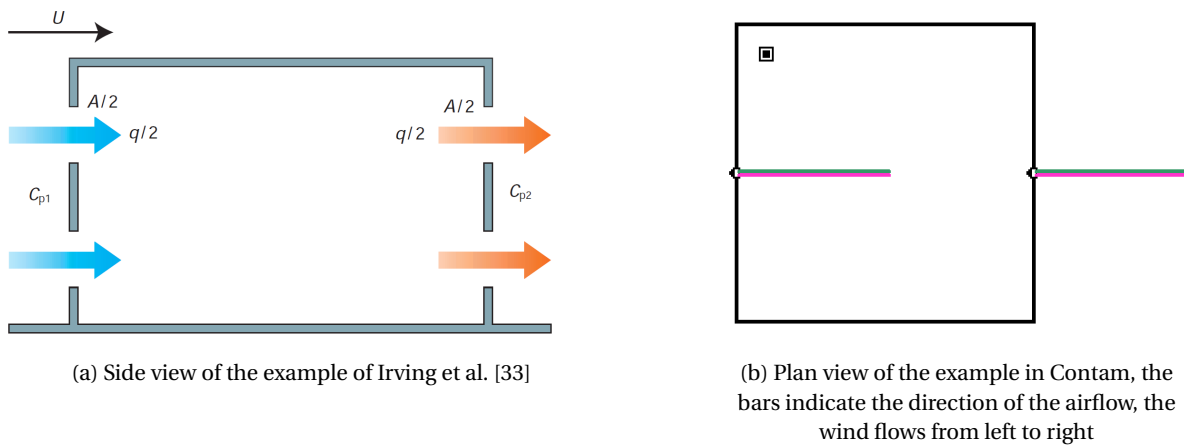


Figure C.2: Crossflow ventilation, wind driven

To make a good comparison five cases are checked. For each case a different variable of formula C.1 is changed. Case 1 is the initial case and for Case 2 the C_d value is altered, see table C.1. The results indicate that the literature and the Contam calculation show the same results for all cases. The rounding error is neglectable.

| Case: | 1 | 2 | 3 | 4 | 5 |
|------------------------------|--------|--------|--------|--------|--------|
| C_d = | 0.6 | 0.9 | 0.6 | 0.6 | 0.6 |
| U [m/s]= | 10 | 10 | 5 | 10 | 10 |
| ΔC_p = | 1.2 | 1.2 | 1.2 | 0.1 | 1.2 |
| A [m ²] = | 1 | 1 | 1 | 1 | 3 |
| ρ [kg/m ³]= | 1.2041 | 1.2041 | 1.2041 | 1.2041 | 1.2041 |

Hand Calculation

| | | | | | |
|---------------------------|-------|-------|-------|-------|--------|
| q [m ³ /s] = | 4.648 | 6.971 | 2.324 | 1.342 | 13.943 |
|---------------------------|-------|-------|-------|-------|--------|

Result Contam

| | | | | | |
|---------------------------|-------|-------|-------|-------|--------|
| q [m ³ /s] = | 4.648 | 6.971 | 2.324 | 1.342 | 13.943 |
|---------------------------|-------|-------|-------|-------|--------|

Table C.1: Comparison between hand calculation and Contam

C.2. Example Buoyancy

In Contam 2d floor plans are drawn to create model, see Figure C.3. Apart from that, the elevation and height of each floor is specified. Because of this only simple rectangular buildings can be draw. This if often not a problem because the floor area doesn't influence the airflow trough the openings.

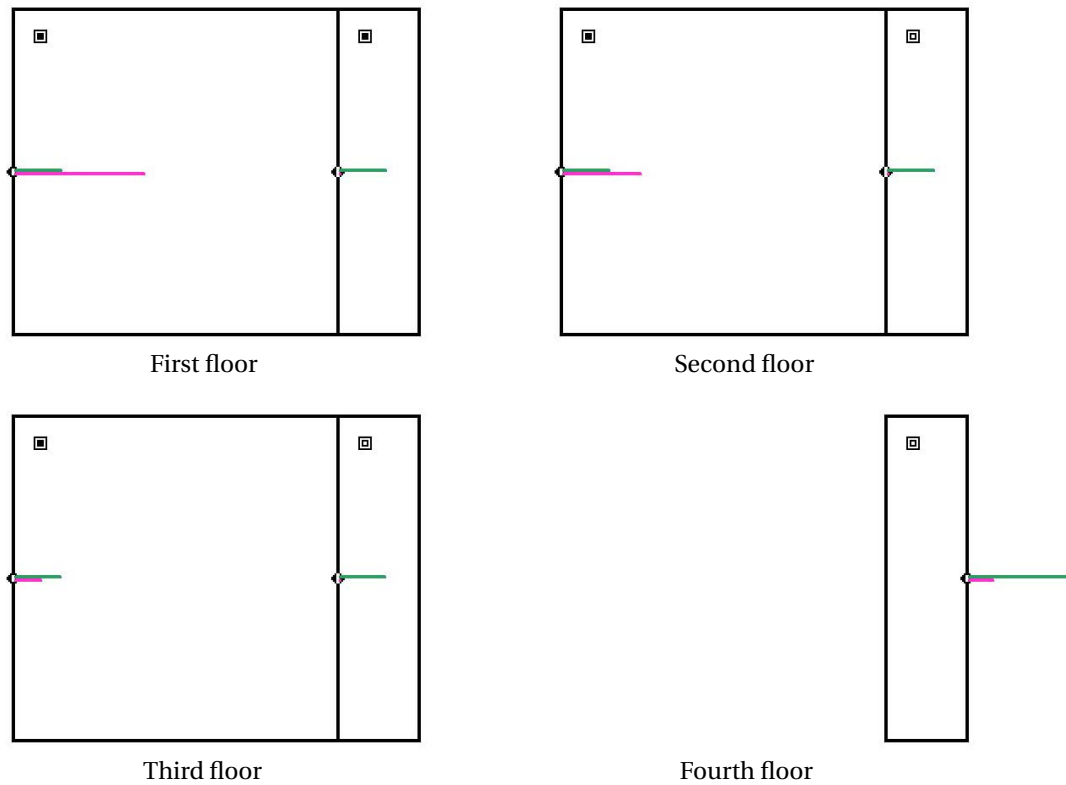


Figure C.3: Floorplans in Contam

Now the stack effect will be verified. This is done on the basis of a simple building, see Figure C.4. Wind is neglected in this example. The internal temperature is $28\text{ }^{\circ}\text{C}$ while the external temperature is $25\text{ }^{\circ}\text{C}$. The resistance of the openings inside the building are negligible while the inlet and outlet have a certain size, see C.2. The positive direction of each opening is shown in Figure C.4.

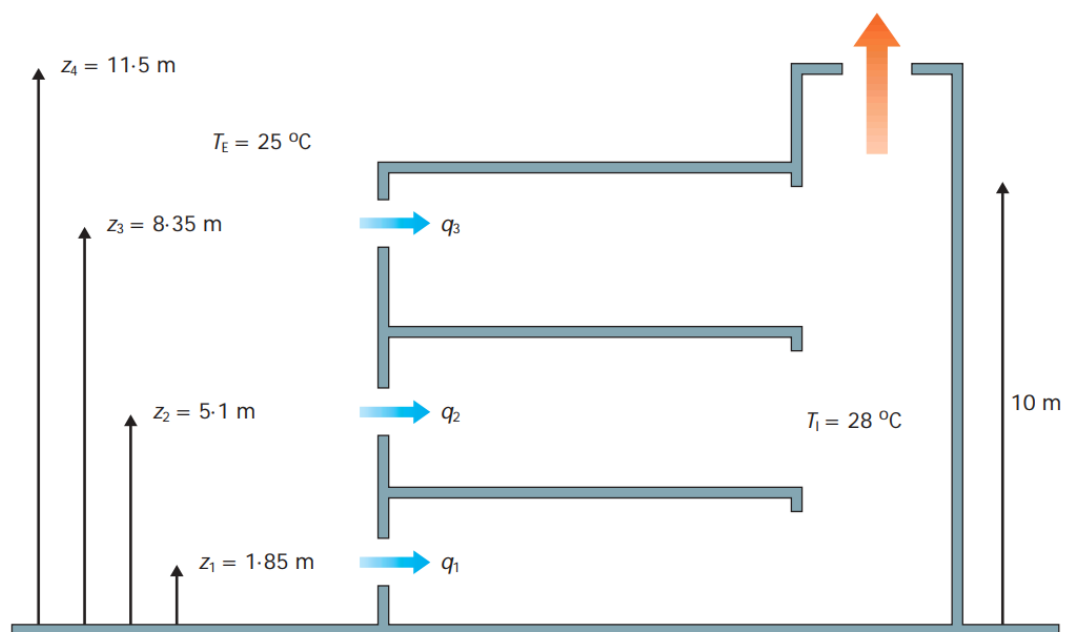
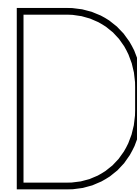


Figure C.4: Example building used to verify Contam [33]

The hand calculation is explained in section 4.3.2 of Natural ventilation in non-domestic buildings [33]. The results of Contam are slightly different compared to the results of the hand calculation, but the error is small, see Table C.2. The neutral height could be the main problem for this error. The neutral height is estimated in the hand calculation, which is less accurate. Also a wrong estimation has a bigger influence on the openings close to the neutral plane and indeed opening 3 has the biggest error. All in all, the results of Contam appear to be accurate.

| Opening: | z_i [m] | A_i [m] | Cd_i | Results hand calculation | Results Contam | |
|-----------------|-----------|-----------|--------|--------------------------|----------------|--------------|
| | | | | q_i [m/s] | q_i [m/s] | error |
| 1 | 1.85 | 0.579 | 0.61 | 0.448 | 0.445 | 0.64% |
| 2 | 5.1 | 0.747 | 0.61 | 0.448 | 0.445 | 0.70% |
| 3 | 8.35 | 1.286 | 0.61 | 0.448 | 0.441 | 1.49% |
| 4 (outlet) | 11.5 | 4.048 | 0.61 | 1.344 | 1.331 | 0.94% |

Table C.2: Comparison between hand calculation and Contam



Glass calculation

The design strength of float glass is calculated with NEN2608:2014

8.3.1 Niet-voorgespannen glas

(1) De rekenwaarde voor de buigtreksterkte ($f_{mt;u;d}$) van niet-voorgespannen glas moet zijn bepaald volgens vergelijking (6).

$$f_{mt;u;d} = \frac{k_a \times k_e \times k_{mod} \times k_{sp} \times f_{g;k}}{\gamma_{m;A}} \quad (6)$$

waarin:

- $f_{mt;u;d}$ is de rekenwaarde van de buigtreksterkte van niet-voorgespannen glas, in N/mm^2 ;
- k_a is de factor voor het oppervlakte-effect volgens 8.3.3(3), 8.3.3(4) en 8.3.3(5);
- k_e is de factor voor de randkwaliteit van de ruit, waarbij bij spanningen op de rand k_e volgens 8.3.3(2) moet zijn toegepast. Voor de overige situaties moet $k_e = 1$ zijn toegepast;
- k_{mod} is de modificatiefactor afhankelijk van de belastingsduur en de referentieperiode volgens 8.3.3(6);
- k_{sp} is de factor voor de oppervlaktestructuur van de ruit volgens 8.3.3(1);
- $f_{g;k}$ is de karakteristieke waarde van de buigtreksterkte van glas, in N/mm^2 , waarbij $f_{g;k} = 45 N/mm^2$;
- $\gamma_{m;A}$ is de materiaalfactor van glas, waarbij:
 - $\gamma_{m;A} = 1,6$ voor situaties waarbij de wind of isochore druk de overheersende veranderlijke belasting is;
 - $\gamma_{m;A} = 1,8$ voor overige situaties.

Figure D.1: Calculation design strength of float glass, NEN2608:2014

A linear calculation is used so $K_a = 1$

For float glass $K_{sp} = 1$ and $f_{g;k} = 45 N/mm^2$

K_{mod} and $\gamma_{m;A}$ depend on the duration of the load:

- $K_{mod} = 1$, $\gamma_{m;A} = 1.6$ for wind load
- $K_{mod} = 0.61$, $\gamma_{m;A} = 1.8$ for snow load

The using the variables mentioned above, design values of the strength are:

Wind load: $f_{mt;u;d} = \frac{1 \cdot 45}{1.6} = 28.13 N/mm^2$

Snow load: $f_{mt;u;d} = \frac{0.61 \cdot 45}{1.8} = 15.25 N/mm^2$ (assumed to be dominant)

Estimation stiffness supports

The supports will be divided in two groups, supports at ground level and supports attached to the building. The supports at ground level are labels S0v, see Figure E.1.

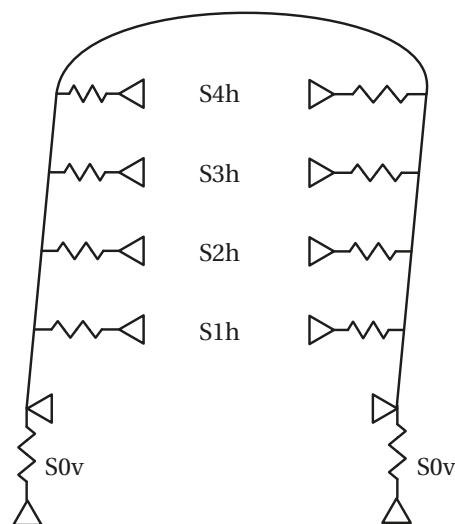


Figure E.1: Names of the supports, h for horizontal and v for vertical

E.1. Supports at ground level

The assumption is made that a pile foundation is used and the stiffness of one pile determines the stiffness of one support. The piles are assumed to be 200mm with a strength class of C45/55.

To make an educated guess for the foundation stiffness some information about the ground layers is needed. The top layer (> 200 cm) is a combination of sandy sediment and clay [79]. Later on the ground is raised with sand by the local government to make the area ready for construction. This is illustrated in Figure E.2. In a large part of Delft, a sand layer is positioned between -6 NAP and -2 NAP [79]. This can be used for light constructions. A heavier construction like Spoorzone Delft must be constructed on a stronger layer and is build on piles of 18m [80].

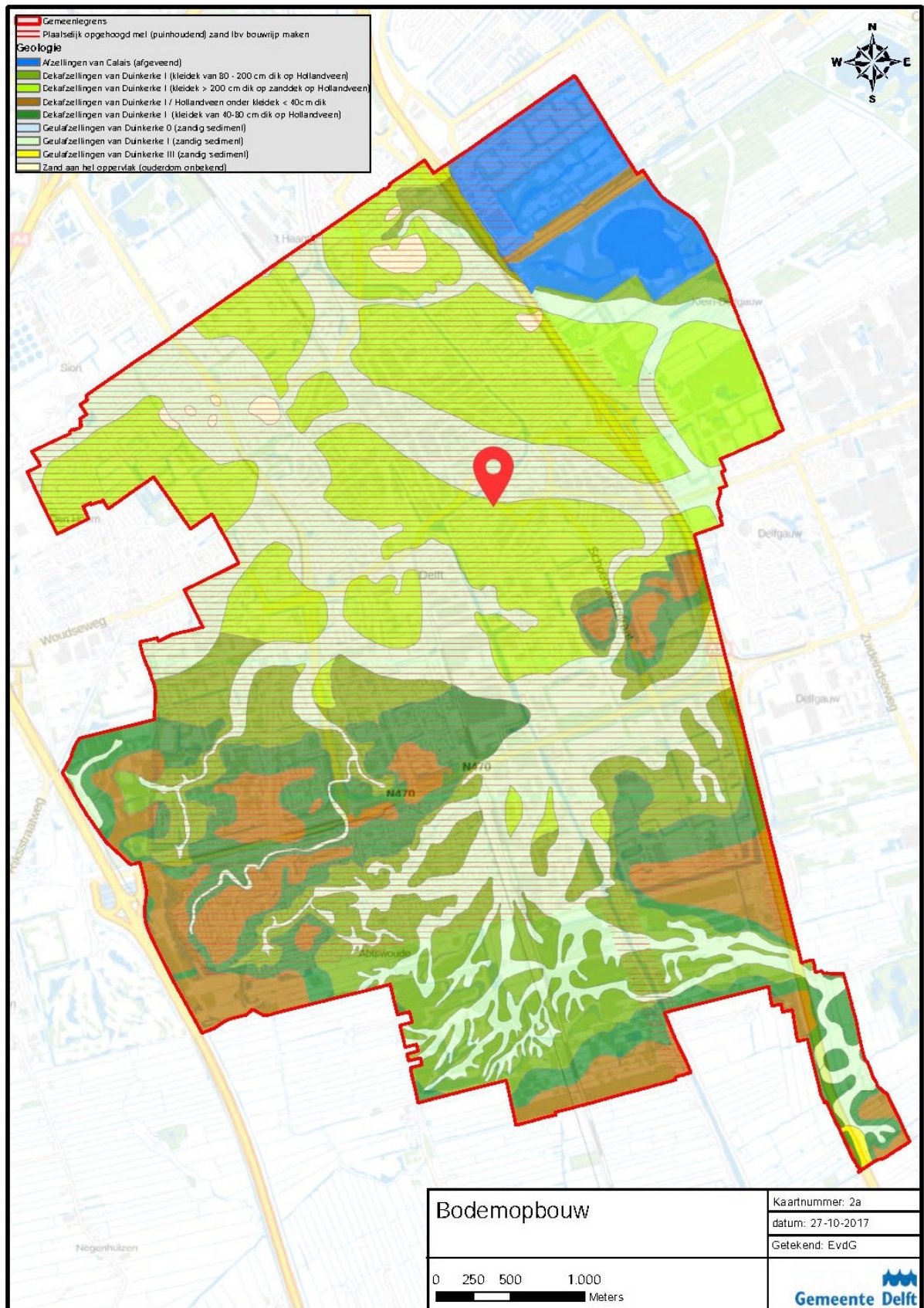


Figure E.2: Map of the ground layers in Delft, the Mijnbouwstraat 110 is marked [79]

Let us assume a length of 10m to determine the stiffness of the supports. The stiffness will be calculated with a method described by Braam [63], because it is a simple and quick method to calculate the pile stiffness. A pile foundation can be considered to be springs, elastic spring stiffness of the pile ($k_{p,el}$) and the elastic support the pile tip ($k_{p,t}$), see Figure E.3. The resulting vertical spring stiffness of the pile becomes:

$$\frac{1}{k_p} = \frac{1}{k_{p,el}} + \frac{1}{k_{p,t}} \quad (E.1)$$

The order of magnitude of the spring stiffness k_p is about 0.2-0.5 times the elastic pile stiffness $k_{p,el}$ [63]. For long piles the higher values are correct and for short piles lower values are correct. When the assumption is made that the pile tip is β times the elastic stiffness of the pile, Equation E.1 can be rewritten as:

$$\frac{1}{k_p} = \frac{1}{k_{p,el}} + \frac{\beta}{k_{p,el}} \quad (E.2)$$

$$k_{p,el} = \frac{E_c A_c}{l_p} \quad (E.3)$$

The stiffness of the pile is:

$$k_p = \frac{k_{p,el}}{1 + \beta} = \frac{E_c A_c}{(1 + \beta) l_p} \quad (E.4)$$

- piles of 200mm with a strength class of C45/55, length of 10 m
- $E_c = \frac{f_{cd}}{\epsilon} = \frac{45/1.5}{1.75 \times 10^{-3}} = 17140 \text{ N/mm}^2$ In tables higher values (short term loading) can be found but the value calculated here is for long term loads [81].
- For short piles the spring stiffness $k_p = 0.2 \cdot k_{p,el} \rightarrow \beta = 1$. For long piles $k_p = 0.5 \cdot k_{p,el} \rightarrow \beta = 4$. Short piles are stiffer than long piles. It is better to be conservative and assume less stiff supports. Therefore β is a bit higher than the lower limit of $1 \rightarrow \beta = 2$.

The stiffness of one pile becomes 22.9 MN/m and is calculated with Equation E.4. The equation is discussed in Section 7.2.4. The assumption is made that the horizontal support at ground floor level is rigid.

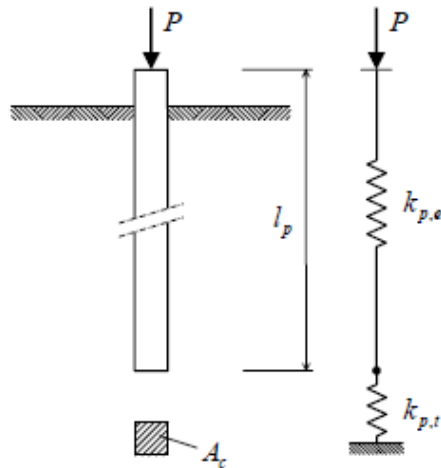


Figure E.3: Scheme for the determination of the spring stiffness of the pile

E.2. Supports attached to the Building

The facade will be supported at multiple points connected to the existing building. The stiffness of these supports will be determined with the help of the Dutch National Annex of NEN-EN1990, Basis of structural design. In the code a deformation limit for non-industrial buildings is:

$$u_{lim} \leq \frac{1}{300} \cdot z \tag{E.5}$$

This deflection occurs due to the wind load. The limit described is the upper limit and most buildings are not designed with a utilisation factor of 1.0. It is more realistic to assume that utilisation factor lower, like 0.5. In this case the deformation will occur when the building is subjected to 2 x wind load.

The supports for the structure are pendulum supports, see Section 7.2.1. Because the supports are orientated in different angles each support is unique, to simplify the situation each support will have the same stiffness. This will be accomplished by only the weakest direction of the building. This is when the wind hits the building perpendicular to the long direction of the building, this is illustrated in Figure E.5 (when $b > d$).

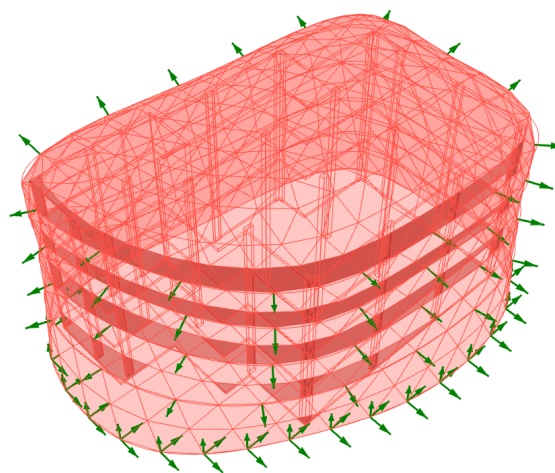


Figure E.4: The supports are illustrated with green arrows, on the bottom pinned supports and pendulums elsewhere

E.2.1. Wind load

The buildings will be simplified to a rectangular box. To calculate the wind load the C_f factors are needed. The dimensions of the rectangular building and corresponding C_f factors are shown in Figure E.5.

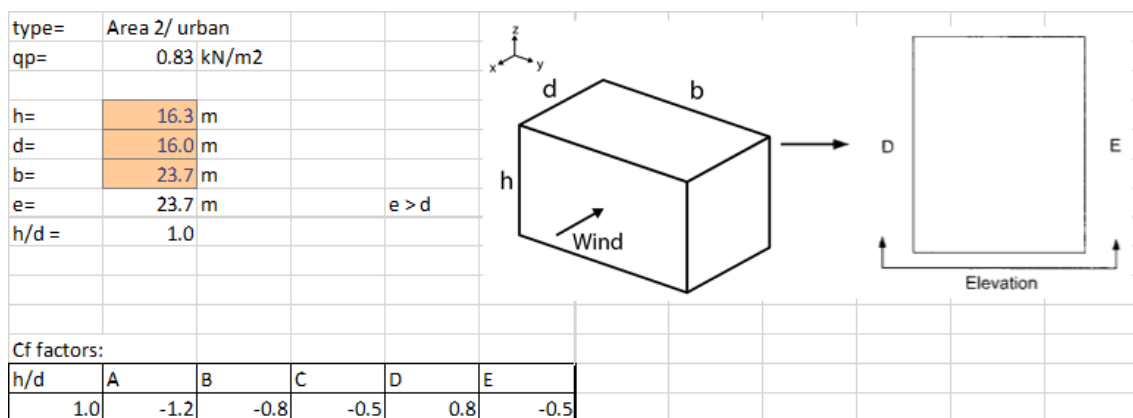


Figure E.5: Calculation of the C_f factors based on NEN-EN 1991-1-4, Coefficients D is on the windward side and Coefficient E is on the leeward side.

Figure E.6 Drawing A

Currently, the building is designed to withstand a certain wind load and stay within the deformation limits. With the load and deformation the stiffness of the building can be calculated.

Figure E.6 Drawing B

The building will be replaced by a set of uncoupled springs. To determine the stiffness of each spring the load and deflections must be known at that point. The springs at the bottom are determined in Section E.1.

Figure E.6 Drawing C

The load closest to the spring will be used to calculate the stiffness. The green box illustrates which part of the load will be used to calculate the spring stiffness, this works in 3D. The deformation limit is $z/300$, where z is the height of the building.

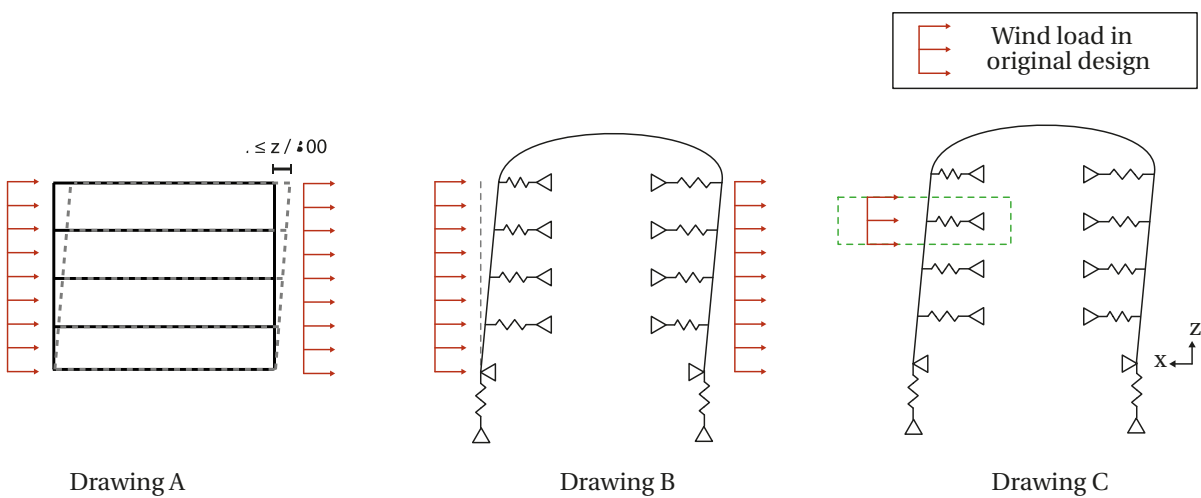


Figure E.6: h

With equation 5.3 of the NEN-EN 1994-1-1 the load on the structure can be calculated:

$$F_w = c_s c_d \cdot c_f \cdot q_p(z_e) \cdot A_{ref} \quad (\text{E.6})$$

- $c_s c_d = 1$ in this calculation
- $q_p(z_e) = 0.83$ the peak velocity pressure at a building height of 16m in Delft (area 2)
- $c_f = 1.3$ is the force coefficient, D + E
- $A_{ref} = \Delta v_z \cdot \Delta v_y$ is the reference area on the structure. Δv_y is the distance between two supports in y direction and Δv_z is the distance between two supports in z direction.
- If utilisation factor of, for example, 0.5 is taken into account, the load must be multiplied by 2 to reach the deformation limit. This is less conservative because the supports stiffens will be higher. For example when utilisation factor = 0.5, $S1h = 0.6$ MN/m and when utilisation factor = 1.0, $S1h = 0.3$ MN/m. The latter is more conservative, therefore the utilisation factor = 1.0.

Lastly, the stiffness of the supports can be calculated with the following formula:

$$k = \frac{F_w}{u_{lim}} \quad (\text{E.7})$$

E.2.2. Results

The names of the supports are shown in Figure E.1. With the equations E.5 - E.7 the stiffness k of the other supports can be determined, the results are presented in Table E.1. The horizontal distance between the supports is 2 m.

| Support | h [m] | Δv_z [m] | Δv_y [m] | F_w [kN] | u_{lim} [m] | k [MN/m] |
|---------|--------|------------------|------------------|------------|---------------|----------|
| S0v | -0.17 | - | - | - | - | 22.9 |
| S1h | 3.68 | 3.4 | 2.0 | 7.34 | 1.23E-02 | 0.30 |
| S2h | 6.78 | 3.1 | 2.0 | 6.69 | 2.26E-02 | 0.15 |
| S3h | 9.88 | 3.1 | 2.0 | 6.69 | 3.29E-02 | 0.10 |
| S4h | 12.745 | 3.7 | 2.0 | 7.98 | 4.25E-02 | 0.09 |

Table E.1: Stiffness of the supports

E.3. Support reactions

E.3.1. Ground supports

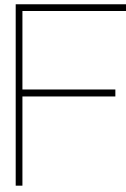
| Support | Pinned support | | | | Springs support | | | |
|---------|----------------|------|--------|--------|-----------------|------|--------|--------|
| | Node | Case | Fz min | Fz max | Node | Case | Fz min | Fz max |
| G1 | 429 | LC2 | 28260 | 67030 | 204 | LC8 | 34610 | 76420 |
| G2 | 430 | LC2 | 23110 | 57490 | 205 | LC8 | 30460 | 60270 |
| G3 | 431 | LC2 | 27880 | 63470 | 206 | LC5 | 22700 | 40380 |
| G4 | 432 | LC2 | 26820 | 61990 | 207 | LC5 | 21950 | 38760 |
| G5 | 433 | LC2 | 23730 | 60290 | 208 | LC8 | 23020 | 63020 |
| G6 | 434 | LC2 | 26810 | 67570 | 209 | LC8 | 28290 | 77490 |
| G7 | 435 | LC2 | 23580 | 57670 | 210 | LC8 | 29290 | 63950 |
| G8 | 436 | LC2 | 30610 | 74620 | 211 | LC8 | 30660 | 66650 |
| G9 | 437 | LC2 | 32840 | 71400 | 212 | LC8 | 34780 | 59890 |
| G10 | 438 | LC2 | 26110 | 61110 | 213 | LC8 | 32220 | 56450 |
| G11 | 439 | LC2 | 24540 | 58410 | 214 | LC8 | 25310 | 58080 |
| G12 | 440 | LC2 | 23690 | 56800 | 215 | LC8 | 21140 | 46660 |
| G13 | 441 | LC2 | 26030 | 59520 | 216 | LC8 | 25800 | 52250 |
| G14 | 442 | LC2 | 23750 | 58540 | 217 | LC8 | 27270 | 60930 |
| G15 | 443 | LC2 | 20700 | 57640 | 218 | LC8 | 31530 | 66930 |
| G16 | 444 | LC2 | 23990 | 61160 | 219 | LC8 | 40380 | 70880 |
| G17 | 445 | LC2 | 29600 | 66700 | 220 | LC5 | 38850 | 67740 |
| G18 | 446 | LC2 | 27300 | 60000 | 221 | LC5 | 24160 | 42760 |
| G19 | 447 | LC2 | 21000 | 56390 | 222 | LC4 | -21780 | 21000 |
| G20 | 448 | LC2 | 21210 | 58240 | 223 | LC4 | -22400 | 38420 |
| G21 | 449 | LC2 | 25790 | 61990 | 224 | LC4 | 11720 | 58700 |
| G22 | 450 | LC2 | 25410 | 59350 | 225 | LC8 | 28150 | 69610 |

E.3.2. Supports attached to building

| Support | Pinned support | | | Springs support | | |
|---------|----------------|------|--------|-----------------|------|--------|
| | Node | Case | F [N] | Node | Case | F [N] |
| B1 | 248 | LC2 | 14040 | 23 | LC2 | 1654 |
| B2 | 249 | LC2 | 7866 | 24 | LC2 | 851.2 |
| B3 | 250 | LC4 | 6252 | 25 | LC2 | 2070 |
| B4 | 251 | LC4 | 5155 | 26 | LC2 | 2879 |
| B5 | 252 | LC2 | 5717 | 27 | LC2 | 626.1 |
| B6 | 253 | LC2 | 16510 | 28 | LC2 | 2315 |

| Support | Pinned support | | | Springs support | | |
|---------|----------------|------|--------|-----------------|------|--------|
| | Node | Case | F [N] | Node | Case | F [N] |
| B7 | 254 | LC4 | 5831 | 29 | LC4 | 2006 |
| B8 | 255 | LC2 | 5034 | 30 | LC2 | 3909 |
| B9 | 256 | LC4 | 3125 | 31 | LC4 | 2513 |
| B10 | 257 | LC2 | 6637 | 32 | LC2 | 856.6 |
| B11 | 258 | LC2 | 17240 | 33 | LC2 | 1311 |
| B12 | 259 | LC4 | 3129 | 34 | LC2 | 1442 |
| B13 | 260 | LC4 | 4189 | 35 | LC4 | 1481 |
| B14 | 261 | LC4 | 4688 | 36 | LC4 | 1177 |
| B15 | 262 | LC4 | 6281 | 37 | LC3 | 1453 |
| B16 | 263 | LC4 | 6103 | 38 | LC4 | 3301 |
| B17 | 264 | LC4 | 3601 | 39 | LC4 | 4439 |
| B18 | 265 | LC3 | 1192 | 40 | LC4 | 1487 |
| B19 | 266 | LC4 | 5686 | 41 | LC4 | 3661 |
| B20 | 267 | LC4 | 8994 | 42 | LC4 | 5475 |
| B21 | 268 | LC4 | 7356 | 43 | LC4 | 1899 |
| B22 | 269 | LC2 | 9506 | 44 | LC2 | 1520 |
| B23 | 292 | LC2 | 20370 | 67 | LC2 | 1318 |
| B24 | 293 | LC4 | 5643 | 68 | LC4 | 162.3 |
| B25 | 294 | LC2 | 5330 | 69 | LC2 | 3584 |
| B26 | 295 | LC2 | 7289 | 70 | LC2 | 4469 |
| B27 | 296 | LC4 | 2485 | 71 | LC2 | 865 |
| B28 | 297 | LC2 | 18160 | 72 | LC2 | 2057 |
| B29 | 298 | LC4 | 3000 | 73 | LC2 | 1629 |
| B30 | 299 | LC2 | 6831 | 74 | LC2 | 3221 |
| B31 | 300 | LC2 | 3343 | 75 | LC2 | 3058 |
| B32 | 301 | LC2 | 2701 | 76 | LC2 | 2164 |
| B33 | 302 | LC2 | 14880 | 77 | LC2 | 1885 |
| B34 | 303 | LC3 | 2104 | 78 | LC2 | 1822 |
| B35 | 304 | LC3 | 3402 | 79 | LC2 | 1931 |
| B36 | 305 | LC4 | 3983 | 80 | LC4 | 318.2 |
| B37 | 306 | LC4 | 5266 | 81 | LC3 | 1160 |
| B38 | 307 | LC4 | 5159 | 82 | LC4 | 2682 |
| B39 | 308 | LC3 | 7772 | 83 | LC4 | 2966 |
| B40 | 309 | LC2 | 15390 | 84 | LC2 | 1871 |
| B41 | 310 | LC2 | 16580 | 85 | LC4 | 2700 |
| B42 | 311 | LC4 | 14000 | 86 | LC4 | 4250 |
| B43 | 312 | LC4 | 13980 | 87 | LC4 | 3884 |
| B44 | 313 | LC4 | 8268 | 88 | LC2 | 917.9 |
| B45 | 336 | LC2 | 32610 | 111 | LC2 | 814.5 |
| B46 | 337 | LC2 | 8950 | 112 | LC4 | 226.6 |
| B47 | 338 | LC4 | 5318 | 113 | LC2 | 1190 |
| B48 | 339 | LC4 | 4608 | 114 | LC2 | 1362 |
| B49 | 340 | LC2 | 8673 | 115 | LC2 | 272.2 |
| B50 | 341 | LC2 | 33810 | 116 | LC2 | 1183 |
| B51 | 342 | LC4 | 4512 | 117 | LC4 | 839.7 |
| B52 | 343 | LC4 | 4417 | 118 | LC4 | 1936 |
| B53 | 344 | LC4 | 3901 | 119 | LC4 | 2002 |
| B54 | 345 | LC2 | 7520 | 120 | LC2 | 1794 |
| B55 | 346 | LC2 | 38090 | 121 | LC2 | 1559 |
| B56 | 347 | LC2 | 13720 | 122 | LC2 | 791.6 |
| B57 | 348 | LC4 | 5673 | 123 | LC2 | 689.9 |
| B58 | 349 | LC4 | 6959 | 124 | LC4 | 368.8 |

| Support | Pinned support | | | Springs support | | |
|---------|----------------|------|--------|-----------------|------|--------|
| | Node | Case | F [N] | Node | Case | F [N] |
| B59 | 350 | LC4 | 8485 | 125 | LC3 | 624.1 |
| B60 | 351 | LC4 | 8772 | 126 | LC4 | 1272 |
| B61 | 352 | LC2 | 6887 | 127 | LC4 | 1264 |
| B62 | 353 | LC2 | 3625 | 128 | LC4 | 285 |
| B63 | 354 | LC4 | 4810 | 129 | LC4 | 900.2 |
| B64 | 355 | LC4 | 9927 | 130 | LC4 | 1679 |
| B65 | 356 | LC4 | 10740 | 131 | LC4 | 1751 |
| B66 | 357 | LC2 | 13500 | 132 | LC2 | 257.4 |
| B67 | 380 | LC2 | 30760 | 155 | LC3 | 181.9 |
| B68 | 381 | LC2 | 25000 | 156 | LC2 | 160.3 |
| B69 | 382 | LC2 | 65510 | 157 | LC2 | 455.4 |
| B70 | 383 | LC2 | 29310 | 158 | LC2 | 506 |
| B71 | 384 | LC2 | 10810 | 159 | LC2 | 333.4 |
| B72 | 385 | LC2 | 37210 | 160 | LC2 | 123.3 |
| B73 | 386 | LC2 | 81790 | 161 | LC2 | 1130 |
| B74 | 387 | LC2 | 19010 | 162 | LC2 | 1909 |
| B75 | 388 | LC2 | 27270 | 163 | LC2 | 1612 |
| B76 | 389 | LC1 | 3505 | 164 | LC2 | 525.3 |
| B77 | 390 | LC1 | 12990 | 165 | LC2 | 149.9 |
| B78 | 391 | LC2 | 22150 | 166 | LC2 | 385.2 |
| B79 | 392 | LC2 | 31750 | 167 | LC2 | 749.6 |
| B80 | 393 | LC2 | 30050 | 168 | LC2 | 905.7 |
| B81 | 394 | LC3 | 5028 | 169 | LC3 | 470.8 |
| B82 | 395 | LC2 | 20080 | 170 | LC4 | 405.4 |
| B83 | 396 | LC3 | 9564 | 171 | LC4 | 300.7 |
| B84 | 397 | LC2 | 65470 | 172 | LC2 | 201.2 |
| B85 | 398 | LC2 | 20130 | 173 | LC4 | 345.4 |
| B86 | 399 | LC2 | 34970 | 174 | LC4 | 544.5 |
| B87 | 400 | LC2 | 19150 | 175 | LC4 | 560.5 |
| B88 | 401 | LC4 | 11240 | 176 | LC4 | 439.3 |



Resultant wind force

The definition of the resultant wind force is explained in the Section 6.7.2.

With equation 5.3 of the NEN-EN 1994-1-1 the load on the structure can be calculated:

$$F_w = c_s c_d \cdot c_f \cdot q_p(z_e) \cdot A_{ref} \quad (E.1)$$

- $c_s c_d = 1$ simple situation
- $q_p(z_e) = 0.83 \text{ kN/m}^2$ the peak velocity pressure at a building height of 16m in Delft (area 2)
- c_f the force coefficient depends on the position at the facade.
- A_{ref} is the reference area

To determine the factor c_f first the variable e must be calculated with $e = \min(b, 2h)$. The wind zones for the facade depends on the ratio between e and d and when $e < d$ the zones are divided in four zones, see Figure E1.

- $h = 16.3 \text{ m}$, $d = 16.0 \text{ m}$, $b = 23.7 \text{ m}$
- $e = \min(b, 2h) = 23.7 \text{ m}$
- $h/d = 1$

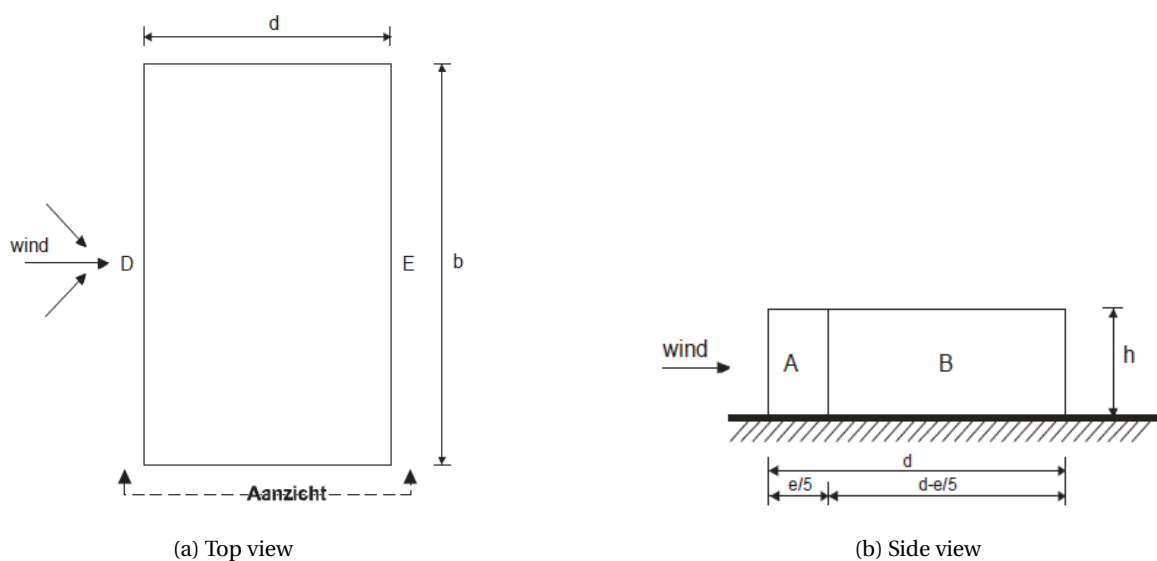


Figure E1: External pressure coefficients for zone A B D E, NEN-EN 1994-1-1

A large part of the roof of the Mijnbouwstraat 106-112 is a flat and some parts are inclined. To simplify the calculation the assumption is made that the complete roof is flat. The assumption can be justified because the resultant wind force in the horizontal plane will be calculated so the inclined roof areas are less important. Also the calculation is just an estimation of the residual wind force. To calculate the residual of the building only the force coefficient for the windward and leeward side is of interest because the sides cancel each other out. When $h/d = 1$ the factor $D = +0.8$ and the factor $E = -0.5$, see Figure E2.

| Façades h/d | c_f for zone | | | | |
|----------------|----------------|------|------|------|------|
| | A | B | C | D | E |
| 5 | -1,2 | -0,8 | -0,5 | +0,8 | -0,7 |
| 1 | -1,2 | -0,8 | -0,5 | +0,8 | -0,5 |
| $\leq 0,25$ | -1,2 | -0,8 | -0,5 | +0,7 | -0,3 |

Figure E2: C_f factors at the facade of a rectangular building (EC1991-1-4)

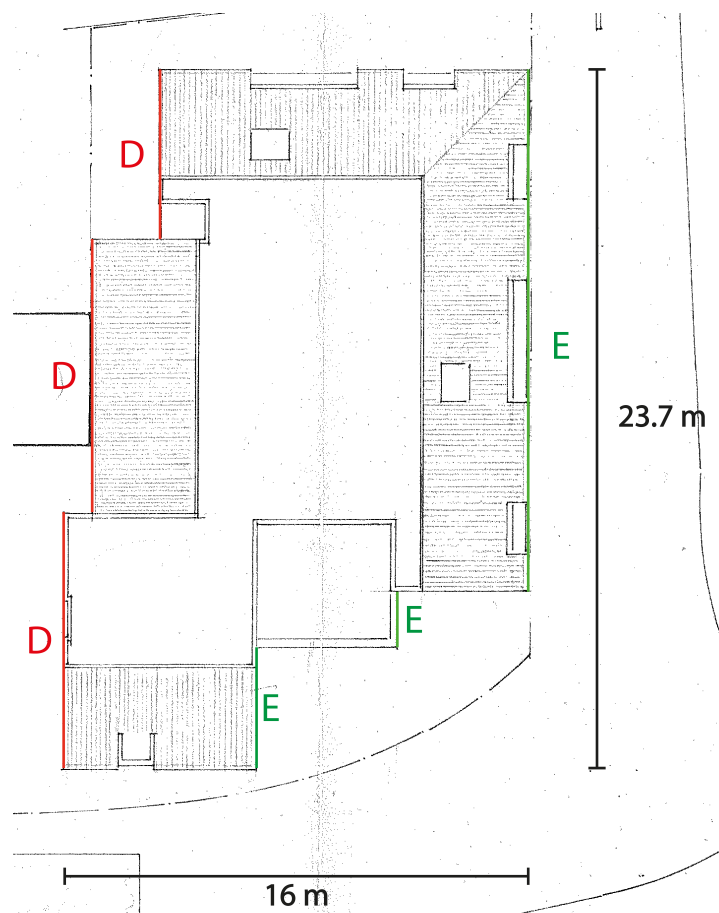


Figure E3

With Equation E.1 the residual wind force on the building is:

$$F_w = 1 \cdot 1.3 \cdot 0.83 \cdot 23.7 \cdot 16.3 = 416.8 \text{ kN}$$



Galapagos-Colibri setup

See Figure G.1

1. Galapagos: controls the process by adjust the sliders according to a genetic algorithm. The GA uses the fitness to determine the next iteration.
2. The process itself. In this simple example a rectangle is made by defining the width and height as input. The goal is to find the rectangle with the largest area. The area is the performance indicator.
3. Colibri parameters (left and middle) and Colibri Aggregate (right). These components of the plugin Colibri are used to store the solutions and open them in DesignExplorer (Figure G.2). Design is a webapp to visualize different designs.

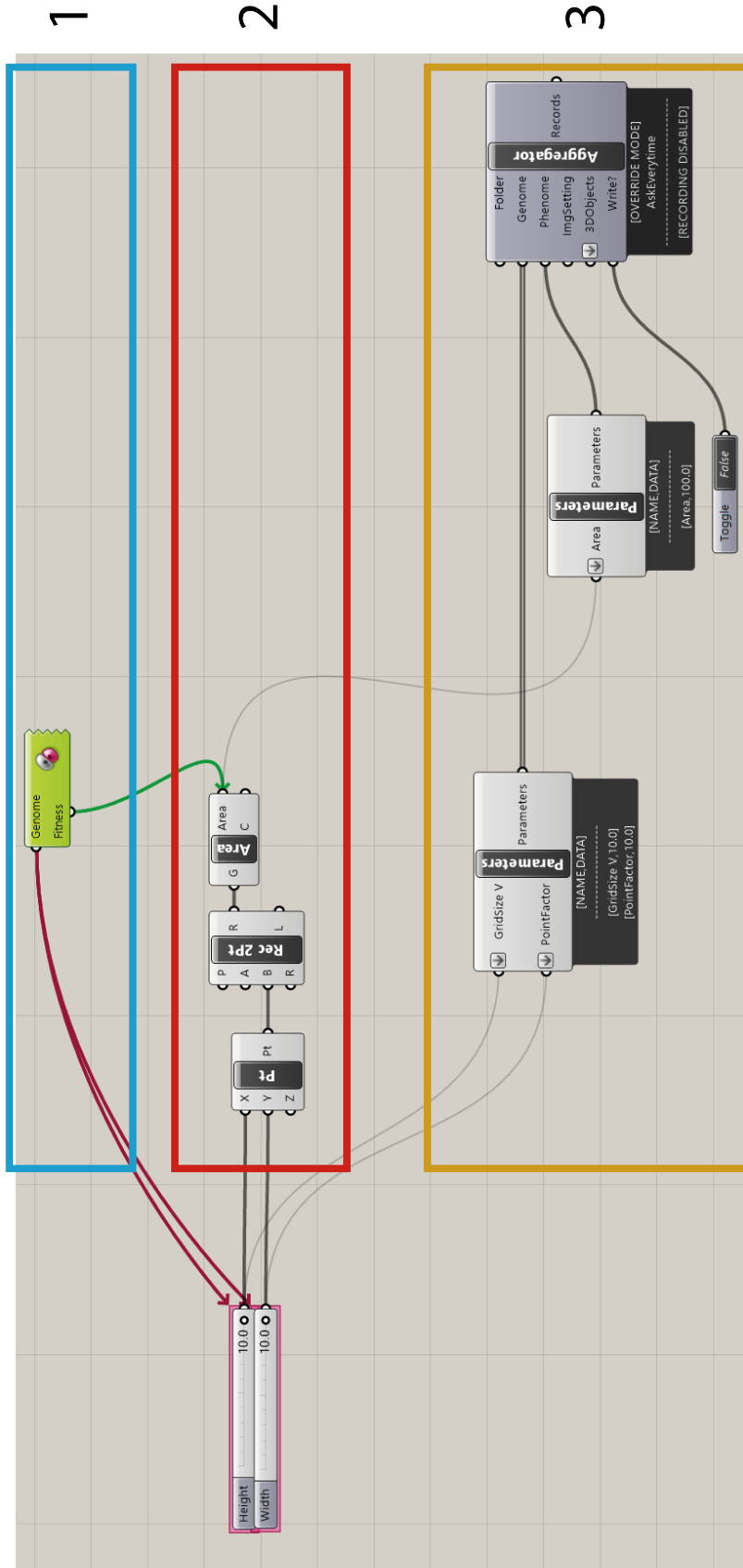


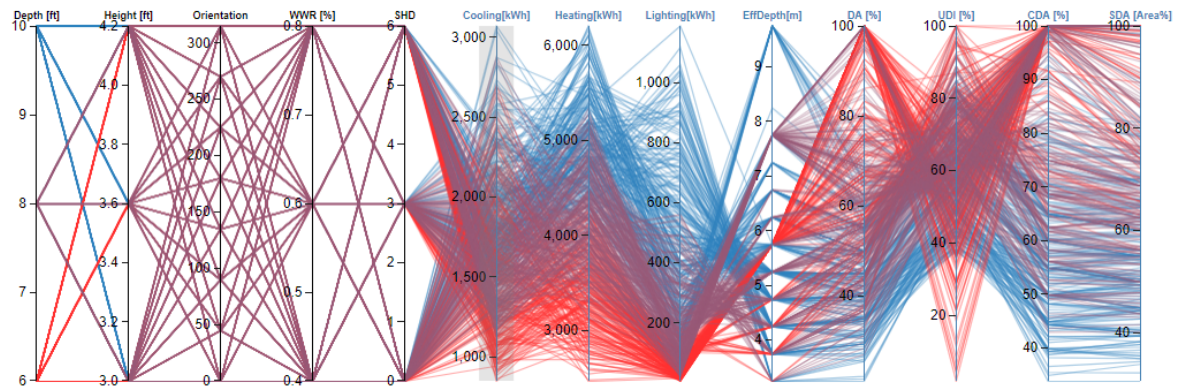
Figure G.1

Design Explorer

Get Data

Reset Selection Exclude Selection Zoom to Selection Save Selection to File My Static Link Tutorial Services Info

Setting L M S



Sort by: Depth [ft]

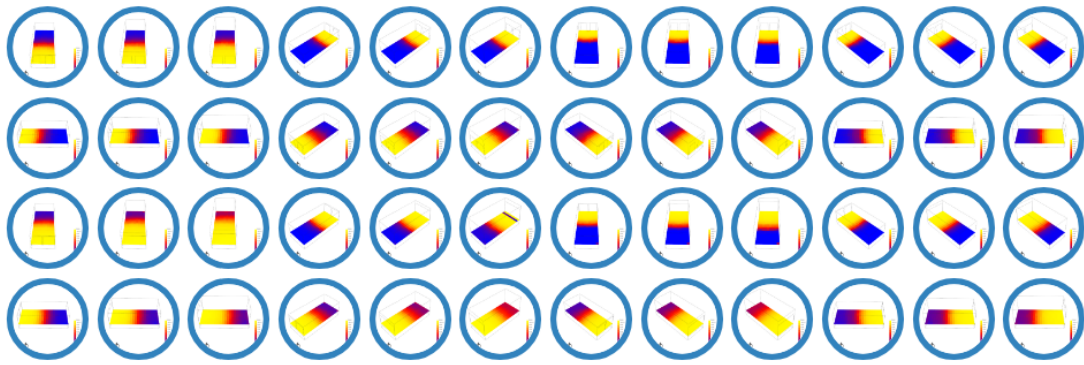


Figure G.2

Bibliography

- [1] Marcello Antinucci, Dirk Markfort, and Kevin O'Rourke. Assistance Documents for EU Member States in developing long term strategies for mobilising investment in building energy renovation (Main Document plus Annexes). Technical Report November, 2013. URL <http://www.epbd-ca.org/Medias/Pdf/EED-Article4-composite-document-final.pdf>.
- [2] Jamal van Kastel. Visual Analytics for Generative Design Exploration: An interactive 3D data environment for a computational design system facilitating the performance-driven design process of a nearly Zero-Energy sports hall, 2018. URL <https://repository.tudelft.nl/islandora/object/uuid:ad6f454b-0e67-4664-88d4-87d2132a1f71?collection=education>.
- [3] Nikolina Sajn. Energy efficiency of buildings: A nearly zero-energy future?, 2016. URL http://www.europarl.europa.eu/RegData/etudes/BRIE/2016/582022/EPRS_BRI%282016%29582022_EN.pdf.
- [4] Christian Anker Hviid and Svend Svendsen. Analytical and experimental analysis of a low-pressure heat exchanger suitable for passive ventilation. *Energy and Buildings*, 43(2-3):275–284, 2011. ISSN 03787788. doi: 10.1016/j.enbuild.2010.08.003.
- [5] A. Greco, T. Konstantinou, H.R. Schipper, R. Binnekamp, E. Gerritsen, R.P. de Graaf, and A.A.J.F. van den Dobbelsteen. Business case study for the zero energy refurbishment of commercial buildings. *Sustainable Built Environment (SBE) Regional Conference*, 2016. doi: 10.3218/3774-6. URL <https://repository.tudelft.nl/islandora/object/uuid:e08c6b3f-b8a3-4d9e-a351-0bbd918708e4?collection=research>.
- [6] Margriet Rutgers. Renovatie ministerie VROM: de stoelendans is gestart. URL <http://www.haacs.nl/renovatie-ministerie-vrom/>.
- [7] Thiemo Ebbert. Refurbishment Strategies for the Technical Improvement of Office Facades. Technical Report February, 2010.
- [8] Miriam Weber and Peter P J Driessen. Environmental Policy Integration: The Role of Policy Windows in the Integration of Noise and Spatial Planning. *Environment and Planning C: Government and Policy*, 28(6):1120–1134, dec 2010. ISSN 0263-774X. doi: 10.1068/c0997. URL <http://journals.sagepub.com/doi/10.1068/c0997>.
- [9] Marc Leijtsens. REKENTOOLS VOOR DUURZAAM GWW Een vergelijkend onderzoek. URL <https://www.dubomat.com/pdf/Rekentoolsvoorduurzamebouwmaterialen.pdf>.
- [10] Windbelasting National Annex. Nen-En 1991-1-4 + a1 + C2 / Nb. Technical Report december 2011, 2014.
- [11] IEMB and BBSR. Lebensdauer von Bauteilen und Bauteilschichten. Technical Report 4, 2006.
- [12] Milan Voorhorst. The use of solar cells to produce energy and enhance the internal comfort of large glazed spaces, 2017. URL <https://repository.tudelft.nl/islandora/object/uuid:34c5fefe-17e9-4be3-9c62-c9eaf84ddb68?collection=education>.
- [13] Planbureau voor de leefomgeving. Leegstand van kantoren 1991-2017, 2017. URL <http://www.pbl.nl/infographic/leegstand-van-kantoren#gemnr=0&year=2017&type=kantoren>.
- [14] Luis Pérez-Lombard, José Ortiz, and Christine Pout. A review on buildings energy consumption information. *Energy and Buildings*, 40(3):394–398, jan 2008. ISSN 0378-7788. doi: 10.1016/J.ENBUILD.2007.03.007. URL <https://www.sciencedirect.com/science/article/pii/S0378778807001016>.
- [15] Peter W. Christensen and Anders. Klarbring. *An introduction to structural optimization*. Springer, 2009. ISBN 9781402086663.

- [16] Robert (Robert Francis) Woodbury. *Elements of parametric design*. Routledge, 2010. ISBN 9780415779876. URL <https://www.routledge.com/Elements-of-Parametric-Design-1st-Edition/Woodbury/p/book/9780415779876>.
- [17] Carlos Roberto Barrios Hernandez. Thinking parametric design: introducing parametric Gaudi. *Design Studies*, 27(3):309–324, may 2006. ISSN 0142-694X. doi: 10.1016/J.DESTUD.2005.11.006. URL <https://www.sciencedirect.com/science/article/pii/S0142694X05000876>.
- [18] Anh Tuan Nguyen, Sigrid Reiter, and Philippe Rigo. A review on simulation-based optimization methods applied to building performance analysis. *Applied Energy*, 113:1043–1058, 2014. ISSN 03062619. doi: 10.1016/j.apenergy.2013.08.061. URL <http://dx.doi.org/10.1016/j.apenergy.2013.08.061>.
- [19] Michael Wetter and Jonathan Wright. A comparison of deterministic and probabilistic optimization algorithms for nonsmooth simulation-based optimization. *Building and Environment*, 39(8 SPEC. ISS.): 989–999, 2004. ISSN 03601323. doi: 10.1016/j.buildenv.2004.01.022.
- [20] G. Slobbe. *Optimisation of Reinforced Concrete Structures*, 2015. URL <https://repository.tudelft.nl/islandora/object/uuid:263afd2e-88d7-4416-a056-e4608ec60122?collection=education>.
- [21] M. Srinivas and L. M Patnaik. Adaptive Probabilities of Crossover and Mutations in Genetic Algorithms. *IEEE Transactions On Systems Man And Cybernetics Transactions On Systems Man And Cybernetics*, 24(4):656–667, 1994.
- [22] Stanley Hunte. Testing the application of CFD for building design: Towards a CFD application as a design tool. page 152, 2010.
- [23] Michiel Zaaijer and Danika Marquis. *Introduction to wind turbines : physics and technology*. 2018.
- [24] Francis Allard and Matheos Santamouris. Natural ventilation in buildings: a design handbook. In *London James James*, page 378. James and James (Science Publishers) Ltd, 1998. ISBN 1873936729. URL https://books.google.nl/books/about/Natural_ventilation_in_buildings.html?id=Fk1SAAAAMAAJ&redir_esc=y.
- [25] Norbert Hölscher and Hans Jürgen Niemann. Towards quality assurance for wind tunnel tests: a comparative testing program of the Windtechnologische Gesellschaft. *Journal of Wind Engineering and Industrial Aerodynamics*, 74-76:599–608, 1998. ISSN 01676105. doi: 10.1016/S0167-6105(98)00054-3.
- [26] Jörg Franke. *Introduction to the Prediction of Wind Loads on Buildings by Computational Wind Engineering (CWE)*, pages 67–103. Springer Vienna, Vienna, 2007. ISBN 978-3-211-73076-8. doi: 10.1007/978-3-211-73076-8_3. URL https://doi.org/10.1007/978-3-211-73076-8_3.
- [27] Céline Paoli. 07- Past and Future of Grid Shell Structures, 2007. URL <http://hdl.handle.net/1721.1/39277>.
- [28] Hee Chang Lim, T. G. Thomas, and Ian P. Castro. Flow around a cube in a turbulent boundary layer: LES and experiment. *Journal of Wind Engineering and Industrial Aerodynamics*, 97(2):96–109, 2009. ISSN 01676105. doi: 10.1016/j.jweia.2009.01.001.
- [29] Fan Qin Meng, Bao Jie He, Jin Zhu, Dong Xue Zhao, Amos Darko, and Zi Qi Zhao. Sensitivity analysis of wind pressure coefficients on CAARC standard tall buildings in CFD simulations. *Journal of Building Engineering*, 16(October 2017):146–158, 2018. ISSN 23527102. doi: 10.1016/j.jobbe.2018.01.004. URL <https://doi.org/10.1016/j.jobbe.2018.01.004>.
- [30] N. G. Wright and G. J. Easom. Non-linear k- ϵ turbulence model results for flow over a building at full-scale. *Applied Mathematical Modelling*, 27(12):1013–1033, 2003. ISSN 0307904X. doi: 10.1016/S0307-904X(03)00123-9.
- [31] P. J. Richards, R. P. Hoxey, and L. J. Short. Wind pressures on a 6 m cube. *Journal of Wind Engineering and Industrial Aerodynamics*, 89(14-15):1553–1564, 2001. ISSN 01676105. doi: 10.1016/S0167-6105(01)00139-8.

- [32] P. J. Richards, R. P. Hoxey, B. D. Connell, and D. P. Lander. Wind-tunnel modelling of the Silsoe Cube. *Journal of Wind Engineering and Industrial Aerodynamics*, 95(9-11):1384–1399, 2007. ISSN 01676105. doi: 10.1016/j.jweia.2007.02.005.
- [33] Steve Irving, Ford Brian, and Etheridge David. *Natural ventilation in non-domestic buildings*. Chartered Institution of Building Services Engineers, 2005. ISBN 1903287561. URL <https://www.cibse.org/Knowledge/knowledge-items/detail?id=a0q20000008I7m2AAC>.
- [34] Rameshwar D. Gupta and Debasis Kundu. Exponentiated Exponential Family: An Alternative to Gamma and Weibull Distributions. *Biometrical Journal*, 43(1):117–130, feb 2001. ISSN 0323-3847. doi: 10.1002/1521-4036(200102)43:1<117::AID-BIMJ117>3.0.CO;2-R. URL <http://doi.wiley.com/10.1002/1521-4036%28200102%2943%3A1%3C117%3A%3AAID-BIMJ117%3E3.0.CO%3B2-R>.
- [35] Meteoblue. Klimaat Rotterdam - meteoblue. URL https://www.meteoblue.com/nl/weer/voorspelling/modelclimate/rotterdam_nederland_2747891.
- [36] Lauri Salokangas. Wooden Tower, Helsinki Zoo. URL http://www.lusas.com/case/civil/wooden_tower.html.
- [37] Alexander de Leon. Two Case-Studies of Freeform-Facade Rationalization. In *Physical Digitality: Proceedings of the 30th eCAADe Conference*, volume 2 of *eCAADe: Conferences*, pages 501–509, Prague, Czech Republic, 2012. Czech Technical University in Prague, Faculty of Architecture, Czech Technical University in Prague, Faculty of Architecture.
- [38] L F M Koning. Digital Fabrication of a Timber Bridge. page 261, 2018.
- [39] Åke Blomsterberg. Best Practice for Double Skin Façades. Technical report, 2007.
- [40] A. Huzefa. Rationalisation of Freeform Glass Facades from Concept to Construction. (September):187, 2013. ISSN 03698718. doi: 10.1039/PL9011700043.
- [41] John Kaiser Calautit, Dominic O’Connor, and Ben Richard Hughes. A natural ventilation wind tower with heat pipe heat recovery for cold climates. *Renewable Energy*, 87:1088–1104, mar 2016. ISSN 0960-1481. doi: 10.1016/J.RENENE.2015.08.026. URL <https://www.sciencedirect.com/science/article/pii/S0960148115302263#undfig1>.
- [42] James Atkinson, Yves Chartier, Carmen Lúcia Pessoa-Silva, Paul Jensen, Yuguo Li, and Wing-Hong Seto. Natural Ventilation for Infection Control in Health-Care Settings. *World Health Organization*, page 133 p., 2009. ISSN 0022-3492. doi: 10.1902/jop.2008.070649. URL http://www.ncbi.nlm.nih.gov/pubmed/23762969http://whqlibdoc.who.int/publications/2009/9789241547857_eng.pdf.
- [43] Jan-Fokko Haan, Michiel van Bruggen, Marco Hofman, Stefan Verbrugge, Marcel Verbeeken, and Bart Cremers. Hybride ventilatie. Technical report, TVVL, 2017. URL <https://www.tvvl.nl/k/n190/news/view/15354/17488/kt-26-hybride-ventilatie-gereed.html>.
- [44] Per Heiselberg. ECBCS Annex 35 - Principles of hybrid ventilation. *IEA Annex 35: Hybrid ventilation in new and retrofitted office buildings*, 2002. ISSN 1395-7953 R0207.
- [45] Michael Humphreys, Fergus Nicol, and Roaf S. *Adaptive Thermal Comfort: Foundations and Analysis*. 2016. ISBN 978-0-415-6916-1.
- [46] B Evans. Integrating fabric and function. *The architects Journal*, 2 June:42–48, 1993.
- [47] Ana Lisa. Berlin’s GSW Headquarters Saves Energy with a Thermal Flue Passive Ventilation System, 2012. URL <https://inhabitat.com/berlins-gsw-headquarters-saves-energy-with-a-thermal-flue-passive-ventilation-system/>.
- [48] Peter White. BRE’s Environmental Building, 2000. URL <http://projects.bre.co.uk/envbuild/index.html>.
- [49] Probe Team. Barclaycard. (March):37–42, 2000.

- [50] Foster and Partners. Arag Headquarters | Projects | Foster and Partners. URL <https://www.fosterandpartners.com/projects/arag-headquarters/>.
- [51] Margo van Voskuilen. De ooievaar die het hoofd van ambtenaren koel hield | NBD-Online, 2017. URL <https://www.nbd-online.nl/nieuws/185161-de-ooievaar-die-het-hoofd-van-ambtenaren-koel-hield>.
- [52] Bjornd Makelaardij. Funda in business: Mijnbouwstraat 110 2628 RX Delft. URL <https://www.fundainbusiness.nl/kantoor/verhuurd/delft/object-48619504-mijnbouwstraat-110/>.
- [53] Jibrán Haider. OpenFOAM course for beginners: Hands-on training, 2018.
- [54] Larson Will. Genetic algorithms: cool name and damn simple. URL <https://lethain.com/genetic-algorithms-cool-name-damn-simple/>.
- [55] G. Sivaraj, K. M. Parammasivam, and G. Suganya. Reduction of aerodynamic drag force for reducing fuel consumption in road vehicle using basebleed. *Journal of Applied Fluid Mechanics*, 11(6):1489–1495, 2018. ISSN 17353645. doi: 10.18869/acadpub.jafm.73.249.29115.
- [56] Chung Yang Huang, Chao Yue Lai, and Kwang Ting Cheng. *Fundamentals of Algorithms*. Number 173. Elsevier Inc., 2009. ISBN 9780123743640. doi: 10.1016/B978-0-12-374364-0.50011-4. URL <http://dx.doi.org/10.1016/B978-0-12-374364-0.50011-4>.
- [57] Sighard F Hoerner. Fluid-Dynamic Drag, Hoerner.pdf, 1993.
- [58] W Klemperer. Luftwiderstandsuntersuchungen an Automodellen. *Z. Flugtech. Motorluftschiffahrt*, (13): 201, 1922.
- [59] Changliang Lai, Junbiao Wang, and Chuang Liu. Parameterized Finite Element Modeling and Buckling Analysis of Six Typical Composite Grid Cylindrical Shells. *Applied Composite Materials*, 21(5): 739–758, 2014. ISSN 1573-4897. doi: 10.1007/s10443-013-9376-x. URL <https://doi.org/10.1007/s10443-013-9376-x>.
- [60] Geometrica. Gridshells | Long Span Structures | Freedomes. URL <http://geometrica.com/en/gridshells>.
- [61] James Taylor-Foster and Timothy Brittain-Catlin. *Understanding British Postmodernism (Hint: It's Not What You Thought)*. ArchDaily, 2017. URL <https://www.archdaily.com/219082/kings-cross-station-john-mcaslan-partners>.
- [62] Thomas Boegl. Peek and Cloppenburg Department Store, 2012. URL <https://www.mimoo.eu/projects/Germany/Cologne/Peek%2526CloppenburgDepartmentStore>.
- [63] C R Braam. *Ontwerpen en dimensioneren van vloeistofkerende constructies LK - https://kb.on.worldcat.org/oclc/67082163*. ENCI Media, 's-Hertogenbosch SE - [210] p. : ill. ; 30 cm., 2001. ISBN 9071806472 9789071806476.
- [64] Lisa Hallberg and Jan-Olof Sperle. Assessing the environmental advantages of high strength steel. *LCM 2011, August 28-31, 2011, Berlin Germany*, 2011. doi: 10.1038/ncomms8872.
- [65] Market bouwbeslag techniek. Glassoorten, Glasopbouw en Gewicht van glas. URL <https://www.market.nl/glassoorten-en-glasopbouw.html>.
- [66] P Crowther. Design for disassembly to recover embodied energy. 1999. URL <http://eprints.qut.edu.au/2846>.
- [67] GKC Ding. The development of a multi-criteria approach for the measurement of sustainable performance for built projects and facilities. 2004. URL <https://opus.lib.uts.edu.au/handle/2100/281>.

- [68] Simone Hegner and Dieter Imboden. An Assessment of Embodied Energy's Relevance for Energy Saving in the Swiss Residential Building Sector. 2007. URL <https://scholar.google.com/scholar?q=%22HegnerS.Embodiedenergyforenergyefficiency%27srelevanceforenergysavingintheSwissresidentialbuildingsector.DiplomaThesis.DepartmentofEnvironmentScience,.>
- [69] P Frey, P Anderson, M Andrews, and C Wolf. Building reuse: Finding a place on American climate policy agendas. 2010. URL https://www.researchgate.net/profile/Rafael_Garcia_Cueto/publication/243458572_Urban_Heat_Island_Urban_analysis_assessment_and_measuring_mitigation_in_cities_of_extreme_dry_weather/links/0046352f1554739241000000/Urban-Heat-Island-Urban-analysis-assessment.
- [70] Roger Plank. The principles of sustainable construction. *The IES Journal Part A: Civil and Structural Engineering*, 1(4):301–307, nov 2008. ISSN 1937-3260. doi: 10.1080/19373260802404482. URL <http://www.tandfonline.com/doi/abs/10.1080/19373260802404482>.
- [71] Robert Smirke. OKATHERM - REFERENCES The Great Court at The British Museum. pages 4–7, 2000.
- [72] Darren Anderson, Zbigniew Czajewski, Stuart Clarke, Ian Feltham, Paul Geeson, Marcin Karczmarczyk, Richard Kent, David Killion, Zbigniew Kotynia, Maciej Lewonowski, Robert Lindsay, Philip Monypenny, Chris Murgatroyd, Johnny Ojeil, Raf Orlowski, Andrzej Sitko, and Darren Woolf. Złote Tarasy, Warsaw , Poland. *The Arup Journal*, 1, 2008.
- [73] Karamba. PARAMETRIC STRUCTURAL MODELING User Manual. pages 6–92, 2012. URL http://www.karamba3d.com/wp-content/uploads/downloads/2012/04/KarambaManual_0_9_084.pdf.
- [74] Jianguo Cai, Yixiang Xu, Jian Feng, and Jin Zhang. Nonlinear Stability of a Single-Layer Hybrid Grid Shell. *Journal of Civil Engineering and Management*, 18(5):752–760, 2012. ISSN 1392-3730. doi: 10.3846/13923730.2012.723325.
- [75] J.L. Coenders. Structural Design - Special Structures April 2008. (April), 2008.
- [76] Duco. Plaatsingsinstructies Tronic DUcoMax, 2018. URL <http://www.duco.eu/nl-nl-producten/nl-nl-basisventilatie/nl-nl-elektronisch-gestuurde-ventilatiooesters/nl-nl-tronicmax>.
- [77] Andrea. London Blog Pt. 6 - "Restful Sunday", 2013. URL <http://researchandramblings.blogspot.com/2013/07/london-blog-pt-6-restful-sunday.html>.
- [78] B.J. Polidoro W.S. Dols. NIST Technical Note 1887 CONTAM User Guide and Program Documentation. Technical report, 2007.
- [79] Giessen Status. Bodemkwaliteitskaart gemeente Delft 2018. Technical report, gemeente Delft, 2017.
- [80] Anja Klaver. Brief OBS - Spoorzone Delft, 2012.
- [81] R. Braam and P. Lagendijk. *Conconstructieer gewapend beton*. 2011.